The transfer of radionuclides from sea to land in sea spray

Patrick M. Nelis

Submitted for the Degree of

Doctor of Philosophy

University of Edinburgh

June 1990

Contents

Acknowledgements

This study was begun while the author was in receipt of a Research Studentship from the Natural Environment Research Council. The NERC also provided the funds for travel between Edinburgh and the fieldwork site at Drigg in W. Cumbria.

I would like to thank Derek Branford, Dave Horrill and Mike Unsworth for their assistance in the completion of this study and their advice in the preparation of this thesis.
I am grateful to Tom Davinson for his efficient management and development of the computer facilities and help with the electronics problems encountered in the course of the γ-ray counting.
Euan Macdonald was a constant and ready source of information on the workings of the GEC, and I thank him for his assistance and patience.
I would like to thank Gordon Turnbull for constructing the frames for the muslin screen collectors.

The fieldwork reported here could not have been performed without the invaluable assistance and enthusiasm of David Simpson, then Warden of the Local Nature Reserve at Drigg. The hospitality shown to me by David and Ceri made my frequent trips to Drigg a great pleasure. I would like to thank them for their kindness and generosity.

This project would not have been completed without the encouragement and support of Teresa Anderson, to whom this document is dedicated.

Declaration

No part of this thesis has been submitted for any other degree or professional qualification.

In accordance with the University of Edinburgh regulation 3.4.7, I here state that:

- this thesis has been composed by myself
- the work involved in the data collection and analysis reported here is my own

Patrick M. Nelis

When he would stand like that
on the other side, white-haired,
swinging his blackthorn

at the marsh weeds,
he prophesied above our scraggy acres,
then turned away

towards his promised furrows
on the hill, a wake of pollen
drifting to our bank, next season's tares.

from *The Other Side* by **Seamus Heaney**, 1972.

Abstract

This thesis reports on an investigation into the transport inland in sea spray of radionuclides discharged into the Irish Sea from the nuclear plant at Sellafield in Cumbria. The work was carried out in response to a concern about the increased incidence of childhood leukaemia in the vicinity of Britain's nuclear reprocessing facilities. It is proposed that the sea spray transfer is a important pathway of discharged radioactivity into the human environment.

The inland transfer of contaminated sea spray was investigated on the beach at Drigg, between 6 and 10 km south of the BNFL Sellafield marine discharge pipeline, through which significant levels of radionuclides have been flushed since 1952. The radionuclide concentrations of coastal marram grass vegetation and collected on exposed muslin screen passive droplet collectors are reported. The method used to determine the mass of sea-salt collected by the exposed screens is described and the results of these measurements presented.

The collection of the natural atmospheric radionuclide ^{7}Be on the exposed muslin screens was used to extract the effects of the changing wind flow on the collection of the spray droplets at different distances inland. This allowed an elucidation of the true reduction in the radionuclide air concentrations with distance from the sea. The Sellafield-produced radionuclides present on the exposed screens were found to decrease with distance inland at the same rate as the collected sea-salt, implicating the sea spray droplets as the carriers of the radioactivity.

A model of the inland transfer of sea spray droplets produced in the surf zone along the shoreline is described. The collection of the contaminated spray in coastal soil, vegetation and muslin screen collectors is simulated. This model gives results which fit the measured reduction in radionuclide air concentrations

with distance from the sea. A successful application to datasets of the inland transfer of spray and radioactivity reported elsewhere is also illustrated.

The analysis of the changing surface air concentration with distance inland illustrated that the initially rapid reduction measured here and elsewhere is due more to the spray droplets being mixed to higher altitudes than their deposition to the ground. An analysis of a sea spray collection event in which very high radionuclide air concentrations were measured calculates that under certain conditions 1 km of coastline can produce 1.54×10^5 Bq of $^{239+240}$Pu and 1.10×10^5 Bq of ^{241}Am per hour. This material is thought to be efficiently transported inland in sea spray, and 60% of it is calculated to be still airborne 1 km from the coast.

It is concluded that the sea spray transport of marine discharged radioactivity transfers significant levels of long-lived radionuclides to the land, much of it in the respirable size range, and that this material can be carried to large distances from the sea. This pathway merits further investigation as the causes of the increased leukaemia incidence in West Cumbria are sought.

Chapter 1

Introduction

Concern first arose about the increased incidence of cancers in the vicinity of British nuclear establishments on the broadcast of a Yorkshire Television documentary, "Windscale – The Nuclear Laundry", in 1983. The committee set up to investigate the findings of this programme published its findings in the Black Report in 1984 [40]. An increased incidence of childhood leukaemia in Seascale, situated 3 km from the British Nuclear Fuels plc (BNFL) reprocessing plant at Sellafield, W. Cumbria, was confirmed in this report. This conclusion prompted an investigation of leukaemia incidence in the locality of Britain's only other nuclear reprocessing plant, the Dounreay Nuclear Establishment, operated by the United Kingdom Atomic Energy Authority (UKAEA) in Caithness. The Committee on Medical Aspects of Radiation in the Environment (COMARE), established in fulfilment of the recommendations of the Black Report, accepted the existence of an increased incidence of leukaemia in young people in the vicinity of Dounreay [14].

The reprocessing plants at Sellafield and Dounreay are responsible for the discharge of radioactivity levels to the local environments which are much in excess of releases from other nuclear installations. The discharges have been substantially greater at Sellafield, which has the highest authorised discharges in the U.K. [14]. Radioactivity is released both to the atmosphere and in liquid wastes discharged to the sea.

Conventional radiological dose and risk estimates have suggested that the dis-

charges from the reprocessing plants are too small to be the cause of the increased cancer incidence [14][40]. This conclusion was reached after consideration of how the radiation exposure of young people living close to the nuclear installations was enhanced by the radioactivity released from the nuclear plants. The pathways of radiation exposure considered in the dose estimates of the local populations were from both external radiation, by airborne and deposited radionuclides, and from internal exposure after inhalation of airborne radionuclides and the ingestion of radionuclides present in soil and foodstuffs. The radioactive discharges to sea and atmosphere have been shown to contribute to the radiation exposure of the local populations, but to only a fraction of the extent of other radionuclides present naturally in the environment to which the population in all areas of the country are being exposed.

Other mechanisms whereby the authorised environmental discharges could be implicated were sought by the investigating bodies. The existence of unrecognised pathways of radioactivity into the human environment, or the use of incorrect factors in estimating the dose received from inhaled and ingested radionuclides would require a re-calculation of the radiation exposure of the local populations. The discovery of unforseen mechanisms of leukaemia induction by radiation would also make a re-consideration of the health effects of the discharged radioactivity necessary [14].

Alternative explanations of the increased cancer incidences, including the possibility that factors other than radiation could be relevant, have also been proposed. Some unrecognized function of the nuclear plants totally unconnected with their radiological significance, such as the use or release of certain chemicals, could be the cause of the increased leukaemia incidence. The COMARE surveyed possible mechanisms and stated that current evidence did not point to any particular explanation and that all possibilities need to be further investigated. Even so, this committee supported the hypothesis "that some feature of the nuclear plants leads to an increased risk of leukaemia in young people living in the vicinity of the plants" [14].

A more recent and much publicised study has proposed links between the leukaemia cases in Seascale and the previous radiation exposure of the fathers

of those with the disease while employed at the Sellafield plant [29]. It is proposed that the radiation exposure of BNFL employees can cause some sort of genetic damage which leads to an increased leukaemia incidence in their offspring. Whether this is a single stage process or a result of the genetic damage leading to a reduced immunity in the children, making them pre-disposed to leukaemia incidence, is a matter for discussion. The second mechanism would implicate the enhanced radioactivity levels in the environment around Seascale arising from the marine and atmospheric discharges from the Sellafield plant.

1.1 Aims of the Present Study

A potentially important pathway of the released radioactivity into the human environment involves the transfer to land of radioactivity discharged initially to the sea. Radionuclides can become airborne in sea spray produced at sea and so be transported inland by the wind. That radioactivity dumped to sea could return to land by such a mechanism had been disregarded until the early 1980s. The COMARE have called for a further investigation of the sea to land transfer of discharged radionuclides in sea spray [14].

The transfer of radionuclides from sea to land in sea spray results in the transport into the human environment of high levels of certain radionuclides which are not present naturally, and in quantities which swamp the activities of these radionuclides present from the fallout from the nuclear bomb tests in the atmosphere in earlier years. As releases from other nuclear establishments are of a much lower order, the two reprocessing plants are alone in causing contamination of their locality with these radionuclides.

Radionuclides of significance in this respect are the various plutonium isotopes ^{238}Pu, ^{239}Pu and ^{240}Pu and other transuranic isotopes such as ^{237}Np, ^{241}Am, ^{243}Cm and ^{244}Cm (these elements are referred to as actinides, as they are in the series of elements beyond actinium in the periodic table). These radionuclides all decay with the emission of high energy alpha (α-) particles which are known to leave high density energy deposits in material they pass through. They are of particular importance when produced by nuclei present inside the body as they

are capable of causing great damage to nearby tissue. The plutonium isotopes are a particularly significant source of radiation exposure after inhalation as they are retained in the lungs for periods over 100 days [13]. The other transuranics are also of significance in this respect [21].

There is a need to understand more fully the mechanisms of the transfer of the contaminated sea spray inland from the sea. It has been the aim of this study to plot the reduction in airborne intensity of sea spray borne radioactivity with distance inland, and to elucidate the major processes by which this reduction occurs. Thus a model of the sea to land transfer of radioactivity in sea spray can be developed, from which estimates can be made of the extent of the inland transfer in a wide range of meteorological conditions. A successful model will also allow an extrapolation from the results of measurements of radionuclide air concentration at a few points to other sites. This will allow a reduction in the number of measurements necessary to adequately monitor the dose to which the populations local to the nuclear installations are being exposed.

The input of radioactivity into the foodchain can also be estimated from the model by allowing calculations of the deposition of radioactivity to vegetation and crops. This will again allow further estimates of the ingested levels of different radionuclides arising from the liquid discharges to the sea. Knowledge of the inland transfer of respirable aerosol will allow an increased accuracy in the dose estimates arising from inhalation of sea spray.

The measurements have been performed in the vicinity of the BNFL Sellafield plant. Large activity levels in liquid discharges to sea have resulted in easily measurable levels of radionuclides present in sea spray being transferred inland from the Irish Sea. Although measurements have been made of only one actinide, ^{241}Am, the conclusions drawn from the study will be valid also for the plutonium isotopes, which are presently being transferred in larger amounts, and the other transuranics. It is perceived that in future years the ^{241}Am present in the inland transfer of sea spray will become the most significant source of the exposure of the local population from this pathway [38]. Thus the measurements of the intensity of the sea to land transfer of radionuclides performed in the course of this study and the sea to land transfer model introduced, will be of use in estimating the

possible long term deleterious health effects to the general public of the release to sea of radioactive wastes from Britain's nuclear reprocessing plants.

1.2 Liquid effluent discharges from Sellafield

The BNFL site at Sellafield in W. Cumbria is organised into three major operating units. The Reprocessing Operation Division, centred on the Windscale works, is responsible for the reprocessing of irradiated nuclear fuel and the conditioning of radioactive wastes. The Reactor Division is responsible for the operation of the four Magnox type Nuclear reactors at the Calder Hall Power Station. The Waste Management Unit is responsible for the Storage and Disposal Site at Drigg. The UKAEA also has its Northern Research Laboratories on the Sellafield Site [4].

Since 1952, and currently with the permission of the Department of the Environment and the Ministry of Agriculture, Fisheries and Food, there have been routine discharges of radioactivity from the plants at Sellafield into the North East Irish Sea (See the map in Figure 2.1). This procedure received an endorsement in a government White Paper in 1959, with the outlook that some exposure of the general public was unavoidable if the benefits of electricity generation by nuclear power were to be enjoyed by the nation as a whole [35].

The majority of the transuranic radionuclides in the Sellafield effluent are present in the liquid wastes arising from the nuclear fuel reprocessing operations [66]. The waste from these processes is routed to holding tanks which are emptied twice daily. The majority of the ^{137}Cs and ^{106}Ru discharged to the sea are present in recycled water from the Magnox fuel storage ponds. This water is discharged continuously to the sea after treatment to remove some of the activity present [4]. (^{137}Cs and ^{106}Ru are among the isotopes referred to as fission products, as they are produced in the fission of uranium and plutonium nuclei.)

The activity levels discharged from the Windscale site increased steadily during the 1950s and 1960s, reaching their peak in the mid-1970s [4][38]. The peak annual ^{137}Cs discharge was in 1975, with an activity of over 5000 TBq, equivalent to 1.35×10^5 Ci, being disposed of into the sea. (The Becquerel (Bq) is the SI unit for the activity of a radioactive substance and is equivalent to one nuclear

disintegration per second. The old unit of activity was the Curie (Ci), equal to 3.7×10^{10} Bq, being approximately the activity of 1 g of radium). The annual discharge of ^{137}Cs was still more than 2000 TBq until 1982, but has since been substantially reduced, with only 12 TBq (324 Ci) of ^{137}Cs being disposed of to the sea in 1987. The peak ^{241}Am discharge rate was in 1974 with 120 TBq (3240 Ci) being dumped in the course of the year. This fell off rapidly in subsequent years, the annual ^{241}Am discharge being reduced to 0.7 TBq (19 Ci) in 1987.

Over the whole period of low-level waste disposal to the Irish Sea, very significant levels of radioactivity have been released. A total of 40 000 TBq (1.1×10^6 Ci) of ^{137}Cs activity, 740 TBq (2.0×10^4 Ci) of Pu α-activity, and 520 TBq of ^{241}Am activity have been discharged until the end of 1987. There has also been a total release of over 21000 TBq (5.7×10^5 Ci) of the beta emitter ^{241}Pu in this period. This Pu isotope has a short half-life of only 14.4 years and decays into ^{241}Am. As there is a significant annual discharge of ^{241}Pu in current discharges, 32 TBq in 1987, there will be a significant ingrowth of ^{241}Am from ^{241}Pu in future years.

Large activity levels of ^{106}Ru have also been discharged into the Irish Sea. The mean annual discharge of this isotope between 1969 and 1972 was 1100 TBq, very similar to the ^{137}Cs levels [34]. The ^{106}Ru discharge was reduced from 550 TBq in 1983 (40% of the ^{137}Cs discharge that year) to 22 TBq in 1987 (185% of the ^{137}Cs released that year).

1.2.1 Behaviour of the radionuclides in Irish Sea

The ^{137}Cs discharged to sea from Sellafield remains mostly in solution, and is rapidly dispersed from the region of outfall by the general circulation of water in the Irish Sea. The residual current in this region carries the water-borne radioactivity southwards along the Cumbrian coast to Liverpool Bay. From here it is flushed from the area in the northward movement of Atlantic water, leaving by the North Channel between the Mull of Kintyre and N.Ireland [41] (See Figure 2.1). The ^{137}Cs which goes into solution is thought to have a lifetime in the Irish Sea of around 200 days [42]. A fraction of the ^{137}Cs will become attached to particles in the sea. Early measurements showed that less than 5% of the ^{137}Cs in the surface seawater is present in the suspended sediment [35].

More recently, however, McKay et al. collected surface seawater samples which contained a much greater proportion of sediment-associated ^{137}Cs [52]. These authors stated that this may be a result of the permanent adsorption of ^{137}Cs released in previous years to the sedimentary particles. Thus the soluble and particulate associated ^{137}Cs are no longer in strict equilibrium.

The behaviour of the discharged actinides contrasts sharply with that of the ^{137}Cs. It has been estimated that, far from being rapidly removed from the Irish Sea, about 33% of the total Pu and 50% of the total ^{241}Am discharged since the early 1950s is still present on the sea bed within a coastal strip extending only 30 km from the Cumbrian coast [65]. In the region of 95% of the discharged Pu is thought to be lost from the water column to the sea bed sediments close to the end of the discharge pipe [35]. It may be the case that the actinides are not available to the water column at all on discharge, as it has been reported that the Pu and ^{241}Am are attached to a ferric hydroxide floc in the effluent prior to the discharge [65], and it has been suggested that the actinides are carried to the sea bed with this floc on discharge [38]. The actinides are thought to desorb from the floc onto the neighbouring sediments on the sea bed over a period of about 200 days, and are subsequently moved throughout the Irish Sea from the region off Sellafield with the general sediment transport [39][66]. Sediment can also become suspended, for example, by biological activity, and be carried from the region by the water currents. This mechanism of the transport of the discharged actinides away from the region off Sellafield is supported by studies of sediment cores taken far from Sellafield, which imply that the activity present is due to the sedimentation of material which has been previously contaminated [35].

Any of the Pu and ^{241}Am which remains unattached to particles will behave similarly to the majority of the discharged ^{137}Cs and will follow the general water circulation and be flushed from the region. This happens to only about 5% of the Pu and less of the ^{241}Am [52]

The discharged ^{106}Ru activity seems to have behaved in a similar fashion to the released actinide activity. This isotope strongly attaches to sedimentary particles in the sea. It too is rapidly lost from the water column and 95% of the ^{106}Ru present in the general vicinity of Sellafield is present in the sea-bed

compartment [34].

Both actinide and fission product radionuclides attach themselves to the sediment via a surface active mechanism. The effect of this is that the specific activity of radionuclides on the sediment grains increases for smaller diameter particles, increasing in going from sand to clay particles [34][35].

1.2.2 Radioactivity levels in in-shore sea water

In this section quoted values of the radioactivity concentrations present in in-shore seawater at sites along the Cumbrian coast will be discussed. These measurements will be of use later when an estimate is made of the radionuclide enrichment of the sea spray being transferred inland relative to the bulk seawater from which it is produced.

Eakins et al. measured the activity levels in seawater samples collected from the surf zone at Eskmeals [18]. They found concentrations of $^{239+240}$Pu of 0.4–1.8 $\mathrm{Bq\,l^{-1}}$, ^{241}Am between 0.2–1.5 $\mathrm{Bq\,l^{-1}}$ and ^{137}Cs in the range 6.8–15.2 $\mathrm{Bq\,l^{-1}}$. The majority of the actinides were associated with the suspended particulate material, with over 90% of the ^{137}Cs being in the soluble phase on all occasions.

The most comprehensive series of measurements of the activity levels present in in-shore seawater along the Cumbrian coastline was performed by M^{c}Kay et al. [52]. These workers collected samples of seawater from the surf-zone at St. Bees, Seascale and Eskmeals on 27 occasions between 1980 and 1984 (Figure 2.1). The beach used in the present study, at Drigg, is between Seascale and Eskmeals. The activity levels present in the seawater samples were not found to be significantly reducing with time during the course of these measurements. It is therefore reasonable, as a first assumption, to use these measurements to give an indication of the levels present off Drigg during the course of the sea spray collections performed in this study.

The collected seawater samples were filtered through a 0.45 μm millipore filter. Only 1–6% of the $^{239+240}$Pu activity and 1–4% of the ^{241}Am activity passed through with the filtrate. The ^{137}Cs activity associated with the filtrate varied between 67 and 95%. The suspended sediment loads varied considerably under different surf conditions, varying between 17 and 300 $\mathrm{mg\,l^{-1}}$. The median value

was of the order of $100\,mg\,l^{-1}$. The authors could find no trend relating the observed weather conditions at the time of collection to the particulate loading present in the collected seawater sample.

The ^{241}Am concentrations in the collected samples were very variable, ranging from 0.06 to $3.7\,Bq\,l^{-1}$ at Seascale. The mean ^{241}Am levels at Seascale and Eskmeals were similar, however, being $0.58\pm0.14\,Bq\,l^{-1}$ and $0.51\pm0.11\,Bq\,l^{-1}$ respectively. The ^{137}Cs activity levels were also variable, ranging between 3.0 and $47.9\,Bq\,l^{-1}$ at Seascale. The mean ^{137}Cs concentration in the samples collected at Seascale was $13.2\pm2.1\,Bq\,l^{-1}$, slightly greater than a mean concentration of $8.8\pm1.1\,Bq\,l^{-1}$ in the seawater collected at Eskmeals, which is further from the discharge out-fall. These measured activity levels agree well with those reported for the samples collected at Eskmeals by Eakins et al. discussed above.

1.3 The sea to land transfer of radioactivity

The possibility that radioactivity present in seawater could become airborne in spray droplets and be transferred inland was discussed by Blanchard & Syzdek as early as 1970 [2]. These workers had found that this phenomenon occurred for bacteria, and later reported that viruses present in the the surf zone could be transferred onto a nearby beach [1]. That a similar process does occur for radionuclides present in coastal waters was first reported by Fraizier et al. [26]. They collected samples of a lichen *Ramalina scopulorum* from the coastal region of Normandy in Northern France, near the La Hague reprocessing plant, and found that the concentrations of industrial radionuclides in these samples decreased with increasing distance inland. A similar result was reported in the same area by Martin et al. who found that the ratio ^{238}Pu : $^{239+240}Pu$ in vegetation samples decreased with distance inland, towards the value expected from depositing debris in nuclear bomb-test fallout [49]. Their explanation for this was that aerosols from the surface of the coastal waters were being transported inland and that the sea spray needed to be 10^2 to 10^3 times more concentrated than the local seawater to explain the levels of Pu present in the coastal vegetation.

Cambray & Eakins suggested that a similar transfer must be occurring from

the Irish Sea to explain the levels of radioactivity accumulated in soil in Cumbria, U.K. [7][8]. They measured levels of ^{238}Pu, $^{239+240}$Pu and ^{241}Am much in excess of those expected from nuclear fallout and which could not be explained by considering the direct atmospheric emissions from Sellafield. The excess Pu and ^{241}Am in the soil diminished with distance inland, suggesting a source from the seaward direction. Also, the Pu isotopic ratio, ^{238}Pu : $^{239+240}$Pu, in the samples near the coast was similar to that present in effluent discharged from Sellafield into the Irish Sea. The more inland soil samples had a ratio indicative of nuclear fallout. Again the explanation was that radionuclides discharged into the sea were, in some way, being returned to the land. From an estimation of the deposition rate of sea salt at the coast and the radionuclide levels present at sea, these authors, too, noted that an enrichment of 2 to 3 orders of magnitude in sea spray concentration over that of the seawater was required to explain the amount of Pu and ^{241}Am present in the coastal soil.

Thus, by the early 1980s, it finally became clear that there was a previously disregarded pathway of industrial radionuclides into the human environment. Subsequent study of this sea-to-land transfer has concentrated on determining the nature of the transfer mechanism, the rate at which radionuclides are coming and can be expected to come ashore in future, and the extent of the penetration of the contaminated sea spray inland from the coast. I will discuss this work and the relevant conclusions which can be drawn from it in the following sections.

1.3.1 Mechanism of the sea to land transfer

The mechanism whereby radionuclides in the sea can become airborne to be blown inland is thought to be due to bubble-bursting at the sea surface. Air bubbles rising through the seawater can scavenge some of the particulate material present and transport it to the surface, where the bubbles burst. The particulate material can become incorporated into the spray droplets produced in the bursting process and so become airborne. Interestingly, the mechanism of bubble-bursting was proposed by Horrocks in 1907 to explain the transport to air of bacteria from sewers [36].

The surf zone along the shoreline is an area of intense bubble production,

as air entrapped by breaking waves returns to the surface. This appears to be the region where the major part of the contaminated sea spray originates [18]. Eakins et al. exposed a muslin screen sea spray collector seaward of the surf zone simultaneously with another screen 100 m away, placed 20 m landward of the surf, on a day of relatively strong onshore winds. The land screen, on analysis, was found to have collected 0.83 Bq of $^{239+240}$Pu, compared to 0.015 Bq collected by the sea screen. Around 98% of the $^{239+240}$Pu coming ashore appeared to have been injected into the atmosphere in the surf zone. Also the ratio ^{241}Am : $^{239+240}$Pu found on a series of screens after exposure at different sites along the Cumbrian coastline correlated closely with that present in the sediment suspended in the seawater collected from the surf zone at the time of the exposures [18]. In all the seawater samples more than 90% of the actinides was associated with the suspended sediment.

Sea spray droplets are also produced further out at sea in whitecaps produced by the action of the wind on the water. Radioactivity may, therefore, also become airborne in areas of the sea far from the breaking surf, but this process is thought to be of less importance in the sea to land transfer of radioactivity [19]. The sediment suspended in the seawater carries the majority of the actinides, and as suspended loads are much less at sea than in the surf zone, spray produced at sea will contain a much smaller concentration of contaminated sediment.

This production mechanism, whereby the radionuclides become airborne as a result of bubble-bursting, can also account for the enriched concentrations of radionuclides found in sea spray compared to the seawater from which it is produced. Eakins et al. produced bubbles artificially in the laboratory under the surface of seawater samples taken from the surf zone at Eskmeals, and collected the spray droplets produced [18]. These experiments illustrated that bubbles rising through water and bursting to produce spray preferentially transfer the smaller suspended particles to the droplets. Spray produced by bubble-bursting will therefore contain a greater proportion of smaller particles than the seawater from which it has been produced. Radionuclides are known to be present in increased specific activity on particles of smaller diameter. Thus sea spray can be expected to have a higher concentration of radionuclides than the seawater

[18].

There has been some doubt about the magnitude of the enrichment factor, the ratio of the concentration of radionuclides in the spray to the concentration in the seawater. Large predictions of enrichment in early papers mentioned above have given way to more conservative and likely estimates. Eakins & Lally estimated enrichment factors of 10–20 for Pu and ^{241}Am and 1–3 for ^{137}Cs [19]. Eakins et al. report finding enrichments of this order in their laboratory studies [18]. Pattenden et al., comparing the spray depositing near the high-water mark with seawater collected in the surf zone, determined enrichments of 2–4 for Pu, ^{241}Am and ^{137}Cs [63]. The larger enrichment factors proposed by earlier workers were produced either by considering the spray concentrations relative to seawater collected offshore, and therefore not particularly indicative of conditions in the surf zone, or by comparing the spray to samples of filtered seawater, from which most of the actinides will have been removed, thus exaggerating the enrichment factors (as in Cambray & Eakins [8]).

1.3.2 Measurements of radioactivity in airborne particulate material in Cumbria

In this section and the one following, I will discuss reported results of measurements made of the activity concentrations of Sellafield radionuclides in airborne particulate material and being deposited in the coastal regions of Cumbria.

Pattenden et al. reported results obtained with a high-volume aerosol sampler set up 300m from the high-water line at Eskmeals [62]. The collection filter was changed monthly from November 1978 to October 1979. Table 1.1 gives the mean air concentrations of some radionuclides measured over the 12 month period at Eskmeals and at Milford Haven, a background site far from Sellafield, were only nuclear fallout was being collected. The ^{238}Pu :$^{239+240}$Pu isotopic ratio present in nuclear fallout is 0.05. The ratio of 0.24 present in the particulate material collected at Eskmeals is significantly higher and similar that in the marine discharges from Sellafield. The highest air concentrations determined in a one month period during the entire sampling period at Eskmeals (not necessar-

Nuclide	Annual Mean Air Concentration (μBq m^{-3})		Highest monthly mean air concentration at Eskmeals (μBq m^{-3})
	Eskmeals	Milford Haven	
^{241}Am	2.0	—	4.2
$^{239+240}$Pu	4.2	0.3	10.9
^{238}Pu	1.0	—	2.4
^{137}Cs	61	11	521
^{106}Ru	122	52	635

Table 1.1: Radionuclide air concentrations measured 300 m from high-water at Eskmeals (Pattenden et al [62])

ily in the period November 1978 to October 1979) are also given in Table 1.1. These peak monthly results are themselves averages over long time periods, and it is reasonable to assume that there will have been short periods when much higher airborne concentrations will have occurred. The ^{241}Am : $^{239+240}$Pu ratio in these collections at Eskmeals was 0.48, while the average ^{241}Am : ^{137}Cs ratio was 0.03. The authors noted that the aerosol sampler had a much reduced collection efficiency for particles of greater than 20 μm diameter.

Fry et al. reported on measurements made with an air sampler at Seascale during 1981 [27]. The annual mean air concentrations of $^{239+240}$Pu and ^{241}Am were 4.6 μBq m^{-3} and 2.4 μBq m^{-3}. These agree very closely with the annual means quoted by Pattenden et al. and given in Table 1.1. The mean annual air concentrations of the γ-emitters at Seascale was in the range 300–600 μBq m^{-3}.

McHugh & Hetherington reported on much more short-term collections of airborne particles at 5 sites along the Scottish Irish Sea coast, within 50m of the shoreline [51]. The collections were made with an aerosol sampler operated unsheltered to allow collection of all particles, irrespective of size, and lasted

Site	^{241}Am μBq m^{-3}	$^{239+240}$Pu μBq m^{-3}
1	2.50 ± 0.12	2.65 ± 0.14
2	0.47 ± 0.03	0.36 ± 0.03
3	1.25 ± 0.10	1.30 ± 0.10
4	0.25 ± 0.02	0.25 ± 0.02
5	0.75 ± 0.06	0.69 ± 0.06
Lowestoft	0.13 ± 0.01	0.17 ± 0.02

Table 1.2: Radionuclide air concentrations measured at 5 sites on the Solway coast within 50 m of high-water (McHugh & Hetherington [51])

between 3 and 24 hours. A background collection far from Sellafield was also carried out, at Lowestoft, to assess the contribution likely to be from nuclear fallout. The air concentrations of $^{239+240}$Pu and ^{241}Am estimated from the activity on the filters are given in Table 1.2. The mean ratio ^{241}Am : $^{239+240}$Pu was 1.0. The air concentrations at the five sites varied over an order of magnitude and were at most 19 times that at Lowestoft. The highest air concentrations measured by these workers were of a similar order to those measured on the Cumbrian coastline discussed above. The ^{137}Cs and ^{106}Ru activities in the collected samples were below the detection limit of the γ-ray counting system used to analyse the filters.

Eakins et al. reported air concentrations obtained by exposing muslin screen collectors for short periods of about one hour at distances of 15–120m from the sea [18]. Table 1.3 gives results of the air concentration of $^{239+240}$Pu, ^{241}Am and ^{137}Cs obtained in 1980 on 7 occasions at Eskmeals and on one occasion at St. Bees, of interest here because of the large amount of activity collected. The air

concentrations were estimated by dividing the activity collected on the screen by the air volume considered to have passed through each screen, and assuming that the screen collected the droplets with an efficiency of 20% (See Section 1.6).

These radionuclide air concentrations are generally higher than those quoted above. Muslin screen collectors, however, are thought to collect larger spray droplets more efficiently than the aerosol samplers used by the other workers [18]. The St. Bees exposure was made at a time of very heavy surf and windborne spray was clearly visible as a mist blowing across the foreshore. The higher radionuclide air concentration determined from this exposure can be regarded as indicating the radionuclide air concentrations possible under extreme sea and weather conditions. It is interesting that not only increased air concentrations of $^{239+240}$Pu and ^{241}Am, thought to be preferentially transferred inland in sea spray, were found in this measurement. The air concentration of ^{137}Cs was also much greater at St. Bees on this occasion, illustrating that this radionuclide is also being transported inland in significant amounts by the sea spray transfer mechanism.

The mean ^{241}Am : $^{239+240}$Pu ratio collected on these exposed muslin screens ranged from 0.42 to 0.87. The ^{241}Am : ^{137}Cs ratio ranged from 0.08 to 0.28, with a mean value of 0.16 ± 0.02, higher than that found by Pattenden et al.

1.3.3 Measurements of radioactivity in deposited material in Cumbria

Measurements of the levels of radioactivity deposited on artificial collectors have also been performed in Cumbria. Pattenden et al. collected both wet and dry depositing material on a 40 cm diameter funnel draining into a 25l plastic bottle, positioned 300m from the high-tide mark at Eskmeals [62]. The collection bottle was changed monthly from November 1978 to October 1979. Table 1.4 gives the total deposit in the course of the year and compares this to deposits collected at Milford Haven. The isotopic ratio of ^{238}Pu : $^{239+240}$Pu in the deposits was 0.22, again indicative of material originally discharged into the sea. The highest deposits of each radionuclide in a one month period throughout the whole sampling

Exposure Name	Radionuclide air concentrations (μBq m^{-3})			Wind speed m s^{-1}
	$^{239+240}$Pu	^{241}Am	^{137}Cs	
Eskmeals 1	3.1	1.4	< 9.4	2.3
Eskmeals 2	15.2	6.4	75.9	5.8
Eskmeals 3	22.4	10.3	60.4	5.4
Eskmeals 4	22.0	9.0	72.6	6.8
Eskmeals 5	33.1	12.9	139.1	7.0
Eskmeals 6	30.9	26.9	95.8	5.9
Eskmeals 7	28.1	23.6	104.0	5.8
St Bees	797.4	574.1	2950.2	6.9

Table 1.3: $^{239+240}$Pu, ^{241}Am and ^{137}Cs air concentrations measured 15–120 m from the sea with muslin screen collectors (Eakins et al. [18])

Nuclide	Annual Deposit ($Bq\,m^{-2}$)		Highest monthly deposit at Eskmeals ($Bq\,m^{-2}$)
	Eskmeals	Milford Haven	
^{241}Am	11.5	—	2.2
$^{239+240}Pu$	39.5	0.1	7.0
^{238}Pu	8.5	—	1.5
^{137}Cs	118	13	70
^{106}Ru	274	78	363

Table 1.4: Radionuclides deposited 300 m from the high-water mark at Eskmeals (Pattenden et al [62])

period are also given in Table 1.4. These peak deposits did not necessarily occur during the 12 month period from 11/78 to 10/79.

In a later report, Pattenden et al. discuss measurements made with their deposition collectors simultaneously at five sites along a transect inland from the sea [63]. This transect was positioned in northern Cumbria, its sea-ward end being at Silecroft, approximately 40 km along the coast to the north of Sellafield. Table 1.5 gives the depositing radioactivity at the site closest to the sea, 20m from the high-water mark, in the 12 months from October 1980 to September 1981. These results are all significantly higher than those in Table 1.4, possibly simply due to the fact that the collections were performed much closer to the high-water mark than at Eskmeals.

1.3.4 Penetration inland of the contaminated sea spray

Fraizier et al., in their studies of radioactivity in lichen collected from a coastal site in Normandy, found that the $^{239+240}Pu$ activity in a sample collected over 1 km from the coast was 17% of that in a sample collected 5 m from the shoreline

Nuclide	Annual deposit ($Bq\,m^{-2}$) Transferred inland from sea	Expected from Nuclear Fallout
^{241}Am	30.5	0.1
$^{239+240}Pu$	57.8	0.3
^{137}Cs	624	24
^{106}Ru	355	143

Table 1.5: Radionuclides deposited 20 m from the high-water mark at Silecroft (Pattenden et al. [63])

[26]. This agrees well with the work of Martin et al. in the analysis of coastal vegetation in the same region, who found that the levels of $^{239+240}Pu$, ^{238}Pu , ^{137}Cs and ^{106}Ru in samples collected 1 km inland were 10–30% of those present in vegetation at the high-water mark [49]. Soil cores collected along a transect inland from the sea in Cumbria by Cambray & Eakins showed that the levels of $^{239+240}Pu$ and ^{241}Am transferred inland from the sea were reduced by 50% between 50 and 500 m [8]. Pattenden et al. found that the annual deposit of $^{239+240}Pu$ and ^{241}Am of marine origin at 500 m inland was 11% of that deposited 20 m from the high-water mark, falling to 1% at 2.4 km [63]. Eakins & Lally found that the $^{239+240}Pu$ collected on a muslin screen exposed 1000 m from the Irish Sea was only 3% of that collected on a screen exposed simultaneously 5 m from the high-water mark [19]. With several screens exposed at the same site at different times, as the sea advanced up the beach, the same authors found that the $^{239+240}Pu$ collected when the mean sea to screen distance was 530 m was 16% of that when the sea to screen distance was 23 m.

There is thus a broad agreement in these results from the Normandy coastline made by Fraizier et al. and Martin et al. and those from the Cumbrian coastline.

The activity levels of radionuclides being transferred inland decrease rapidly with distance, being reduced to the order of 10% in the first 1000 m of travel.

Other measurements indicate that the sea spray borne radioactivity can be detected at large distances from the sea. Cambray & Eakins found that levels of $^{239+240}$Pu and ^{241}Am in the soil cores taken 20 km inland were still in excess of those expected from nuclear fallout [8]. Pattenden el al. found that even at 17 km from the sea, the levels of radioactivity depositing were still 4–8 times the expected fallout contribution [63]. The excess could not be explained by taking into account the expected contribution of radionuclides from the atmospheric emissions from Sellafield. Eakins el al. performed analyses on sheep faeces collected in northern England to study the current deposition of Pu on the vegetation being eaten by the sheep [20]. The $^{239+240}$Pu levels in samples collected at Shap, 60 km inland, were double the baseline value reached further inland. From the Pu isotopic ratio this $^{239+240}$Pu could be associated with the Sellafield marine discharges.

The conclusion to be drawn from the results of these studies is that although the inland transfer of radionuclides in sea spray seems to result in a rapid reduction in intensity close to the sea, significant levels of marine discharged radionuclides are still transported to large distances inland.

1.3.5 Comparison with safety limits

There has been a recent reduction in the International Commission for Radiological Protection (ICRP) recommended principal dose limit which should be received by members of the general public. The annual recommended dose limit was reduced from 5 to 1 mSv [38].

Eakins et al. used 5 mSv as the limit of significance for measuring health detriment to the public, and calculated that the upper limit for the air concentration of actinides is 4440 μBq m^{-3} [18]. Actinides are of greatest significance in terms of radiation exposure from inhaled radioactivity.

More recently, authors have taken into consideration the reduced ICRP recommendation of 1 mSv [38][51]. Beyond this, BNFL have set themselves a desired upper limit of exposure of the general public of 0.5 mSv [4]. This was after advice

to the company by both the Radioactive Waste Management Advisory Committee and the National Radiological Protection Board (NRPB). This limit would require the reduction of the maximum permissible actinide air concentration from the level quoted by Eakins et al. to 444 μBq m^{-3}, if a simple correction factor of 10 is assumed to be valid.

The average actinide concentrations measured on the Cumbrian coast (e.g. Table 1.1) are the order of 2% of this limit. However, the sum of the air concentrations of $^{239+240}$Pu and ^{241}Am estimated by Eakins et al. from the muslin screen exposure at St. Bees (See Table 1.3) is a factor of 3 greater than the limit set for themselves by BNFL, and 1.5 times the new limit set by the ICRP. Conditions producing such levels may be quite rare, and not all of the airborne radioactivity will be present in droplets of diameter less than 5 μm. A fraction of the activity, therefore, will not be respirable and so will not contribute to the inhalation dose. It seems certain, however, that in some sea and weather conditions the general public living close to the W. Cumbrian coastline will be exposed to air concentrations of actinides, carried inland in sea spray, which are in excess of current ICRP and NRPB recommended limits.

1.4 Production and transport of sea spray

1.4.1 Production mechanisms and aerosol size distributions

It is generally believed that the major source of the sea-salt aerosol is in bubble bursting at the sea surface [3][80]. The most intense areas of bubble production are in breaking waves, caused either by the action of the wind on the water or along the shoreline, in the surf zone. A breaking wave entrains a large volume of air into the sea, and the produced air bubbles rise to the surface. Bubbles produced below a critical depth will go into solution before reaching the surface, while those which reach the surface burst and eject water droplets into the air. Any particulate material in the sea scavenged by the rising bubble can become airborne in the droplet produced when the bubble bursts at the surface.

The size range of the spray droplets produced in breaking waves, by the action of bubble bursting, range from 0.1 to 150 μm [23]. Gathman has discussed the observable aerosol at a coastal site in terms of three distinct particle populations [30][31]. The smallest class, with diameters less than 0.1 μm, is a background component and is not of local origin. Its concentration can be related to the characteristics of the air mass containing it. The second class of aerosol is populated by marine aerosols which have been produced in earlier high wind conditions and which are well mixed in the marine boundary layer. The concentration of this aerosol is more closely related to wind speeds in the previous 24 hour period than to the current conditions. The third class contains droplets of mostly local origin. The concentration in the air is closely dependent on the current wind speed and local white-water conditions.

Gathman represents the aerosol size distribution in terms of three overlapping log-normal distributions, one for each of the above population classes. The largest class, of local origin and of most interest here, is thus fitted by a profile of the form:

$$\frac{dN(D)}{dD} = A_3\, exp(-(log\frac{D}{D_0})^2) \tag{1.1}$$

where dN(D) is the number of particles with diameters between D and D+dD. Gathman gives the mode diameter D_0 for the largest aerosol a value of 4 μm, and accepts the possibility that this could shift to higher values in increased wind speeds [72]. The amplitude A_3 scales the number of droplets in the air and is very dependent on the current wind speed. The spray volume distribution is thus of the form:

$$\frac{dV(D)}{dD} = A_3\,\frac{\pi}{6}D^3 exp(-(log\frac{D}{D_0})^2) \tag{1.2}$$

Thus dV(D), the volume of spray contained in droplets with diameters in the range D$\rightarrow$D+dD is given by:

$$dV(D) = A_3\,\frac{\pi}{6}S(D)\,dD \tag{1.3}$$

where S(D) is given by:

$$S(D) = D^3\, exp(-(log\frac{D}{D_0})^2) \tag{1.4}$$

A volume distribution of this form is used to represent sea spray droplets produced by breaking waves in the model of the sea-to-land transfer described in Chapter 4.

1.4.2 Measurements of sea spray over land

It is of interest here to consider the results of measurements of sea spray concentration on land. Studies have been performed on coasts all around the world. A range of sea spray collection and analysis techniques have been utilised. Measurements have been performed in a wide range of wind speeds, up to 100 mph ($44\,\mathrm{m\,s^{-1}}$) in one instance [72].

Several studies of the airborne sea spray at coastal sites have been performed. Boyce exposed cheese-cloth screens attached to wire frames on the Carolina coast of the USA with the aim of indicating the relative concentration of sea spray at different sites [5]. The exposed cloths were washed in distilled water and the chlorinity of the solutions determined by titration with silver nitrate. Fujiwara & Umejima exposed cotton gauze screens along lines going inland from the Japanese coast and determined the Cl trapped [28]. Petrenchuk collected bulk aerosol samples by pumping air through filters along the coasts of the Black, Barents and Baltic Seas [67]. More recently Exton et al. and Smith et al. performed measurements using aerosol spectrometers which scatter laser light off suspended particles to determine the size spectra of droplets present in sea spray [23][72]. These measurements were performed on a beach on South Uist in the Western Isles, off the Scottish coast.

There have also been studies of sea-salt sedimentation rates inland. Malloch collected sea-salt deposition into polythene tubes stuck into the ground in Cornwall, U.K. [48]. Williams & Moser determined sea-salt sedimentation onto petri dishes [79]. The dishes were washed and the solution analysed for Na using flame photometry.

These studies have shown that the amount of sea spray present in the air at a site close to the surf zone varies over a wide range. The wind speed at the time of the measurement is a major factor in the volume of sea spray coming ashore. Fujiwara & Umejima found that the salt on their screens increased by

a factor of 100 as the wind speed increased from 3 to 13 $m\,s^{-1}$ [28]. Petrenchuk found a similar change in airborne sea spray concentrations over this wind speed range in measurements on the Black Sea coast, but found a less rapid increase in spray concentration at the higher wind speeds on flatter and more sandy beaches [67]. Boyce reports salt levels increasing by a factor of 4 as winds increased over 7 $m\,s^{-1}$ [5]. Malloch found increased sea-salt deposition only with wind speeds over 14 $m\,s^{-1}$ [48]. The relationship between sea spray transfer inland and wind speed thus varies greatly at different sites. Even in repeated measurements taken at a single site however, there will be no clear relationship between the measured sea spray being collected inland and the current wind speed. The wind speed in the previous 24 hours or so, and the wind direction will affect the salt mass being transferred inland from the sea at a particular time.

Fujiwara & Umejima measured a very rapid reduction in the sea-salt collected on their screens over the first 100 m inland from the sea [28]. Hama & Takagi estimated that 80% of the incoming spray deposited in the first 300 m [33]. Malloch found the deposited salt levels to fall to 10% of the seashore level at 500 m inland, with little further reduction after 2 km [48]. Petrenchuk found great variability in salt loading at the shore, while 2 km inland the salt concentrations were relatively constant [67]. The same author also found different penetration inland at different sites and concluded that the propagation of spray from the sea is determined in substantial measure by the topography of the coastal zone and by the peculiarities of the wind regime in a particular area.

1.5 Fallout of radioactivity from the Chernobyl accident

Some of the measurements performed in the course of this study were affected by the release of radioactivity from the nuclear reactor accident at Chernobyl in the USSR. The accident occurred at around 23:30 GMT on Friday 25^{th} April 1986. The radioactivity released the following day, after travelling along a circuitous path over Europe was finally detected over Britain on Friday 2^{nd} May [71]. The passage of the radioactive plume coincided with very heavy rainfall in areas of

N.Wales, Cumbria and S.W.Scotland and very significant levels of radionuclides were washed to the ground.

The highest level of deposited radioactivity in Britain, 10 000 Bq m^{-2} of ^{137}Cs, was found at Holm Rook in Cumbria [9], a village less than two miles from the collection sites used in the present study. It was therefore not surprising that in collected vegetation samples the levels of ^{137}Cs, ^{134}Cs and ^{106}Ru of Sellafield origin had been swamped by the input of radioactivity deposited from the Chernobyl plume.

The ratio of ^{137}Cs :$^{239+240}Pu$ in airborne particulate material collected at Harwell in early May 1986 was measured as 6×10^5 [9]. Very low levels of the actinides Pu and ^{241}Am released from Chernobyl are therefore thought to have reached Britain to be deposited in the rainfall. The concentrations of these actinides in the collected vegetation samples are not thought to have been significantly increased by the deposition of Chernobyl released radioactivity.

1.6 Muslin screen collection efficiency

During the course of this study pieces of muslin cloth were exposed close to the Irish Sea to collect the sea spray droplets being carried inland by the wind. The muslin cloth used was chosen to be identical to that used in other studies of the sea-to-land transfer of radioactivity in Cumbria [18][19].

The efficiency with which the exposed screens extract the spray droplets and salt particles from the air passing through them will vary with the size of the particles and the wind speed. Little is currently known about the collection characteristics of such collectors, although they have been used in a similar fashion for many years (e.g. [5][28][60]). A better knowledge of the collection efficiency of the screens for particles of varying diameters, in different wind conditions, will shed further light on the data being presented here. Such a study is currently being carried out in the E&MS section at Harwell [53]. Here I will consider the information which can be obtained from the literature to aid in an approximation of the collection characteristics of the screens.

Parkin et al. collected airborne dust in the North Atlantic by exposing terylene

screens on board ships [60]. From a theoretical analysis these workers calculated that these screens should have a collection efficiency of 50% in 7 ms^{-1} winds, for dust particles of diameter greater than 7 μm and a relative density of 3. The collection efficiency was expected to fall to 25% for particles of diameter 2 μm, 7.5% for 1 μm particles and to be zero for particles of diameter less than 0.5 μm. Less dense particles would be expected to be collected with a reduced efficiency.

Eakins et al. exposed a piece of muslin identical to the cloth used in the present study on a beach close to the Irish Sea beside a screen similar to the one described by Parkin et al. [18]. In a wind speed of 4 ms^{-1}, the muslin collected an activity equivalent to 40% of that collected by the Parkin-like screen. If the assumption is made that this reduced efficiency is similar over the entire droplet size range, then droplets over 7 μm diameter will be collected at 20% efficiency by this muslin and droplets of size 2 μm will be collected at 10% efficiency. Eakins et al. also found that, contrary to what might be expected, the collection efficiency of the muslin screens reduces in higher winds, because the open area of the cloth increases as it is stretched [18].

1.7 ^{7}Be in the Atmosphere

Significant levels of the radionuclide ^{7}Be were found in the vegetation samples collected in the course of this study and on the muslin screens after their exposure. ^{7}Be is a naturally occurring radionuclide, of half-life 53.3 days, produced in the atmosphere by cosmic ray spallation of nitrogen and oxygen. As the concentrations of ^{7}Be in the collected samples have been of use in the analysis of the results of this study, a short discussion of the behaviour of this radionuclide in the atmosphere will be presented.

The rate of production of ^{7}Be in the atmosphere is a function of the product of the flux of low energy neutrons produced by incoming cosmic rays and the air density. There is a broad layer of maximum production at an altitude around 12 km which, depending on latitude and time of year, is positioned either in the upper troposphere or lower stratosphere [44]. The Earth's magnetic field deflects incoming cosmic rays towards the poles and so the rate of production is greater

Aerosol Size Range (μm)	Percentage of associated ^{7}Be
< 1.1	81.5 ± 3.0
1.1–2.0	8.3 ± 2.3
2.0–3.3	3.5 ± 1.1
3.3–7.0	3.1 ± 1.5
> 7.0	3.6 ± 2.5

Table 1.6: Percentage of ^{7}Be associated with different sized aerosol in surface air. (Data from Ludwick et al. [47])

at higher latitudes. The rate of production decreases with distance through the troposphere because of the attenuation of the cosmic rays, falling by a factor of about 200 between the tropopause and the surface [68]. The tropospheric production is thought to change relatively little with increasing latitude [44].

On production, the ^{7}Be rapidly becomes attached to the particulate material present in the atmosphere. The ^{7}Be-bearing aerosol in the stratosphere has a size $\leq 0.1\mu$m, and is thought to have a residence time above the tropopause of 1 year, much in excess of the life-time of ^{7}Be. Except for the regular, but infrequent, injections of stratospheric air into the troposphere, e.g. in folding events, the flux of ^{7}Be to the surface is determined predominantly by the rate of production within the troposphere [75].

Ludwick et al. report on measurements of the size spectrum of the ^{7}Be-bearing aerosol in surface air [47]. Their results are reprinted in Table 1.6. These results show that around 80% of the ^{7}Be activity is associated with the sub-μm diameter aerosol in surface air, the other 20% being predominantly attached to particles of less than 10 μm diameter.

Table 1.7 gives some reported results of measured air concentrations of ^{7}Be at ground level. Due to incomplete mixing, the surface air concentrations are not typical of the troposphere, being a factor of at least 10 less than the mean tropospheric concentration [32]. Feely et al. found wide variation in the mean air concentration measured at 28 different sites [25]. Even between sites at a similar latitude, such as Beaverton, Oregon (46^{0} N 123^{0} W) and Rexburg, Idaho (44^{0} N 112^{0} W) the mean air concentration differed by a factor of 2, from $2664\,\mu\mathrm{Bq\,m^{-3}}$ to $5254\,\mu\mathrm{Bq\,m^{-3}}$.

The very high mean value quoted in Table 1.7 from the work of Shapiro et al. was measured in a particularly arid environment, with long periods between precipitation events allowing build up of ^{7}Be in the troposphere. The highest monthly air concentration recorded by these workers was $15\,\mathrm{mBq\,m^{-3}}$, almost twice their mean value. Air samples collected after rainfall were found to have the lowest concentrations of ^{7}Be.

Table 1.8 gives some results of measured ^{7}Be deposition rates. All workers report that the main mechanism of ^{7}Be deposition is by wash-out of the suspended ^{7}Be-bearing aerosol by precipitation. Olsen et al. found a high correlation between the deposition of ^{7}Be and ^{210}Pb, a radionuclide which is a daughter of ^{222}Rn which emanates from the ground [58]. The correlation between two radionuclides with such different sources is taken as evidence that scavenging by precipitation is the major deposition mechanism.

Also given in Table 1.8 are the average concentrations of ^{7}Be in rain, the assumption made that all the deposition was by wash-out. This will tend to over-estimate the concentrations in rain as there is likely to be a dry depostion component in the fallout. Olsen et al. measured both wet only and bulk ^{7}Be deposition and found that dry deposition accounts for about 10% of the total fallout [58].

Significant and repeated seasonal variations in the level of ^{7}Be present in air and rain have been measured by almost all workers. The ratio of peak level to trough is typically around 2 [17][25][32], but values of around 5 and over have also been reported [25][59][64]. The timing of the peak levels, often in the spring in the Northern Hemisphere, agrees well with increases in the tropospheric inventory

of ^{7}Be due to folding of stratospheric air into the troposphere [17][59]. Other workers have explained the seasonal variation in their data by considering the lifting of the tropopause in summer, thus increasing the rate of production in the troposphere [37][75]. Feely et al., however, from analysis of their great amount of data, contend that no single factor is predominant in influencing the level of ^{7}Be in air at the surface [25]. They propose that local meteorological conditions, such as varying levels of precipitation and tropospheric mixing, can have a large effect on the measurements of ^{7}Be at a site, often totally disguising the seasonal increases in the inventory of ^{7}Be in the troposphere.

Several workers have measured ^{7}Be concentrations in air and deposition at coastal sites and at sea [15][76][81][82]. No mention has been made of the possibility of ^{7}Be transfer from water to air, subsequent to its deposition in the sea, having an effect on measured air concentrations. Wagenbach et al. in measurements 6 km inland in Antarctica found that the suspended sea salt aerosol reached an annual peak in the local autumn, later than the ^{7}Be maximum in summer [76].

This review of the data concerning ^{7}Be in the atmosphere shows that the instantaneous levels in air and rain are very variable at a site, changing with the time of year and the local meteorological conditions. The ^{7}Be levels differ greatly at different sites, making it difficult to estimate accurately the expected concentration at a point at any time.

Location	Latitude	^{7}Be Mean air concentration (μBq m^{-3})	Reference
Chilton, U.K.	51° N	2130	Peirson [64]
California, U.S.A.	34° N	8000	Shapiro et al. [69]
Washington, U.S.A.	46° N	4200	Crecelius [15]
Munich, W.Germany	49° N	3630	Hotzl & Winkler [37]
28 stations	80° N–90° S	2790	Feely et al. [25]

Table 1.7: Ground level air concentrations of ^{7}Be

Location	^{7}Be deposition rate (μBq m^{-2} s^{-1})	^{7}Be concentration in rain (Bq l^{-1})	Reference
Chilton, U.K.	29	1.4	Peirson [64]
Washington, U.S.A.	43	0.5	Crecelius [15]
Connecticut, U.S.A.	120	2.7	Turekian et al. [75]
Bermuda	90	1.7	Turekian et al. [75]
Maryland, U.S.A.	72	2.4	Dibb[17]

Table 1.8: Measurements of deposited ^{7}Be and typical concentrations in rainfall

Chapter 2

Experimental Methods and Techniques

In the course of this study, samples of indigenous vegetation were removed from sand dunes close to the West Cumbrian coastline. Also, muslin cloth aerosol collectors were exposed near the Irish Sea for periods ranging from 1 hour to over 1 month. All the vegetation and cloth samples have been analysed, in Edinburgh, for their radionuclide content by γ-ray analysis. The muslin screens were subsequently washed, and the chloride ion concentration in the resulting solution measured with the use of a Ion Specific Electrode. Thus the mass of sea-salt trapped on each screen during its exposure has been determined.

In this Chapter the details of the vegetation sampling and muslin screen exposure programme will be presented. The γ-ray analysis procedure for measuring the radionuclides present in a sample and the sea-salt measurement technique will then be described.

2.1 The sampling programme

2.1.1 Location of sampling sites

The vegetation collections and the muslin screen exposures were performed on the sand dunes of the beach at Drigg, which extends from 6 to 10 km south of the Sellafield discharge pipeline (Figure 2.1). This site was originally chosen because

of its easy access and the relatively large extent of sand dunes over which the proposed work could be performed. When secluded sites were sought for the long-term exposure of muslin screens, Drigg again proved to be ideal. The southern section of the beach is under the protection of Cumbria County Council as a Local Nature Reserve (LNR) and members of the public are discouraged from trespassing onto this region. Permission was given by the Warden of the LNR, allowing the setting up of muslin screen holders behind the fenced-off section of the sand dunes, an ideal site for undisturbed exposure for extended periods.

The grass collections and screen exposures were performed along 4 transects at different positions on the dunes, shown in Figure 2.2. The transects A, B, C and D extend to over 300 m inland from the high-water mark, along lines bearing 240° from magnetic north. This is the direction of the prevailing wind in this region. The topography of the sand dunes along the lines of the transects B, C and D was surveyed with a theodolite. Figures 2.3, 2.4 and 2.5 illustrate the relative position of each site, the height being relative to an arbitrary point at the bottom of the frontal dune. The positions of the grass collection and screen exposure sites on the transects are illustrated.

2.1.2 Marram grass collections

The first attempts to plot the inland penetration of the contaminated sea spray were performed by measuring the radionuclide content of samples of vegetation collected at different distances inland from the sea, after the work of Fraizier et al. [26] and Martin et al. [49].

It was necessary to collect the same plant species at the different distances from the sea because plants with different surface and leaf characteristics have different efficiencies for the collection of depositing pollutants and plants with different growth patterns will have varying retention properties [10,46]. Marram grass (*Ammophila arenaria*) was selected for this study as it grows over a large area of this dune system, from close to the high-water mark to around 350 m inland. The same sort of coverage could not be obtained with any other plant.

Sets of marram grass samples were collected along 3 transects across the dune system at Drigg on 6 occasions. Two collections were taken from each of the three

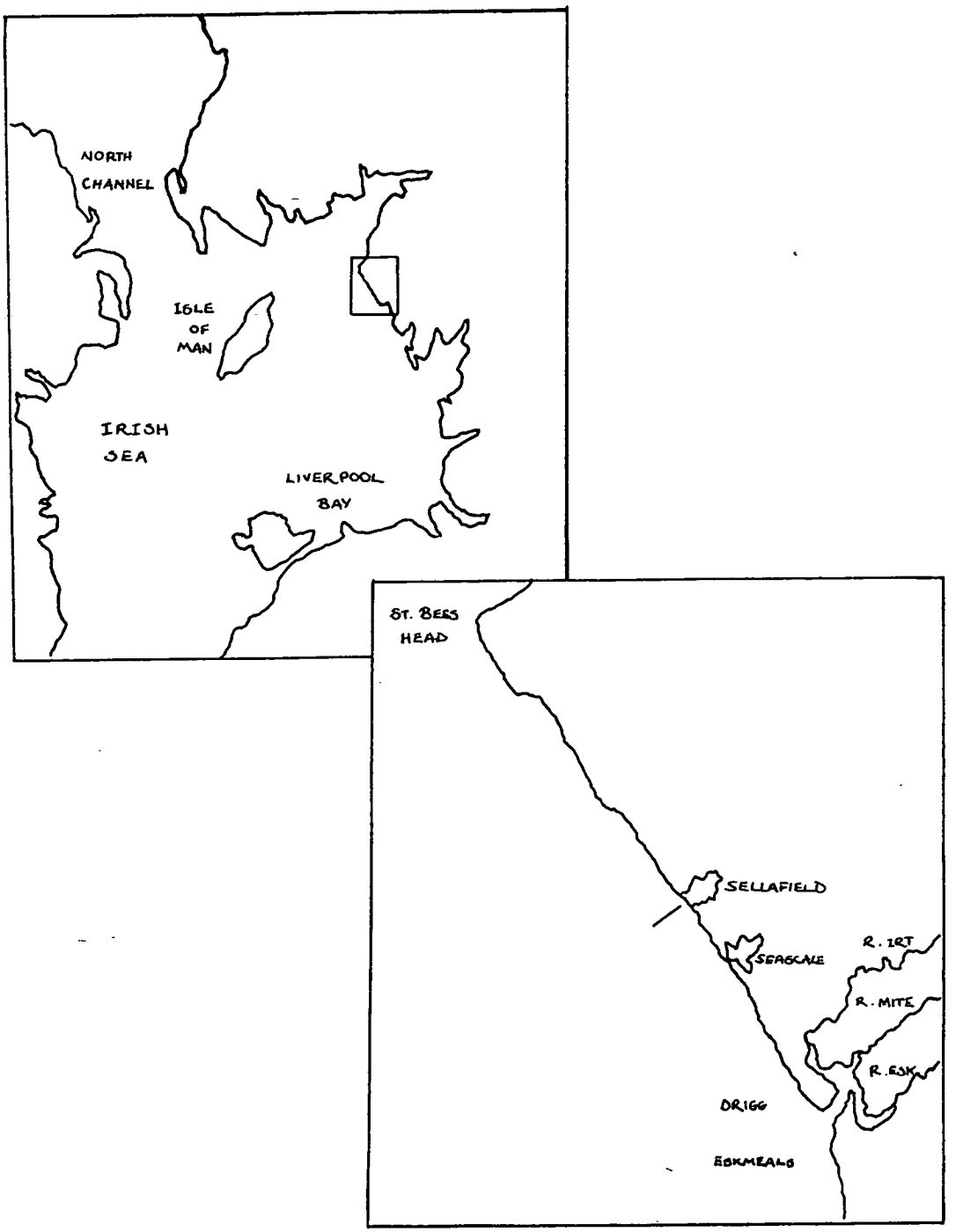

Figure 2.1: Maps of the Irish Sea illustrating the positions of the Drigg beach and the BNFL Sellafield discharge pipe-line

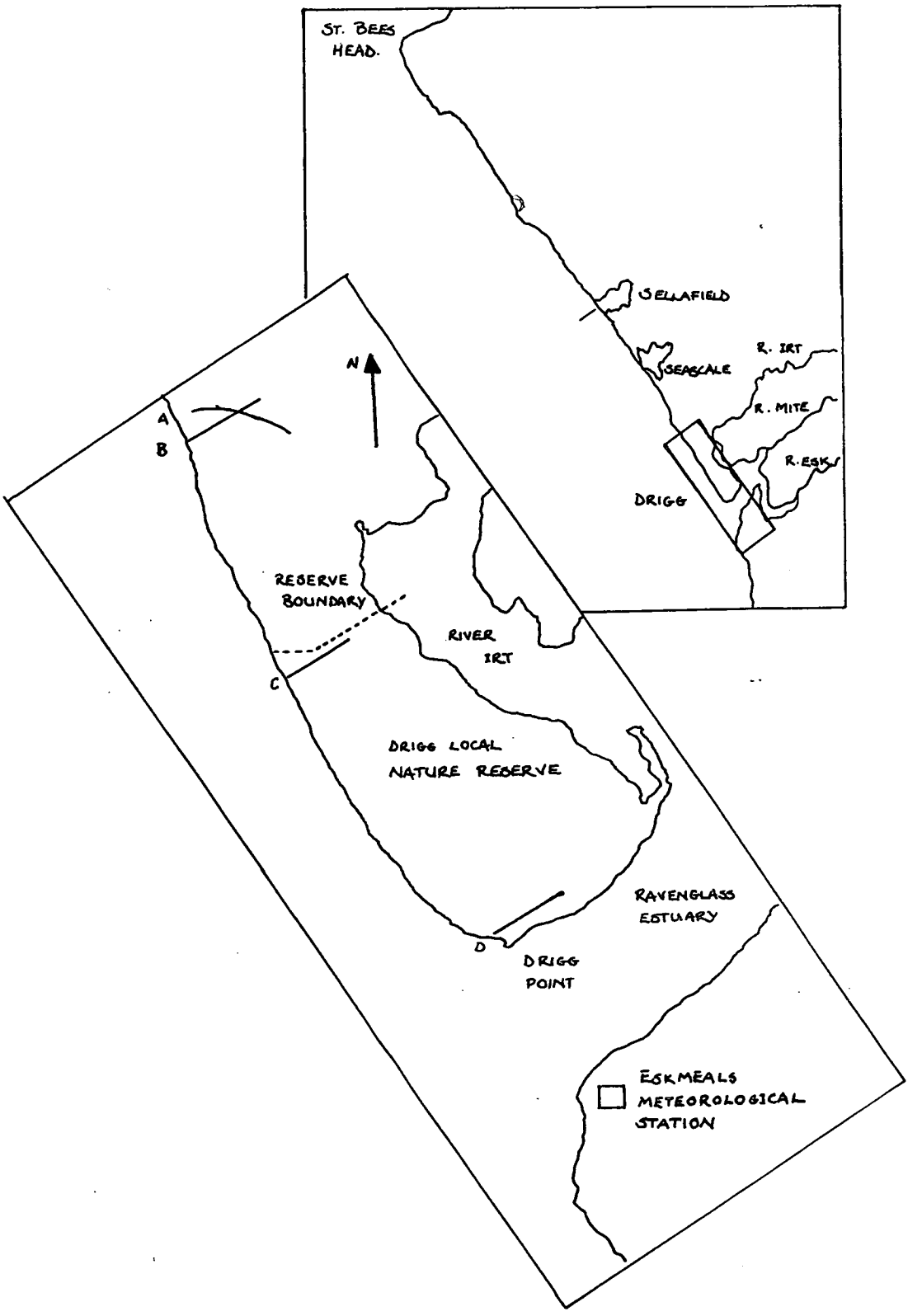

Figure 2.2: Map showing the relative positions of the sampling transects on the beach and the position of the Meteorological Office station at Eskmeals

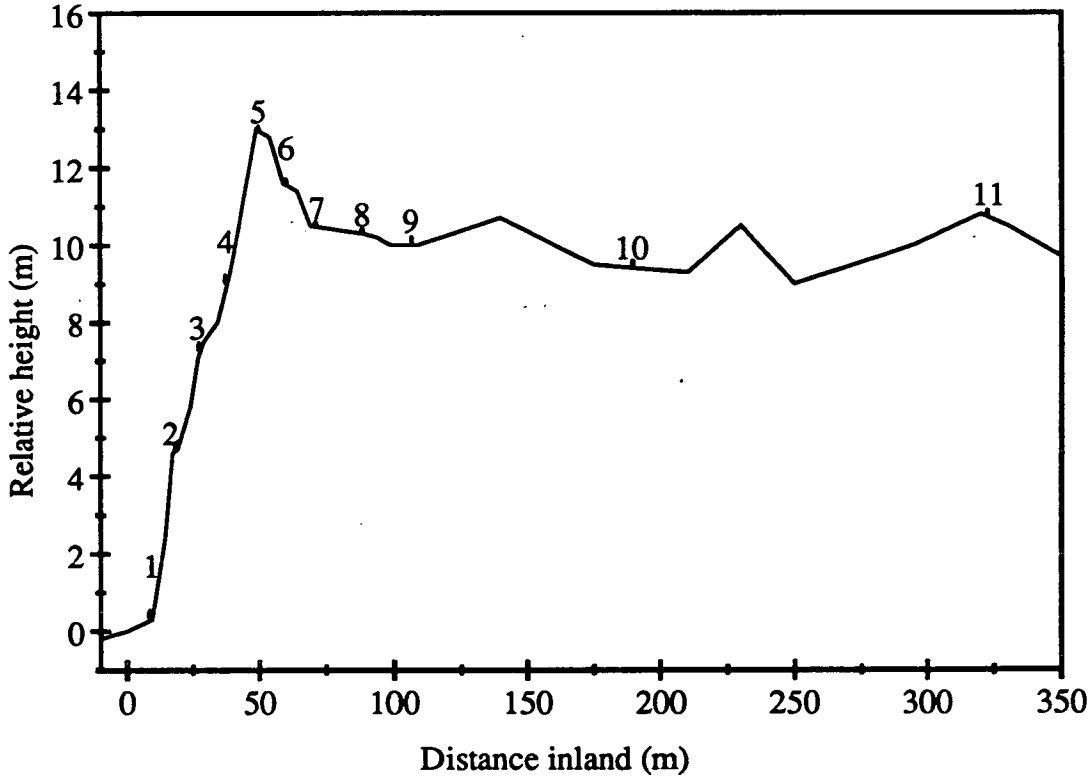

Figure 2.3: Survey along the transect at Drigg B showing the positions of the marram grass collection sites.

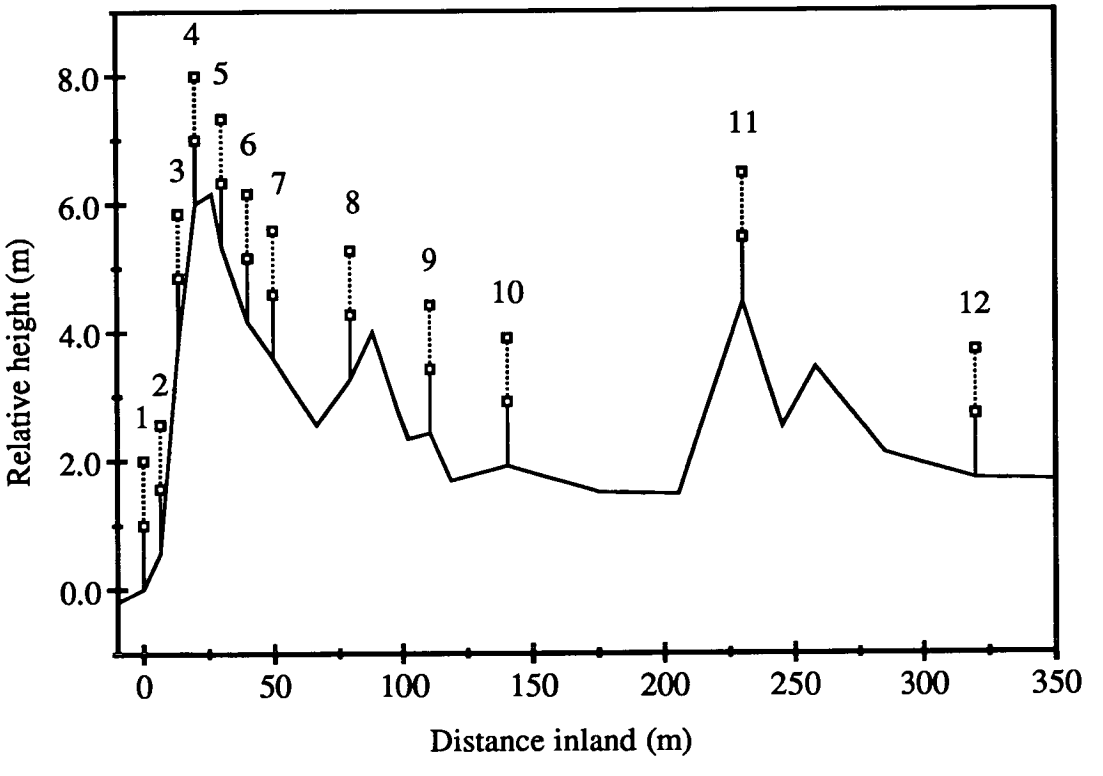

Figure 2.4: Survey along the transect at Drigg C showing the positions of the muslin screen exposure and marram grass collection sites

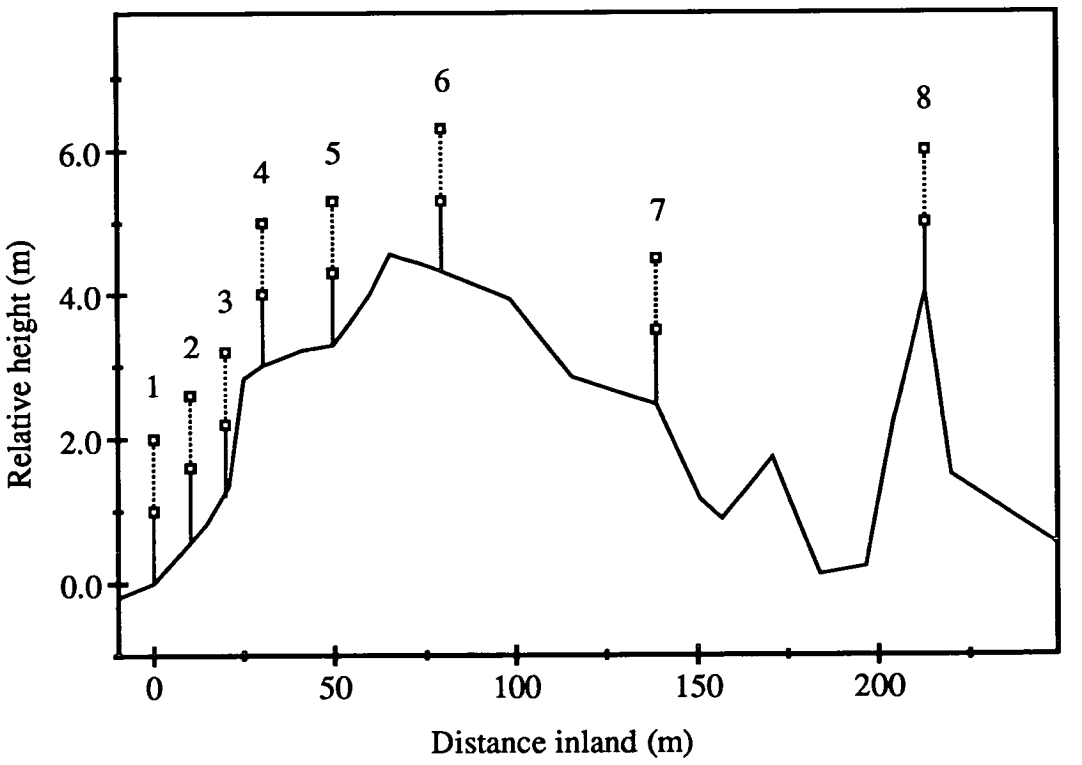

Figure 2.5: Survey along the transect at Drigg D showing the positions of the muslin screen exposure sites

transects A, B and C, as shown in Table 2.1.

Collection Marram A1 was not carried out by the author, but the single sample was obtained for analysis. Transect A is a line going inland from the site where the A1 sample was taken. This transect was not marked out before sampling and Figure 2.2 gives a representation of the line followed on this occasion. The distances of the collection sites along Transect A from the sea were approximated by eye. In all the later collections the transect was marked out along a straight line prior to collection and the position of each site relative to the high-water mark measured.

Different methods of grass collection were used on different occasions, however. In the grass collections performed along Transect B, all the grass within a measured area at the collection site, down to about 1 cm from the ground, was clipped. The collection regime followed in Drigg A2 was returned to in Drigg C1 and C2. Grass was taken from similar sized clumps around each of the collection sites. The grass was not clipped to the ground. Only top-most shoots were taken and herbage obviously from previous seasons was removed from the sample to ensure that similarly aged grass was collected along the transect.

The grass collections at Drigg C were performed around the sites used for the muslin screen exposures. No grass was growing around exposure site 1.

Prior to γ-ray analysis the collected vegetation samples were dried overnight in an oven at 80° C. The grass was then ground to a particle size of less than 0.7 mm and presented to the γ-ray detectors for analysis in perspex holders. The weight of analysed grass was measured.

2.1.3 Muslin screen exposures at Drigg C and D

The exposed muslin screens were cut from rolls of bleached muslin obtained from Evans' Textile Group, Manchester. The cloth is made from thread of approximately 0.2 mm in diameter and has holes sized around 0.25 mm^2. The cloth is identical to that used to make the muslin screens used in the sea spray work of Eakins et al. [18][19].

The screens exposed at Drigg C were stretched across rectangular wooden frames of dimension 80 by 62.5 cm. The screens therefore had an exposed area of

Transect	Collection Name	Date of collection	No. of samples
A	Marram A1	October 1985	1
A	Marram A2	5^{th} December 1986	5
B	Marram B1	27^{th} April 1987	11
B	Marram B2	3^{rd} July 1987	11
C	Marram C1	3^{rd} November 1987	11
C	Marram C2	6^{th} February 1988	11

Table 2.1: Details of the marram grass collections along the transects at Drigg

$0.5\,m^2$. The bottom of each screen was set between 0.8 and 1 m from the ground.

Seven sets of 12 screens were exposed along the Drigg C transect between 21^{st} March and 23^{rd} September 1988. Details of the dates of the individual exposures are given in Table 2.2.

Sets of muslin screens were also exposed for long periods along Transect D, near Drigg Point (Table 2.3). The muslin screens exposed here were stretched between two poles positioned approximately 2 m apart. The screens were 0.5 m high and were set up with their bottom edges approximately 1 m from the ground. Some of these exposures at Drigg D were carried out simultaneously with others at Drigg C.

In addition to these relatively long-term muslin screen exposures, some sets of screens were exposed for much shorter periods of around 1 hour. It was thought unlikely that enough sea spray would be collected in the course of these short exposures to allow measurement of the radionuclides present on the screens. An early test had shown, however, that measurable amounts of sea-salt could be

Exposure Name	Date put out	Date taken in	Time (Days)
Muslin C1	21/3/88	30/3/88	9
Muslin C2	30/3/88	20/4/88	21
Muslin C3	20/4/88	10/5/88	20
Muslin C4	10/5/88	7/7/88	58
Muslin C5	7/7/88	14/7/88	7
Muslin C6	14/7/88	17/8/88	34
Muslin C7	17/8/88	23/9/88	37

Table 2.2: Dates of the muslin screen exposures along the Drigg C transect

Exposure Name	Date put out	Date taken in	Time (Days)
Muslin D1	13/7/88	3/8/88	21
Muslin D2	3/8/88	17/8/88	14
Muslin D3	17/8/88	23/9/88	37
Muslin D4	23/9/88	22/10/88	29

Table 2.3: Dates of the muslin screen exposures along the Drigg D transect

Exposure Name	Date	Sites Used	Exposure Time (mins)
Muslin S1	30/1/89	1,4,5,6,7,8	90
Muslin S2	31/1/89	1,4,5,6,7,8	134
Muslin S3	1/2/89	1,4,5,6,7,8	130
Muslin S4	7/2/89	4,5,6,7,8	120
Muslin S5	8/2/89	4,5,6,7,8	113
Muslin S6A	9/2/89	4,5,6,7,8	60
Muslin S6B	9/2/89	4,5,6,7,8	76

Table 2.4: Details of the short-term muslin screen exposures at Drigg D

collected in such short periods.

Seven sets of screens were exposed along Transect D for periods ranging from 60 to 130 minutes, the details of which are given in Table 2.4.

2.1.4 Meteorological data during the exposures

It was not possible to record the weather conditions during the muslin screen exposures. There is, however, a Meteorological Office station at Eskmeals, across the Ravenglass Estuary from Drigg Point (Figure 2.2), and the weather data measured at Eskmeals for the periods covered by the screen exposures were obtained. These data included details of the hourly mean wind speed and direction, measured at a height of 10 m. The hourly rainfall and measurements of air temperature and relative humidity were also included. Thus, although no actual measurements were made at the sites themselves during the screen exposures, a good record of the weather conditions prevalent in the general region has been obtained and used in the analysis of the results.

2.2 Gamma-ray analysis

This section gives a brief description of the techniques which have been used to measure the concentrations of radionuclides in the collected vegetation samples and on the muslin screens after exposure.

Unstable radioactive nuclei become more stable by altering their proton to neutron ratio. The resultant nucleus is often created in an excited state and reaches its ground-state by emission of γ-ray photons. For instance, a ^{137}Cs nucleus changes into a stable nucleus, ^{137}Ba, by the capture of an orbiting electron. The ^{137}Ba nucleus is formed in an excited state and can reach its lowest energy ground-state by emission of a 661.7 keV γ-ray. (The fraction of the ^{137}Cs decays which result in the emission of a 661.7 keV γ-ray is known as the γ-ray branching ratio of the nucleus, b_γ). This 661.7 keV photon is characteristic of the ^{137}Ba energy levels and so is indicative of the decay of a ^{137}Cs nucleus. Measurement of the count-rate of 661.7 keV photons will allow determination of the number of ^{137}Cs nuclei present in the sample under analysis. The concentration of other radionuclides can be determined by measuring the count rates of other distinctive γ-rays produced in the sample (See Table 2.5).

2.2.1 Ge(Li) detectors

In this section I will give a description of the function of a Ge(Li) detector and how it has been used in this study to determine the levels of radioactive substances in the collected samples. A Ge(Li) detector contains a germanium crystal which has been drifted with mobile lithium ions. The crystal is used in a reverse biased n^--i-p^+ configuration. The high resistivity intrinsic zone is the sensitive region of the crystal. A γ-ray entering this region can interact with electrons and transfer some or all of its energy to them. These excited electrons will cause further ionization of the atoms in the crystal producing many electron-hole pairs which, under the action of an applied electric field, are swept out of the region to form the basic signal information in the γ-ray detection. The life-time of the charge carriers created in the intrinsic region is substantially greater than the time required to collect them at the boundaries [45].

The energy deposited in the sensitive region of the crystal is determined by measurement of the current of electron-hole pairs leaving the intrinsic region. A single γ-ray can produce many charged carriers in an interaction, giving good statistics in the measurement of the current. This is the reason why the energy resolution of a Ge(Li) detector is far superior to that of other γ-ray detectors [56]. Incomplete collection of the charge produced in the intrinsic region and broadening effects of the electronic components following the detector result in a subsequent degradation of the Ge(Li) resolution from the limit imposed by the statistical spread in the number of carriers produced.

After an initial amplification, the current pulse from the pn diode is passed into a shaping amplifier which gives an output pulse of height proportional to the amount of energy deposited by the γ-ray in the sensitive region of the Ge(Li). The output pulses from this amplifier are then passed into a Multichannel Analyser, (MCA), to record the output pulse–height spectrum. When the system has been calibrated using γ-rays of known energy, this pulse–height spectrum will show the relative occurrence of different energy depositions in the sensitive region of the crystal.

A γ-ray will deposit energy in the crystal by undergoing one of three major interactions [22]. In a photoelectric interaction, the γ-ray will transfer all of its energy to a nucleus. If this interaction between an incoming γ-ray and a nucleus occurs in the sensitive region of the crystal, all the energy of the γ-ray will be detected. This will result in the production of a count in the full-energy peak of the spectrum (Figure 2.6).

Another possible interaction is that the γ-ray will undergo Compton scattering by atomic electrons, when only some of the γ-ray energy will be transferred to the crystal. Individual Compton interactions will deposit varying amounts of energy and so give a count in the region of the spectrum lower in energy than the photoelectric peak, in the Compton continuum. It is possible, however, that a γ-ray can deposit all its energy in the sensitive region of the crystal in a series of quickly successive Compton and photoelectric interactions. These interactions can occur so close in time that their current pulses merge into one pulse, which when detected will result in a count in the full-energy peak. A third possible

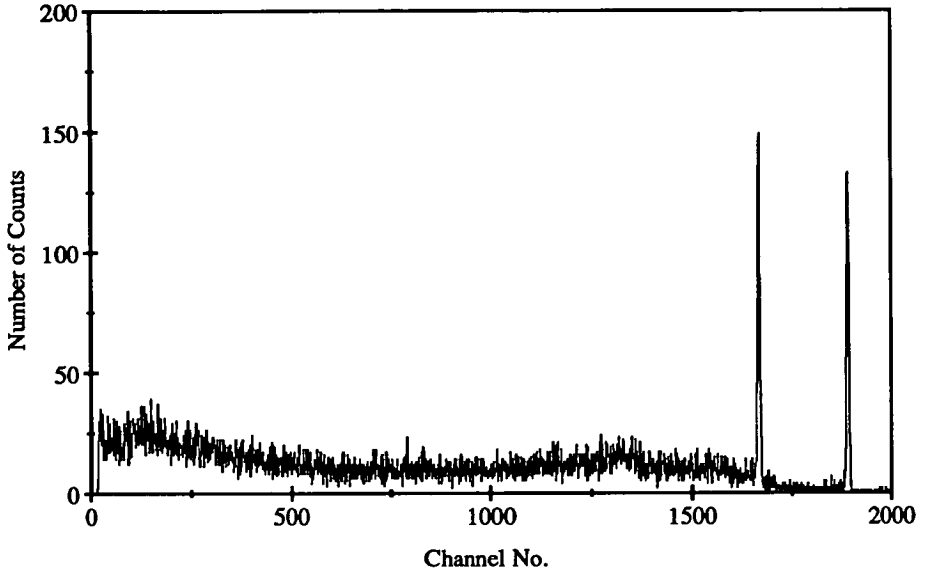

Figure 2.6: A spectrum from a ^{60}Co source showing the full-energy peaks from the 1173 and 1133 keV γ-rays and the lower energy continuum produced by Compton interactions

interaction, pair production, is possible only for γ-rays of energy greater than 1.02 MeV.

Figure 2.6 shows a γ-ray spectrum obtained by detecting γ-rays emitted by a ^{60}Co source with a Ge(Li). The full-energy peaks from the γ-rays of energy 1173 keV and 1132 keV emitted by the source can be seen, along with the low-energy continuum produced by Compton interactions between these γ-rays and electrons in the sensitive region of the detector.

The concentrations of radioactive substances present in the sample being analysed are determined by measuring the count-rates in the γ-ray full-energy peaks in the spectrum resulting from the analysis of the sample with the Ge(Li). In the course of this work the samples were analysed for the presence of several different radioactive isotopes. Details of the radionuclides and the γ-rays used in their measurement are given in Table 2.5. The excellent resolution of Ge(Li) detectors allows the levels of the different radionuclides to be measured from one spectrum.

Radionuclide	Half-life	γ-ray used (keV)	Branching Ratio (b_γ)
^{241}Am	433 years	59.5	0.357
^{7}Be	53 days	477.6	0.104
^{106}Ru	1.0 years	621.9	0.098
^{137}Cs	30.0 years	661.7	0.852
^{134}Cs	2.1 years	795.9	0.854
^{40}K	10^9 years	1460.8	0.107

Table 2.5: Details of the radionuclides measured in the course of this study [6]

2.2.2 Determination of Ge(Li) efficiency

The γ-rays produced in the sample being analysed will be emitted into the whole 4π solid angle, and so only a fraction of these will enter the Ge(Li) detector and allow the possibility of detection. Also it is possible for a γ-ray entering the crystal to remain undetected, if it fails to produce electron-hole pairs in the sensitive region of the detector. A γ-ray will be detected only if it interacts in the intrinsic region of the crystal and will be of use here only if the interaction results in a count in the full-energy peak. Therefore, in order to allow determination of the concentration of each radionuclide in a sample, it is necessary to know the full-energy peak efficiency of the Ge(Li) for the γ-ray being counted. That is, to know what fraction of the γ-rays emitted by the sample result in a count in the full-energy peak in the spectrum.

The full-energy peak efficiency, ε_{FULL}, will be different for γ-rays of different energy. The cross-section for the photo-electric interaction decreases with increasing γ-ray energy [22]. Also, very low energy γ-rays do not often have enough energy to penetrate through the surface dead layer of the crystal into the sensitive region of the detector. These low energy γ-rays are inefficiently

detected. ε_{FULL} is therefore expected to fall off for both lower and higher energy γ-rays.

The geometry of the sample-detector arrangement will affect the fraction of γ-rays emitted into the solid angle occupied by the detector. Different geometries will have different full-energy peak efficiencies at all γ-ray energies.

Each different Ge(Li) will show a different variation of ε_{FULL} with γ-ray energy. Detectors with larger sensitive regions should have a greater efficiency at all energies, as the probabilities of γ-rays interacting in the sensitive region increase. Detectors with slightly thicker windows or insensitive regions will have decreased efficiencies at lower energies.

It is obvious, therefore, that the way ε_{FULL} varies with energy will be dependent on the specific Ge(Li) and the sample-Ge(Li) geometry being used in the measurement. It is necessary to determine the full-energy peak detection efficiency of each γ-ray of interest for each Ge(Li) and in all sample-Ge(Li) geometries which will be used in the γ-ray analyis.

The full-energy peak efficiencies were determined using sources emitting γ-rays at a known rate. The standard samples used in the determination of ε_{FULL} for the Ge(Li)s were obtained from ITE Merlewood. The samples were produced by mixing measured amounts of Amersham International QC99 solution (with added liquid ^{241}Am) into matrices of vegetation and soil, and so contain known activities of 9 radionuclides emitting γ-rays ranging in energy from 60—1800 keV. This source was presented to the Ge(Li) detectors in the exact geometry used in counting the unknown samples. After performing counts with the standard samples, the count-rates in the full-energy peaks of the different γ-rays were obtained, giving the fraction of emitted γ-rays which result in a count in the full-energy peak. This is ε_{FULL}.

Figure 2.7 gives the variation of the full-energy peak efficiency with γ-ray energy for the two Ge(Li)s used in this study, for the exact geometry used in counting the unknown samples. The 19% Ge(Li) detector has a larger crystal and, as expected, has a larger ε_{FULL} for the higher energy γ-rays. At lower energies the smaller crystal is more efficient. This possibility has been discussed by Minemma et al.[54]. In this case it was probably caused by a thicker insensitive

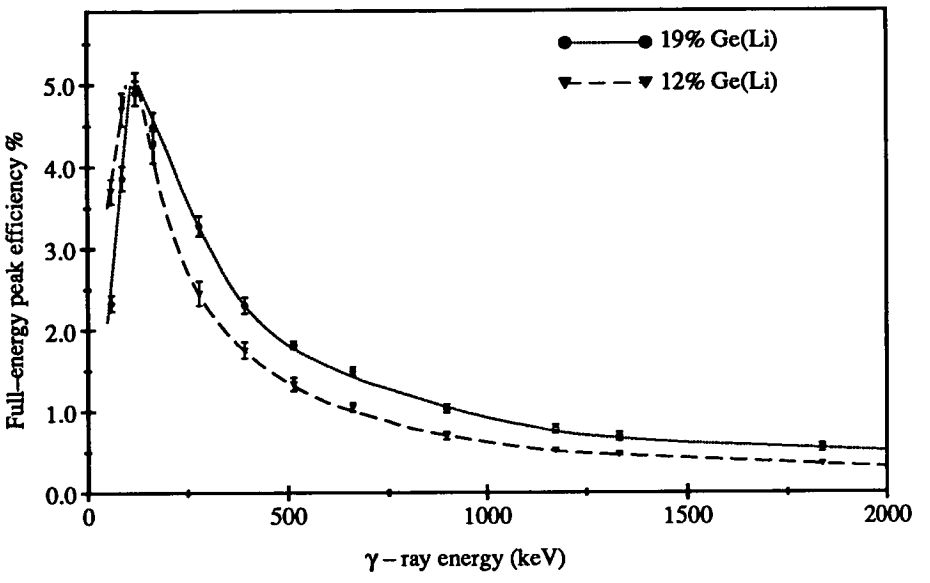

Figure 2.7: The full-energy peak efficiencies for γ-rays of different energy of the Ge(Li) detectors used in this study

region between the sample and Ge(Li) in the case of the larger 19% one, reducing the number of low energy γ-rays which penetrate to the sensitive region and so reducing detection efficiency.

2.2.3 Gamma-ray analysis of unknown samples

The two co-axial Ge(Li) detectors used in this study were manufactured by EG&G ORTEC. The pulses from the 19% model were input into a GEC 4090 computer via an Analogue to Digital Converter. The collected γ-ray spectra were analysed using programs developed at the Nuclear Structure Facility at the Daresbury Laboratory, Cheshire. The 12% model was run with the signals being input to a TRACOR MCA, later replaced by an MCA simulator run on an IBM PC.

The samples were counted for at least 24 hours, but often longer. Longer count times are useful in analysing less active samples as they result in larger peaks and so improved statistics.

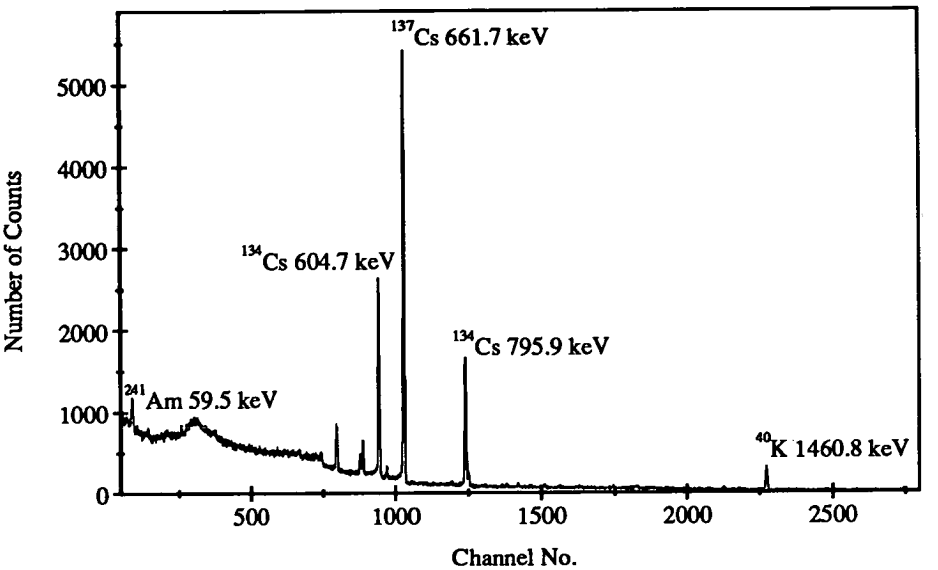

Figure 2.8: A γ-ray spectrum produced by the marram grass sample Marram A2: No.1, measured with the 19% Ge(Li) interfaced to the GEC 4090 computer

A typical γ-ray spectrum obtained by counting one of the marram grass samples with the 19% Ge(Li) is shown in Figure 2.8. The number of counts present in the different peaks were determined using the spectrum analysis software available on the GEC computer. The activity of each of the radionuclides present in the sample was determined using the equation:

$$A = \frac{N_{peak}}{T} \times \frac{1}{\varepsilon_{FULL} \times b_\gamma} \tag{2.1}$$

where A is the activity of the radionuclide in the sample in Becquerels (Bq), N_{peak} is the number of counts in the full-energy peak, T is the duration of the count in seconds, ε_{FULL} is the full-energy peak efficiency of the detector for the γ-ray in the geometry used in the analysis and b_γ is the γ-ray branching ratio of the radionuclide.

2.3 Chloride Ion Analysis

2.3.1 The ion specific electrode

Determination of the amount of sea-salt collected on the muslin screens exposed along transects Drigg C and D was performed using an EIL Model 8004-2 Chloride Ion Specific Electrode. The electrode and reference electrode were plugged into a PYE pH meter used on the mV range, and set for the measurement of monovalent anions. Sections of the exposed muslin screens were washed in distilled water and the chloride ion concentration of the resultant solution measured. From this the mass of sea-salt present on the cloth could be determined.

The sensing tip of the electrode consists of a silver billet electrolytically coated with a layer of silver chloride, AgCl. In solutions containing chloride ions the electrode potential is set by the equilibrium activity of silver ions generated at the electrode by dissolution of the AgCl. The electrode potential is proportional to the logarithm of the chloride activity in the solution. Provided that the ionic strengths of the solutions are held constant, achieved here by adding a constant amount of buffer solution to all the standards and samples, the chloride ion activity will be proportional to the chloride ion concentration, $[Cl^-]$. (The buffer solution is composed of a mixture of 0.5 M ammonium acetate and 0.5 M acetic acid solutions). Thus the voltage E produced by the electrode when placed in a solution of chloride ion concentration $[Cl^-]$ is:

$$E = E_c - m\, log_e\, [Cl^-] \tag{2.2}$$

where E_c and m are the intercept and gradient of a straight line through the points in a plot of E against $log_e\,[Cl^{-1}]$. Calibration of the electrode was performed by making measurements on a set of standard NaCl solutions of molarity ranging from 10^{-3} to 10^0 M. A best fit through the data-points was performed to determine the parameters E_c and m in Equation 2.2. An example of a fit to a set of calibration measurements is shown in Figure 2.9. The electrode was calibrated every day of use, and repeated measurements of the standard solutions were made after every two or three measurements on the unknown solutions to ensure the stability of the system.

The concentration of chloride ions in an unknown solution is determined from the voltage reading E using Equation 2.2, with the values of E_c and m determined from the fit to the calibration points. The number of moles of chloride ions present in the the solution, M_{Cl}, is then determined from:

$$M_{Cl} = V \times e^{(E_c - E)/m} \tag{2.3}$$

where V is the volume of the solution in litres. Chloride ions make up 54.96% by weight of sea-salt [78]. The mass of sea-salt present in the solution, W, is therefore determined from M_{Cl} by

$$W = M_{Cl} \times MW_{Cl} \times \frac{100}{54.96} \tag{2.4}$$

where MW_{Cl} is the molar weight of chlorine, 35.45 g. The error in W, σ_W, is given by

$$(\frac{\sigma_W}{W})^2 = (\frac{\sigma_V}{V})^2 + \frac{1}{m^2}(\sigma_E^2 + \sigma_{E_c}^2 + (E - E_c)^2(\frac{\sigma_m}{m})^2) \tag{2.5}$$

where σ_V is the error in the measurement of the volume of the analysed solution, σ_E is the error in the voltage reading on the pH meter, and σ_{E_c} and σ_m are the errors in E_c and m obtained from the uncertainty in the best fit to the calibration points.

2.3.2 Muslin screen analysis

On several occasions an exposed muslin screen was cut into different sections which were washed and analysed for their sea-salt content. Table 2.6 gives the voltages recorded from the analysis of a screen cut into 10 equally sized vertical strips and washed in turn in clean distilled water for 60 seconds. Table 2.7 gives the results of a similar analysis of 10 horizontal strips from another exposed screen. As in all the sea-salt analyses, the electrodes were properly washed in distilled water before each measurement to avoid contamination of the new solution with salt from previous measurements.

As can be seen the from the results quoted in Tables 2.6 and 2.7 the measurements on the different sections of the same screen gave very similar results. These results give confidence in the sea-salt measurement technique utilised here,

Strip No.	Electrode Voltage (− mV)
1	325
2	324
3	323
4	323
5	323
6	323
7	323
8	323
9	323
10	327

Table 2.6: Chloride electrode potential from the measurement of 10 equally sized strips cut from screen no. 9 of the C7 exposure. Each 50 cm^2 section was washed for 60 seconds in 100 mls of distilled water.

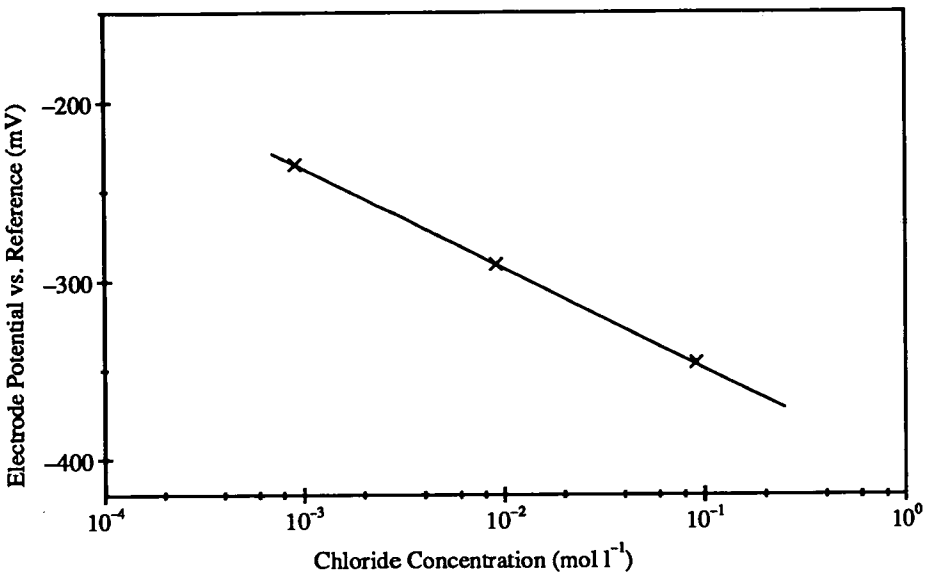

Figure 2.9: Graph showing measurements made on standard NaCl solutions with the chloride specific electode. The line is the best fit to the points and gives the values of the gradient, m and intercept, E_c

particularly the routine of washing equally sized sections of screens in a constant volume of distilled water for a constant time period. It illustrates the repeatability of the sea-salt measurements performed in this study.

These results also imply that the collected sea-salt is evenly distributed over the surface of the muslin screens exposed to collect the sea spray. Thus it does not appear to be necessary to perform an analysis of a whole screen. The results from a fraction of a screen can be scaled to give the sea-salt collected by the whole. Two different sized muslin screens were used in this study. Those exposed along the Drigg C transect were 0.5 m^2 in area, while those exposed at Drigg D were 1.0 m^2. Usually, half of the exposed area of each screen was used in the analysis of the sea-salt content.

The section of the screen to be analysed was cut up into approximate 0.125 m^2 pieces. These pieces were washed in turn in a sample of distilled water for 60 seconds. 10 mls of the buffer was added and the solution stirred. The electrodes were immersed in the solution and the needle allowed to settle before the

Strip No.	Electrode Voltage ($-$ mV)
1	323
2	323
3	323
4	323
5	324
6	324
7	323
8	323
9	324
10	323

Table 2.7: Chloride electrode potential from the measurement of 10 equally sized strips cut from screen no. 7 of the C7 exposure. Each 50 cm^2 section was washed for 60 seconds in 100 mls of distilled water.

voltage reading was recorded. The volume of the solution was measured. All the screens comprising an exposure set were analysed in the same fashion on the same day, with the stability of the measurement system being continuously monitored.

It was also deemed to be unnecessary to repeatedly wash each piece of cloth to remove all the sea-salt present. It was found from repeated washings of screens that a constant fraction of the removable sea-salt was removed in the first wash. Thus it was possible to determine the mass of sea-salt present on a screen by determining the mass washed into the distilled water solution on the first wash.

It is, however, necessary to know what fraction of the sea-salt present on a screen was washed off. This was done by re-washing screens repeatedly in fresh distilled water samples. Repeat washings of $0.5\,m^2$ sections of cloth were performed on seven occasions. The results of these sea-salt analyses are given in Table 2.8. It can be seen that on the occasions when a section of screen was washed for a third time the mass of sea-salt removed was smaller than the uncertainty in the mass removed during the first wash. The mass of salt present in the solution after the third wash was always found to be so small. Repeat washings therefore came to be performed only once on each screen. Table 2.8 illustrates that the mass of sea-salt removed in the first wash as a fraction of the total salt removed, was stable and repeatable. An average of $84 \pm 2\%$ of the total sea-salt removed in two washes was washed from the $0.5\,m^2$ pieces of cloth during the first.

Table 2.9 gives the results obtained in rewashing half of the smaller screens exposed along Drigg C, and on the occasions when only one quarter of the Drigg D screens were analysed. Repeat washings showed that $94 \pm 3\%$ of the salt present on these smaller screens was removed during the first wash. The sea-salt is apparently more efficiently removed from smaller areas of cloth. The important point here is not that the washing process is more efficient on smaller pieces of muslin, but that, no matter what area of screen was washed, a constant and measurable fraction of the sea-salt which could be removed, was removed in the first wash. From the mass of sea-salt present in the water solution after one wash, the mass initially on the screen could be calculated.

Screen Name	Mass of sea-salt in solution (g)			% age of total removed in first wash
	1^{st} wash	2^{nd} wash	3^{rd} wash	
D3 No. 5	1.92±0.10	0.28±0.01	—	87±6
D4 No. 3	0.342±0.017	0.054±0.005	—	86±6
S2 No. 8	0.079±0.004	0.0129±0.0007	—	86±6
S4 No. 4	0.111±0.006	0.0180±0.0010	0.0029±0.0002	84±6
S4 No. 8	0.038±0.002	0.0052±0.0003	0.0008±0.0001	86±6
S5 No. 7	0.0048±0.0003	0.0015±0.0001	—	76±6
S6B No. 8	0.0157±0.0008	0.0035±0.0002	—	82±5

Table 2.8: Results of repeated washes on sections of muslin screens on the occasions when 0.5 m^2 of each screen was being washed and analysed. On average 84±2% of the total sea-salt removed was washed off during the first wash.

Pieces of muslin cloth which had not been exposed to the sea winds were also washed and analysed in the same way as the sections of the exposed screens. No chloride could be detected in the solutions resulting from the washing of these clean screens, and so it can be assumed that all the chloride washed from the exposed screens was collected in sea spray during their exposure on the beach at Drigg.

Screen Name	Mass of sea-salt in solution (g)		% age of total removed in first wash
	1^{st} wash	2^{nd} wash	
C3 No. 9	0.0265±0.0012	0.0024±0.0001	92±6
C4 No. 12	0.202±0.013	0.014±0.001	94±6
C5 No. 11	1.07±0.06	0.070±0.005	94±7
C6 No. 12	0.284±0.013	0.0190±0.0009	94±6
D1 No. 9	0.307±0.014	0.0170±0.0008	95±6
D2 No. 8	1.90±0.10	0.128±0.007	94±6

Table 2.9: Results of repeated washes on sections of muslin screens when $0.25\,m^2$ of each screen was being analysed. On average 94±3% of the total sea-salt removed was washed off during the first wash.

Chapter 3

Presentation of Results

In this Chapter the results of the analyses on the collected vegetation and exposed muslin screens will be presented. The concentration of radionuclides in the collected marram grass samples will be reported, followed by the radioactivity levels present on the muslin screen spray collectors after exposure. The mass of sea-salt present on the muslin screens will also be given. The analysis of the weather records collected by the Meteorological Office at Eskmeals will then be discussed.

3.1 Marram grass

The results of the γ-ray analyses of the marram grass samples collected along the transects at Drigg are presented in terms of Bq of each radionuclide per kg of dried herbage. The activity levels present in the Drigg A1 sample, back-dated to the time of collection, are given in Table 3.1. This grass sample was analysed over 16 months after its collection, a period equivalent to over 9 half-lives of the ^{7}Be isotope. The activity level of ^{7}Be in this sample was below the detection limit of the system of 11 Bqkg^{-1} at the time of analysis. This sets the upper limit of the activity in the sample at the time of collection given in Table 3.1. The A1 sample was collected before the deposition in this region of radioactivity released during the accident at the Chernobyl nuclear reactor in April 1986 (See Section 1.5). For comparison with the radioactivity concentrations present in this A1 sample, the results of the γ-ray analysis on the Drigg A2 Sample 1 are also quoted in

Radionuclide	Activity present in Drigg A1 sample October 1985 ($Bq\,kg^{-1}$)	Activity present in Drigg A2, sample 1 5^{th} December 1986 ($Bq\,kg^{-1}$)
^{241}Am	33±4	78±5
^{7}Be	< 6000	824±38
^{106}Ru	78±28	284±12
^{137}Cs	75±2	1395±31
^{134}Cs	4±3	596±11

Table 3.1: Radionuclides present in the marram grass samples collected at Site No.1 of the Drigg A transect, before and after the deposition in this region of radionuclides released during the Chernobyl incident in early May 1986.

Table 3.1. The A2 sample was collected from a similar location on 5^{th} December 1986, six months after the deposition of the Chernobyl radioactivity.

Figures 3.1 to 3.5 show the levels of ^{241}Am, ^{137}Cs, ^{134}Cs, ^{106}Ru and ^{7}Be present in the other samples of marram grass collected along the Transects A, B and C. The error bars in these graphs are due solely to the Poisson Statistics of determining the counting rate of the γ-ray used to measure each radionuclide from the full-energy peaks in the spectra produced by the Ge(Li) detector. The uncertainty in the detection efficiency of each γ-ray is not included.

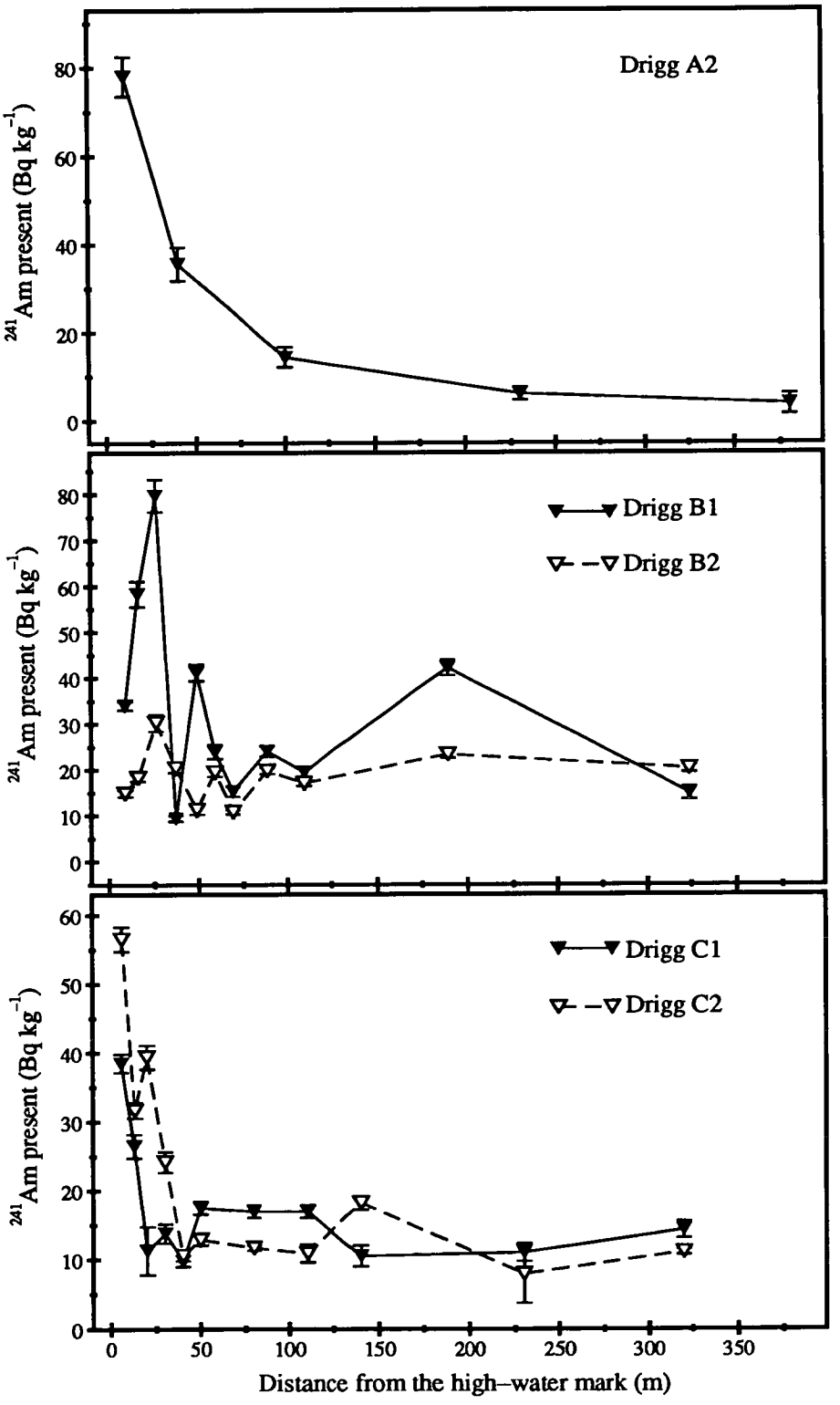

Figure 3.1: ^{241}Am present in marram grass samples collected along transects A, B and C

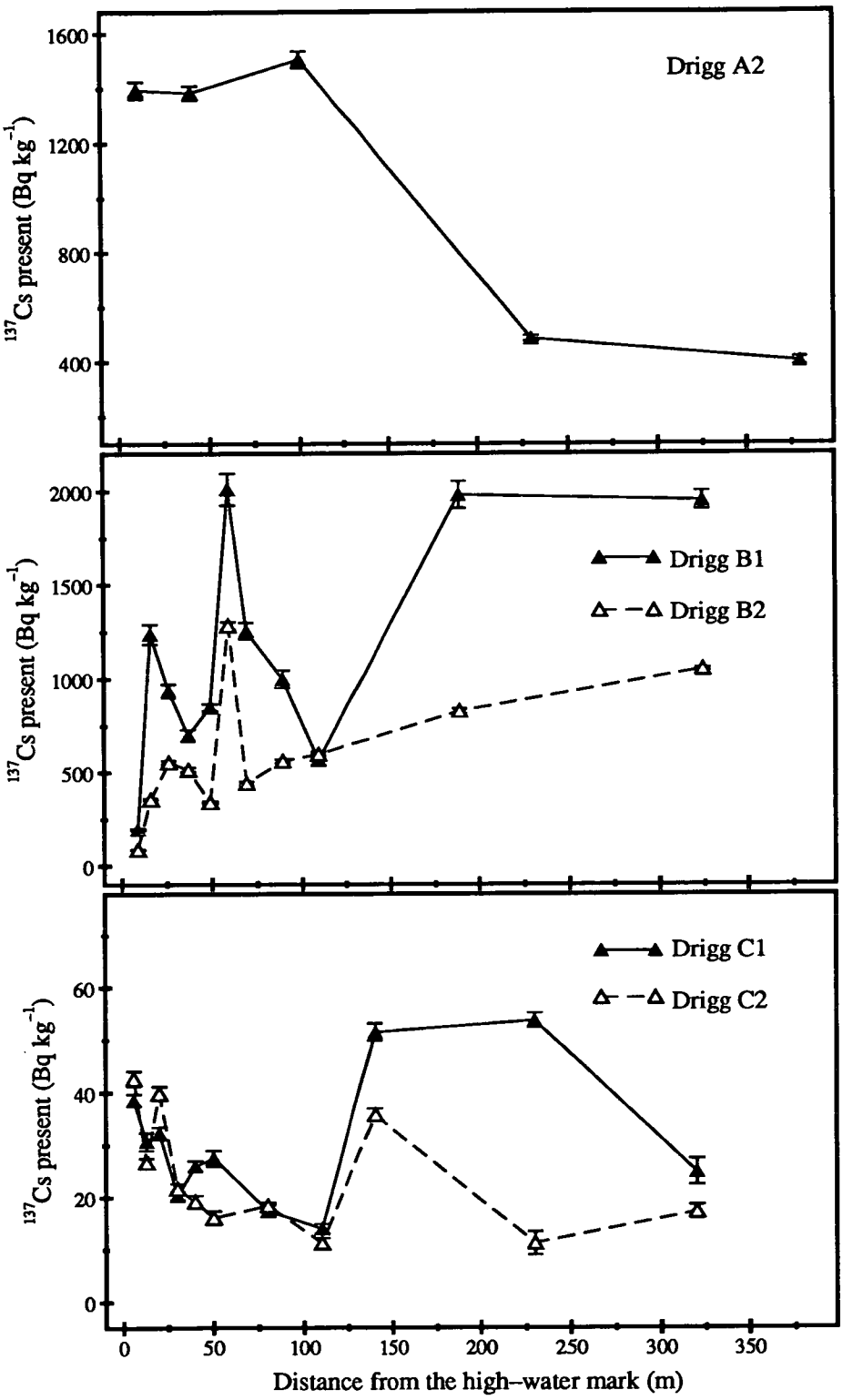

Figure 3.2: ^{137}Cs present in marram grass samples collected along transects A, B and C

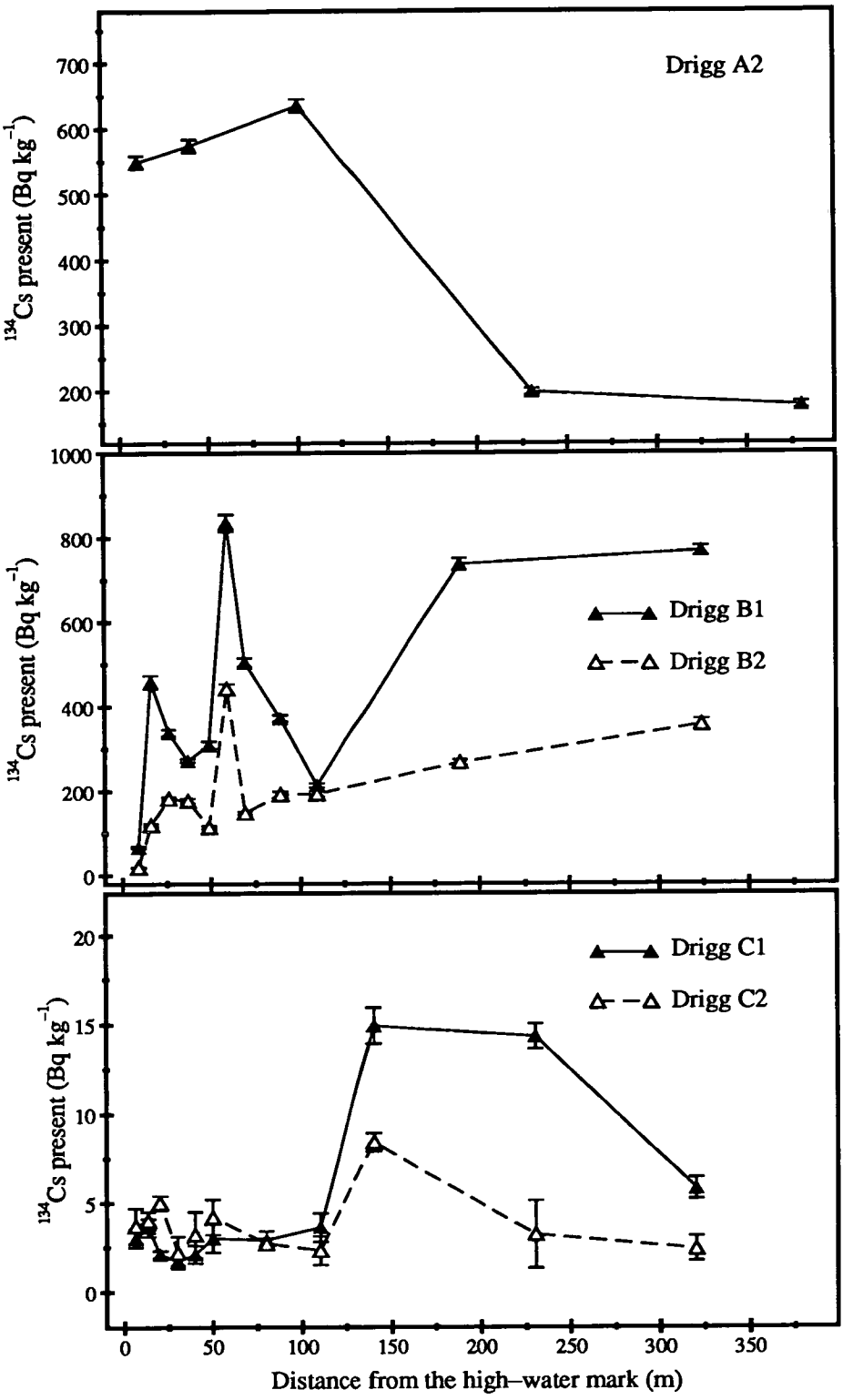

Figure 3.3: ^{134}Cs present in marram grass samples collected along transects A, B and C

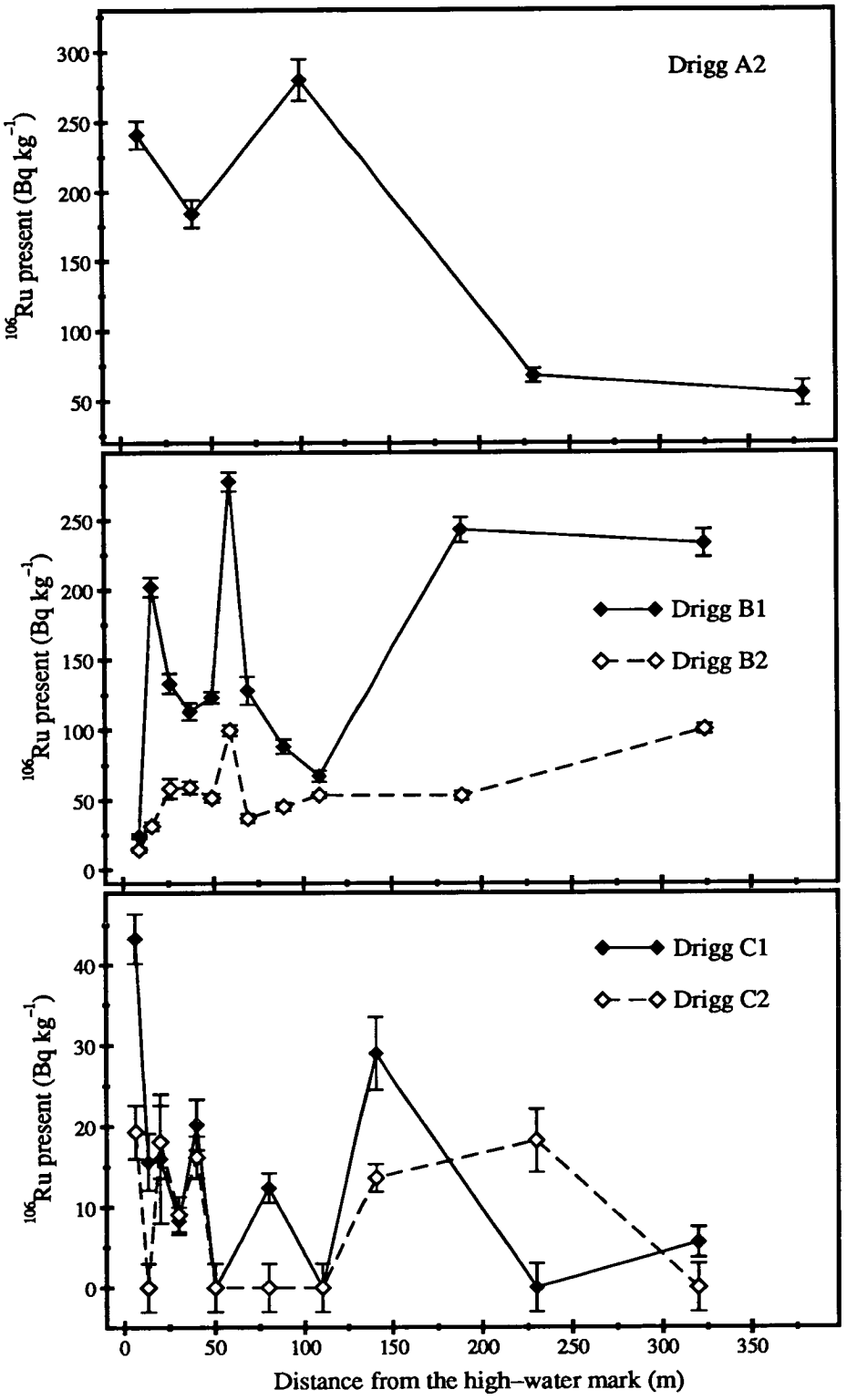

Figure 3.4: ^{106}Ru present in marram grass samples collected along transects A, B and C

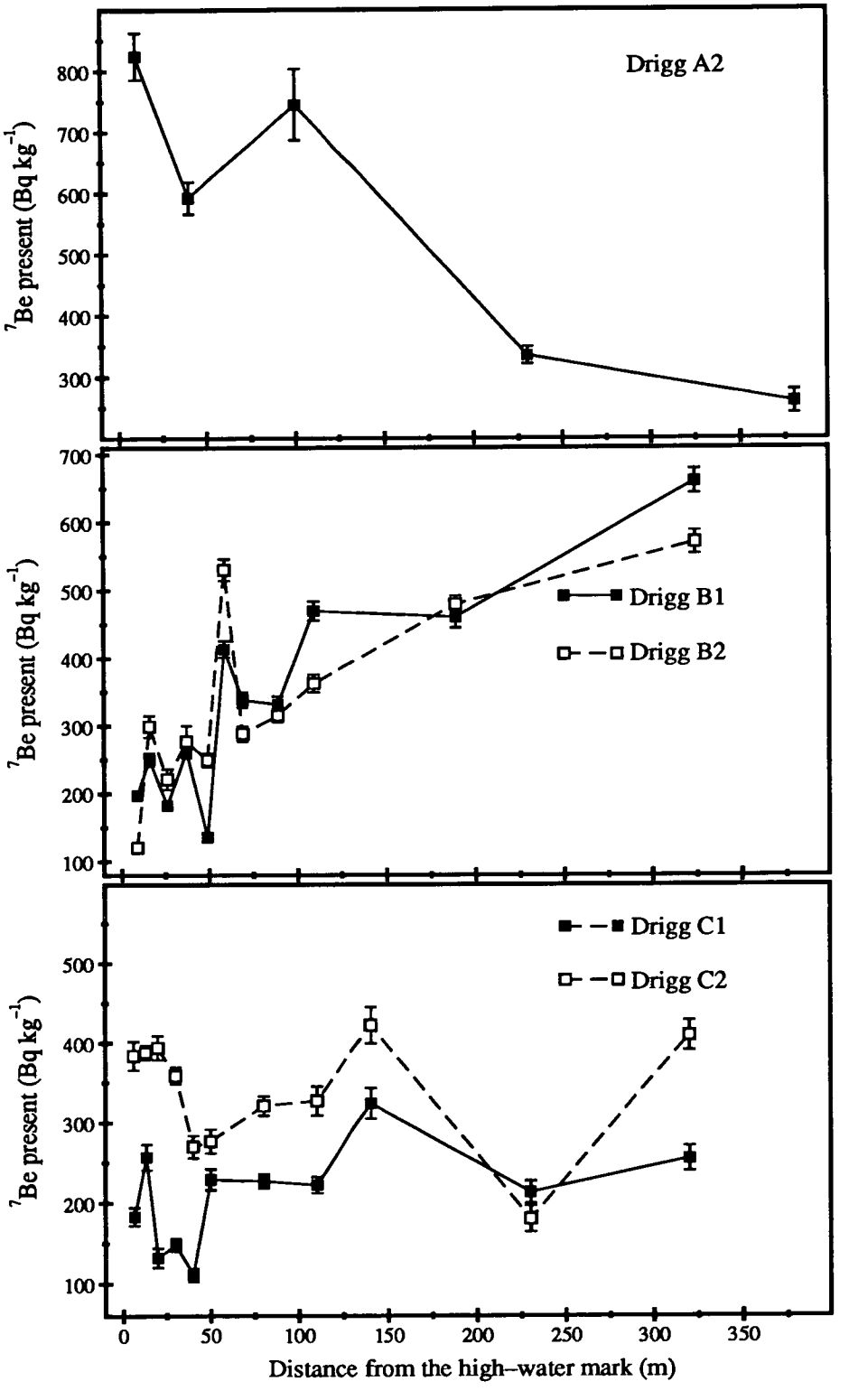

Figure 3.5: ^{7}Be present in marram grass samples collected along transects A, B and C

3.2 Muslin screens

3.2.1 Exposures along Drigg C

The activity levels of ^{241}Am, ^{137}Cs, ^{106}Ru and ^{7}Be and the mass of sea-salt present on the muslin screens after exposure along the Drigg C transect are illustrated in Figures 3.6 to 3.15. The distance inland in these plots is measured from the position of site No.1. The screen holder at site 11 snapped off and fell to the ground at some point in the middle of the C1 exposure; no results are given for this screen.

All the 0.5 m^2 exposed area of each of these screens was used in the γ-ray analysis. The results give the activity present on the whole screen. No ^{134}Cs could be measured on these screens and the levels of ^{106}Ru on the screens from the C2 and C3 exposures were below the detection limits (See Table 3.2). The levels of ^{106}Ru and ^{7}Be have been corrected for the radioactive decay between the end of the screen exposure and the time of the γ-ray analysis. Only half of each screen was used in the analysis of the sea-salt collected. The results have been scaled to give the mass present on a 0.5 m^2 area.

3.2.2 Long-term exposures along Drigg D

The radionuclide activities and salt masses present on screens from the long-term exposures along the Drigg D transect are given in Figures 3.16 to 3.20. Again, no ^{134}Cs could be detected on these screens (See Table 3.2). The distances inland in these diagrams are measured relative to the position of site No.2 on the transect. This is because no results were obtained from site 1 from these exposures along Drigg D. The poles holding screen 1 were washed away in a high tide during exposure D1 and the screen was lost. This fate later befell the poles at site 2, during the D3 exposure. The screen at site 8 was found wrapped around one of its poles at the end of exposure D3 and so was not collecting spray throughout the whole period. This also occurred at sites 6 and 8 during D4. No results are reported for any of these screens.

The screens exposed along Drigg D had an area of 1 m^2, but only half of

each screen was analysed for γ-rays. The results presented here give the activity present on that $0.5\,m^2$ portion of screen and not the whole screen. The salt measurements also give the mass present on a $0.5\,m^2$ area section.

The D4 screens were not analysed until more than 7 months after the end of the exposure period. The ^{106}Ru and ^{7}Be results had to be significantly corrected to allow for the decay between the end of the exposure and the count. The poor statistics, due to the low counting rates after the delay, gave rise to the larger errors bars in these graphs.

3.2.3 Short-term exposures along Drigg D

As described above for the screens from the long-term exposures, only half the area of the screens exposed for short periods along Drigg D were subjected to γ-ray and sea-salt analysis. The results of these measurements are again given in terms of the activity and mass of sea-salt present on the analysed $0.5\,m^2$ portion of the screens.

Of the screens exposed for short periods, only those in the S4 set collected measurable levels of ^{241}Am and ^{137}Cs. These results are presented in Figure 3.21. The distance inland in this figure is the mean sea to screen distance during the S4 exposure. Only those screens from exposures S1, S3 and S4 contained measurable levels of ^{7}Be at the time of γ-ray analysis. These results are plotted in Figure 3.22. The positions of the exposed screens are here plotted relative to the position of site 1 on the transect, and not with reference to the position of the surf at the time of the exposure. The collected ^{7}Be has its source in the atmosphere and not in the sea, and the sea to screen distance is therefore of no consequence.

The screens from all the short-term exposures collected levels of sea-salt which could be measured easily by the technique being used. The results of the salt analyses on these screens are presented in Figures 3.23 and 3.24. In these figures the distances inland are again the mean sea to screen distance measured during each exposure period. Table 3.3 indicates the state of the sea at the time of each of the short-term exposures.

Isotope	Detection Limit (Bq)
^{241}Am	0.083
^{7}Be	0.37
^{106}Ru	0.42
^{137}Cs	0.040
^{134}Cs	0.053

Table 3.2: Limits of detection of the radionuclides of interest in the γ-ray analyses of the exposed muslin screens with the 12% Ge(Li) detector. These limits are for counting times of the order of 24 hours

Exposure	State of tide	Description of surf zone
S1	High	Large breakers extending out to over 100 m from water's edge
S2	Low	No appreciable surf
S3	Rising	Similar to S1
S4	High	Very rough. Breakers extend right out to sea
S5	Falling	Calm. Small waves
S6 A,B	Rising	Rough sea. Breakers extend out to 300 m.

Table 3.3: State of surf during short-term exposures at Drigg D

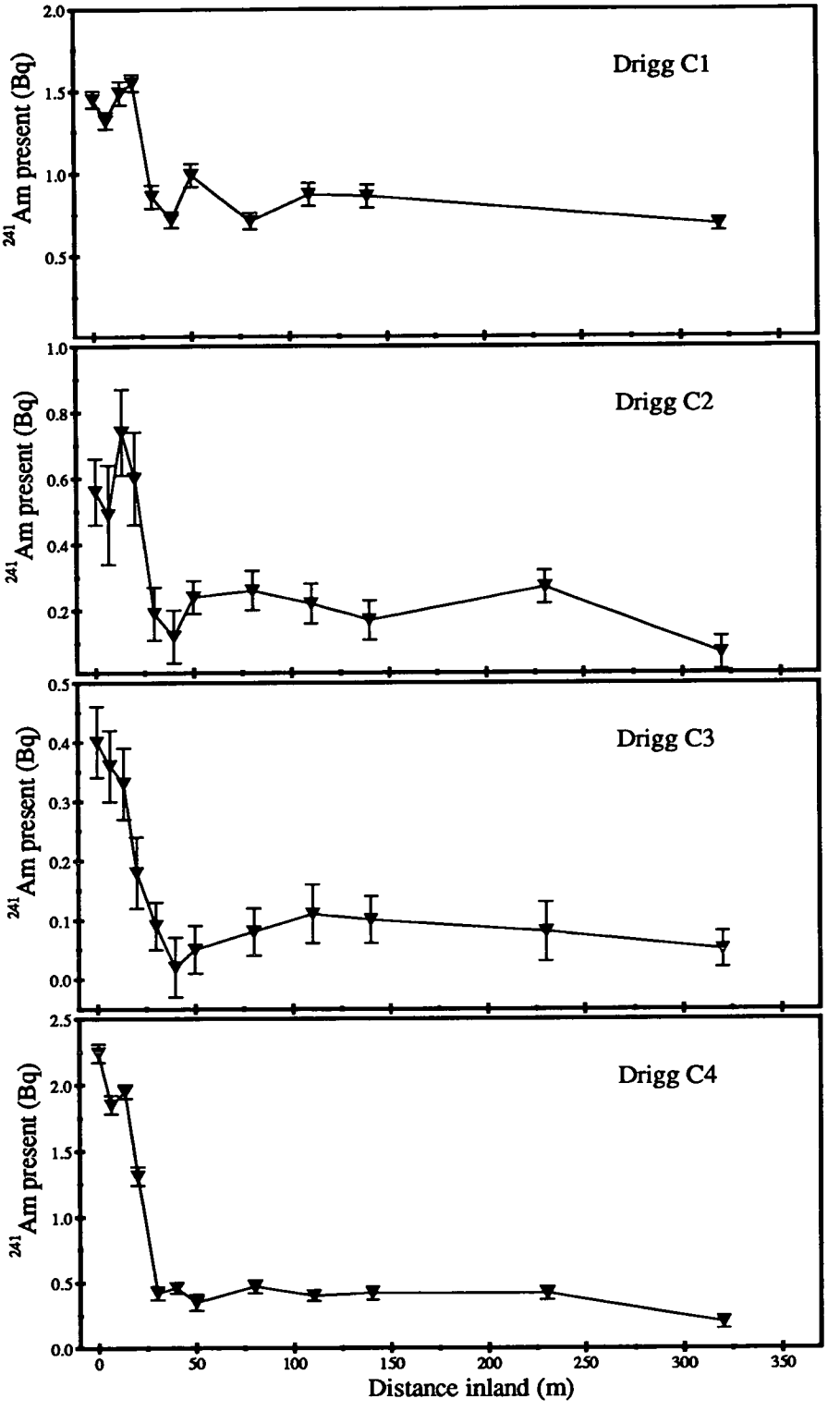

Figure 3.6: ^{241}Am collected on muslin screens exposed along transect C during exposures C1 to C4

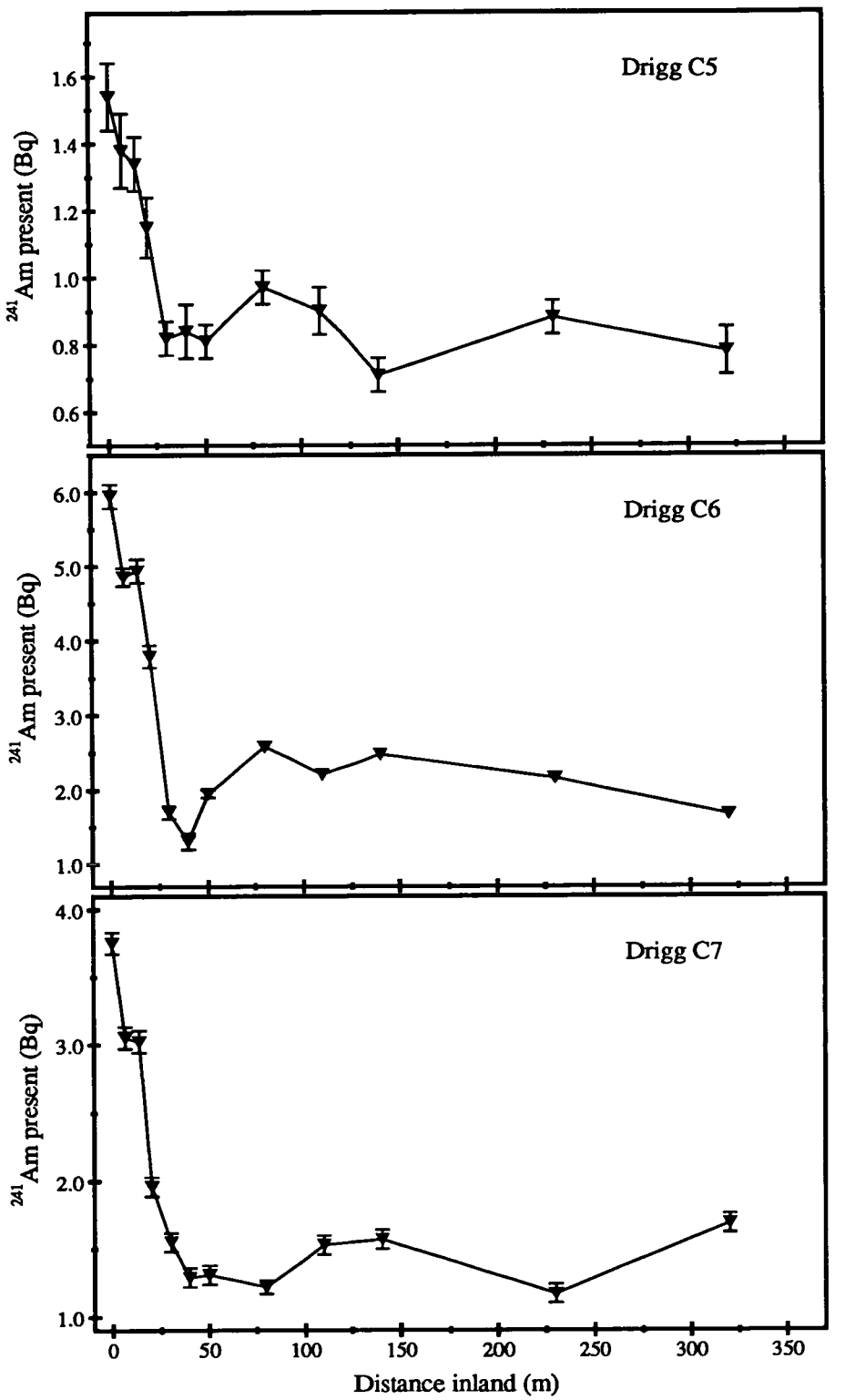

Figure 3.7: ^{241}Am collected on muslin screens exposed along transect C during exposures C5 to C7

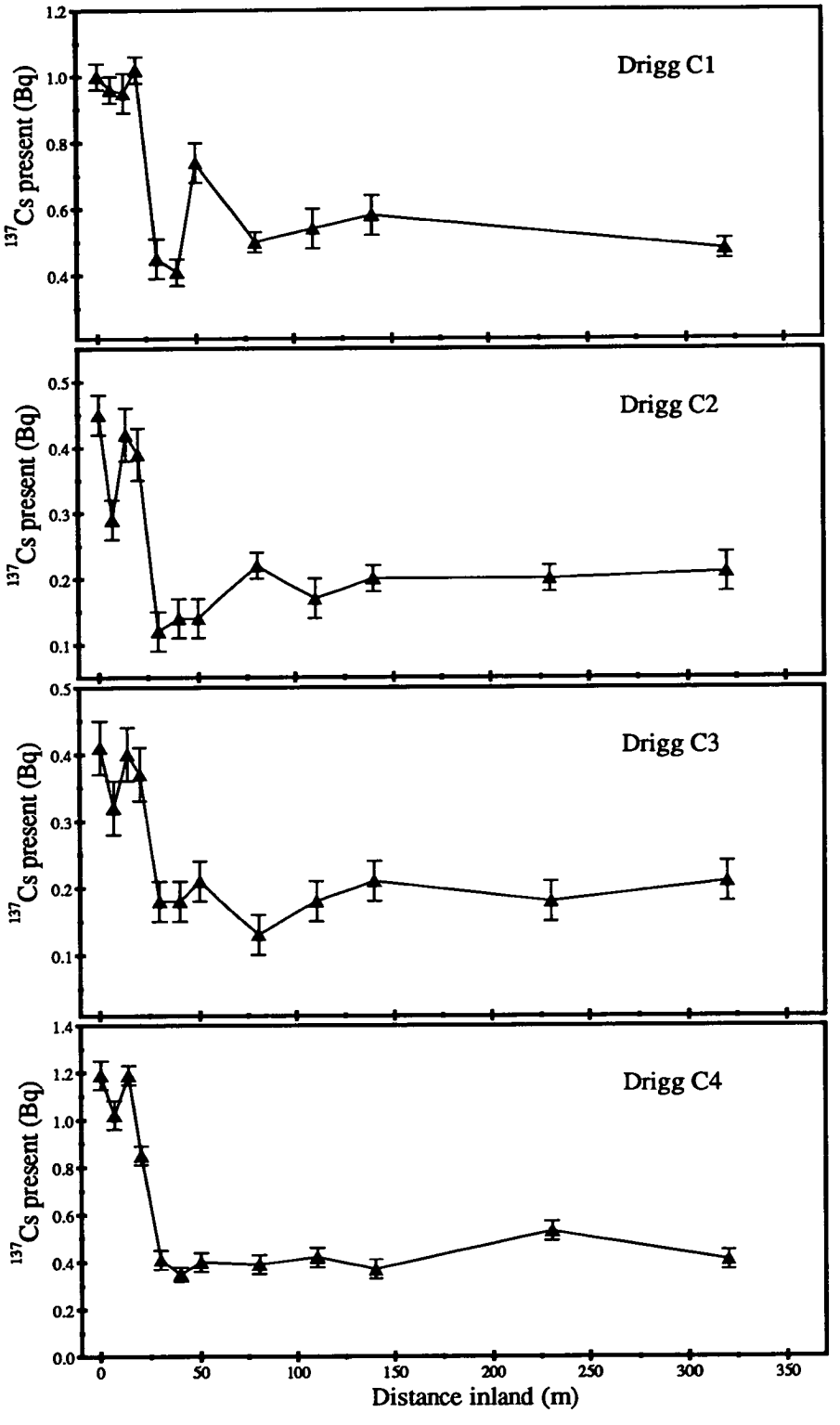

Figure 3.8: ^{137}Cs collected on muslin screens exposed along transect C during exposures C1 to C4

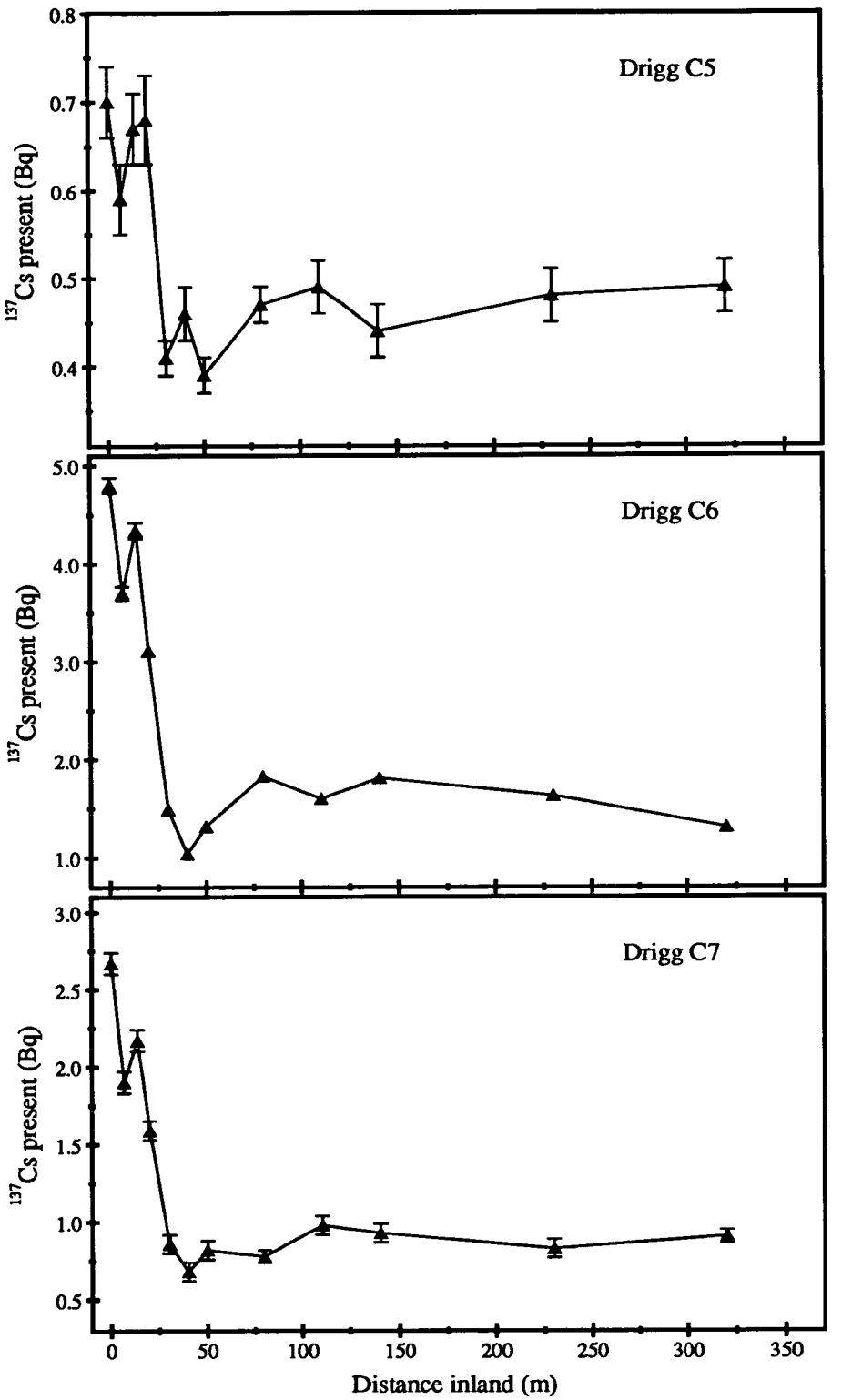

Figure 3.9: ^{137}Cs collected on muslin screens exposed along transect C during exposures C5 to C7

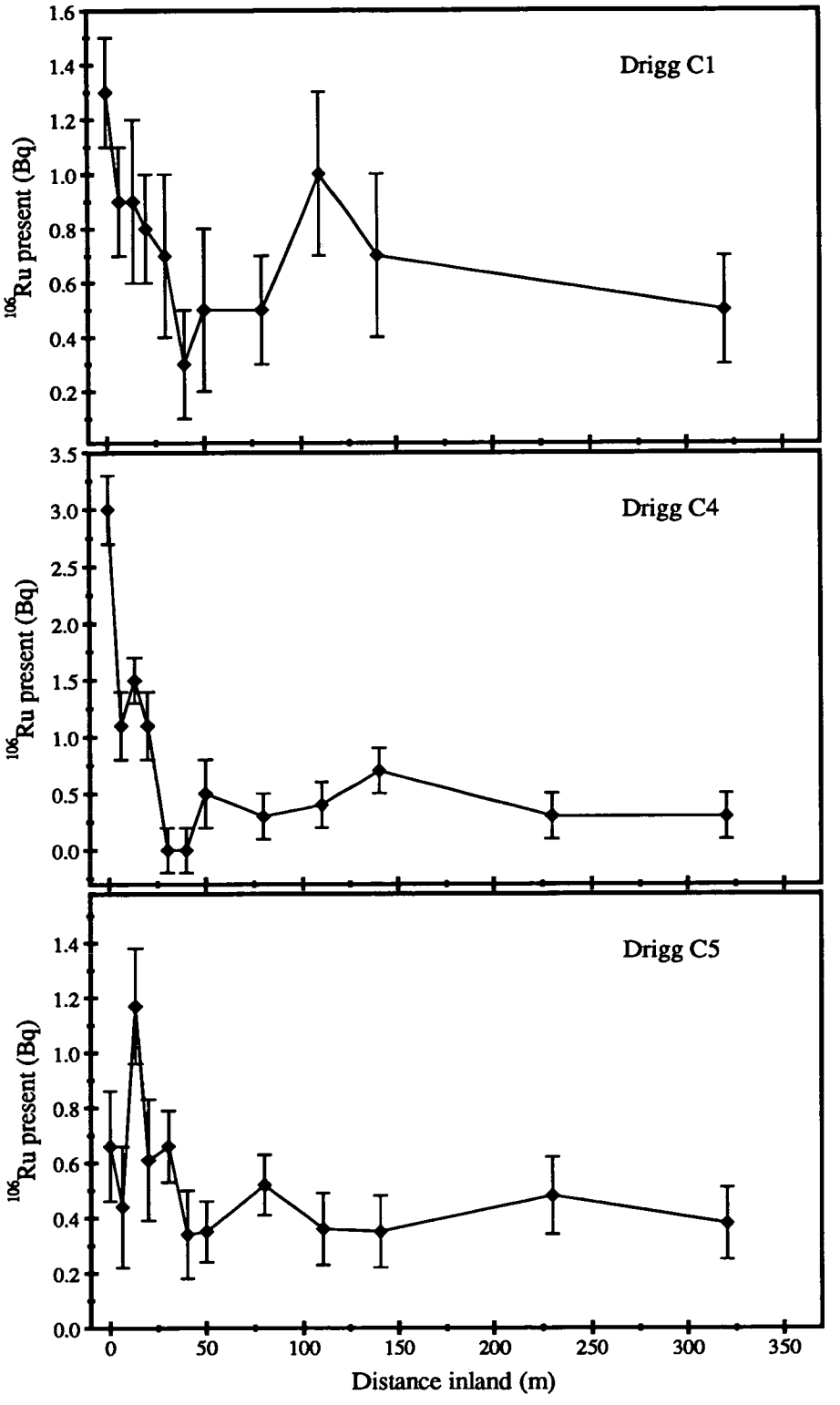

Figure 3.10: ^{106}Ru collected on muslin screens exposed along transect C during exposures C1, C4 and C5

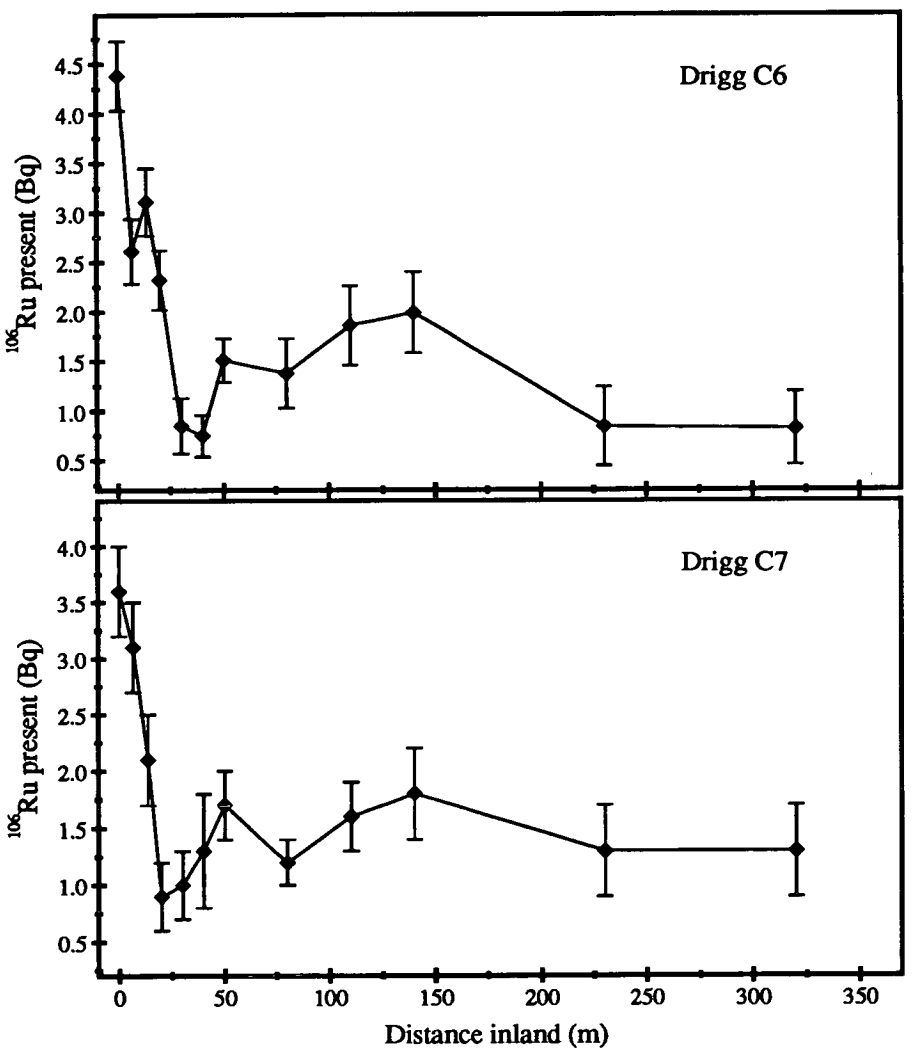

Figure 3.11: ^{106}Ru collected on muslin screens exposed along transect C during exposures C6 and C7

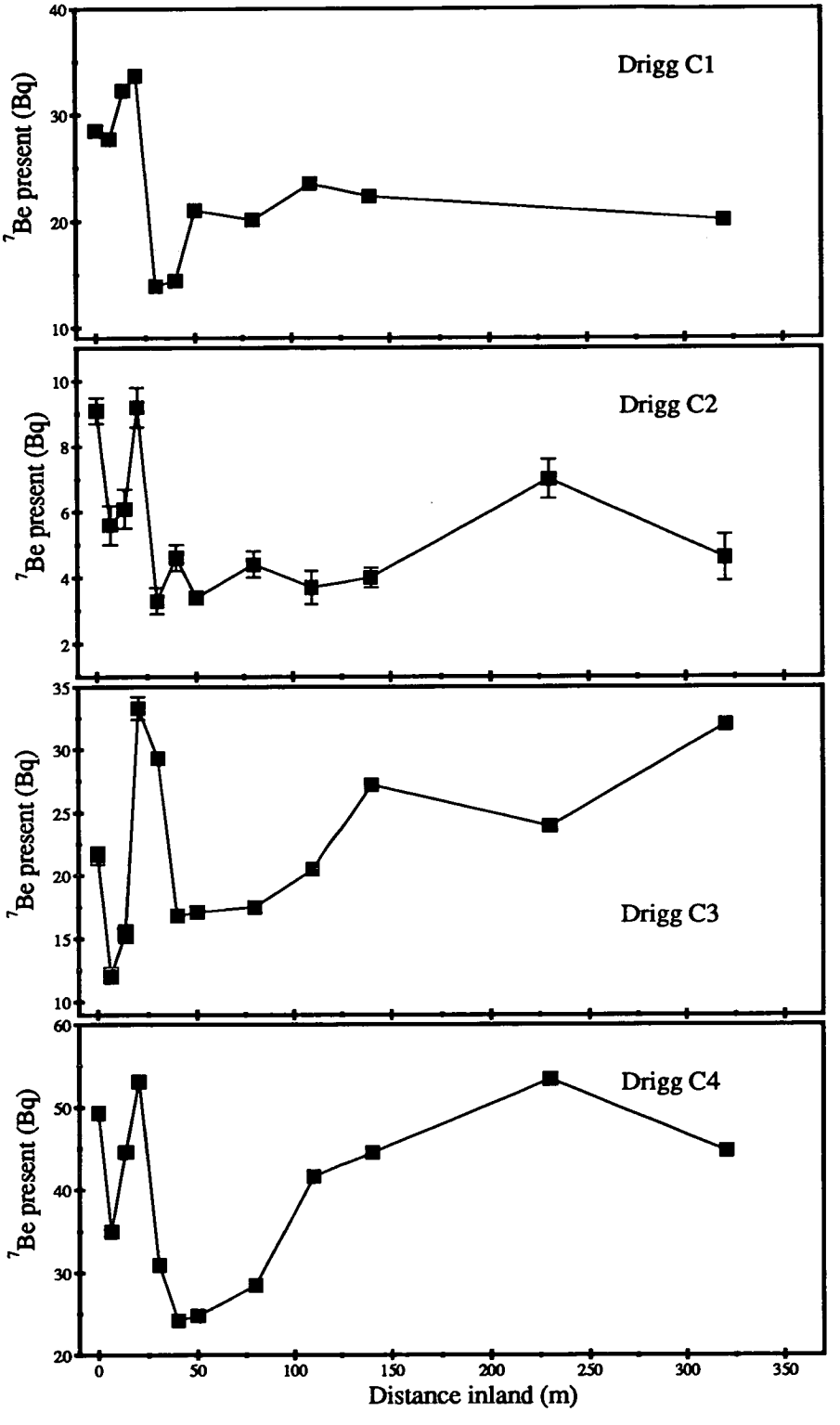

Figure 3.12: ^{7}Be collected on muslin screens exposed along transect C during exposures C1 to C4

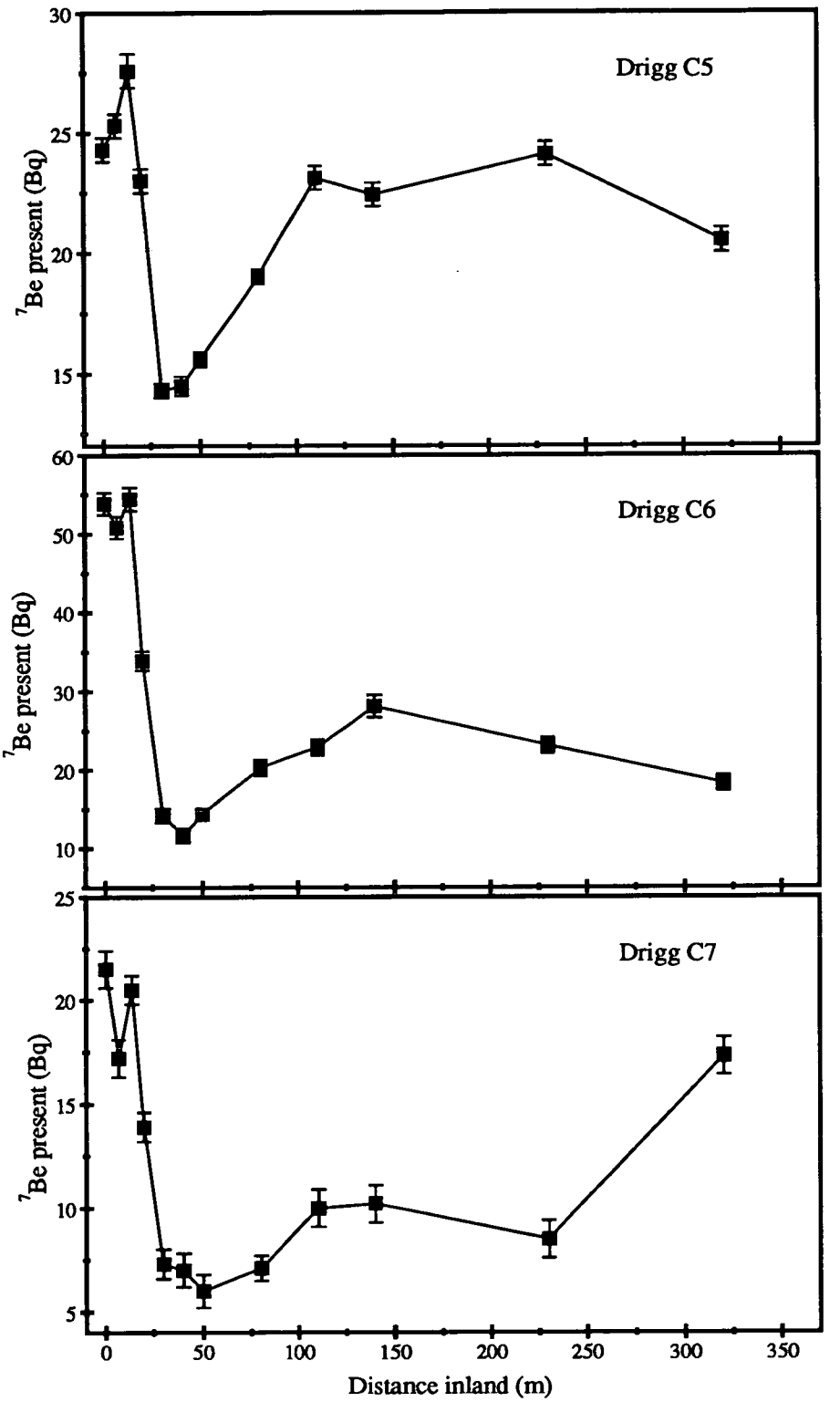

Figure 3.13: ^{7}Be collected on muslin screens exposed along transect C during exposures C5 to C7

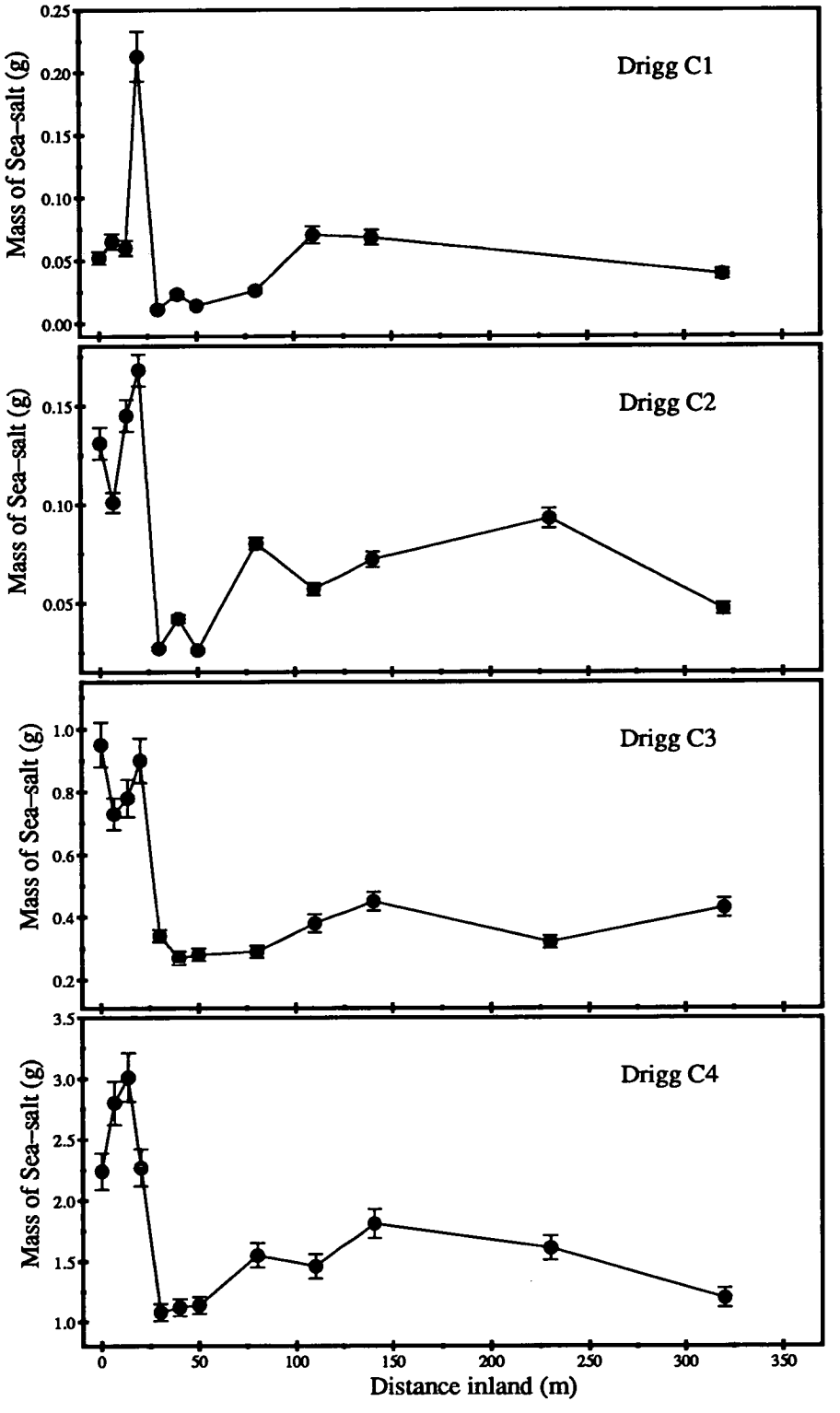

Figure 3.14: Sea-salt collected on muslin screens exposed along transect C during exposures C1 to C4

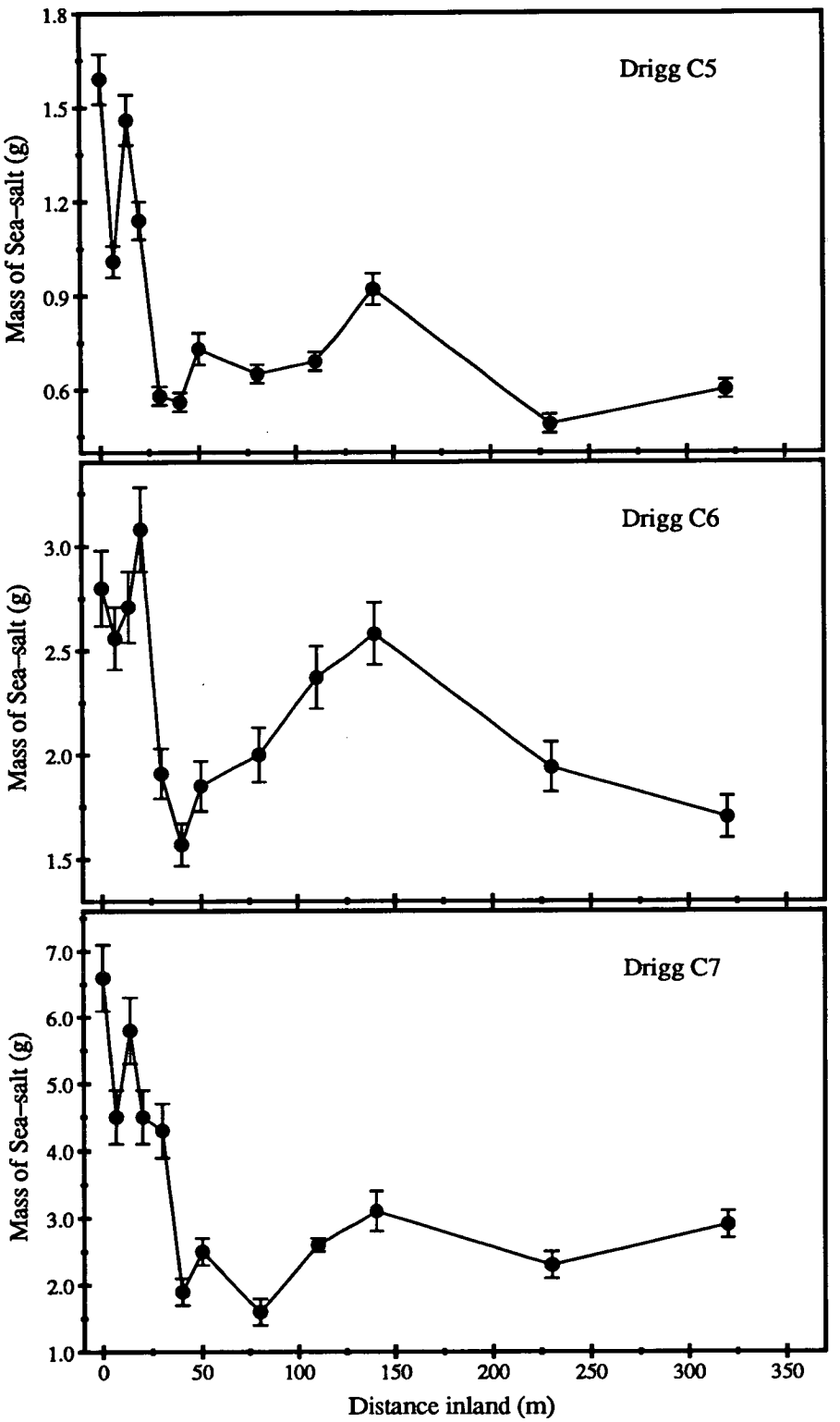

Figure 3.15: Sea-salt collected on muslin screens exposed along transect C during exposures C5 to C7

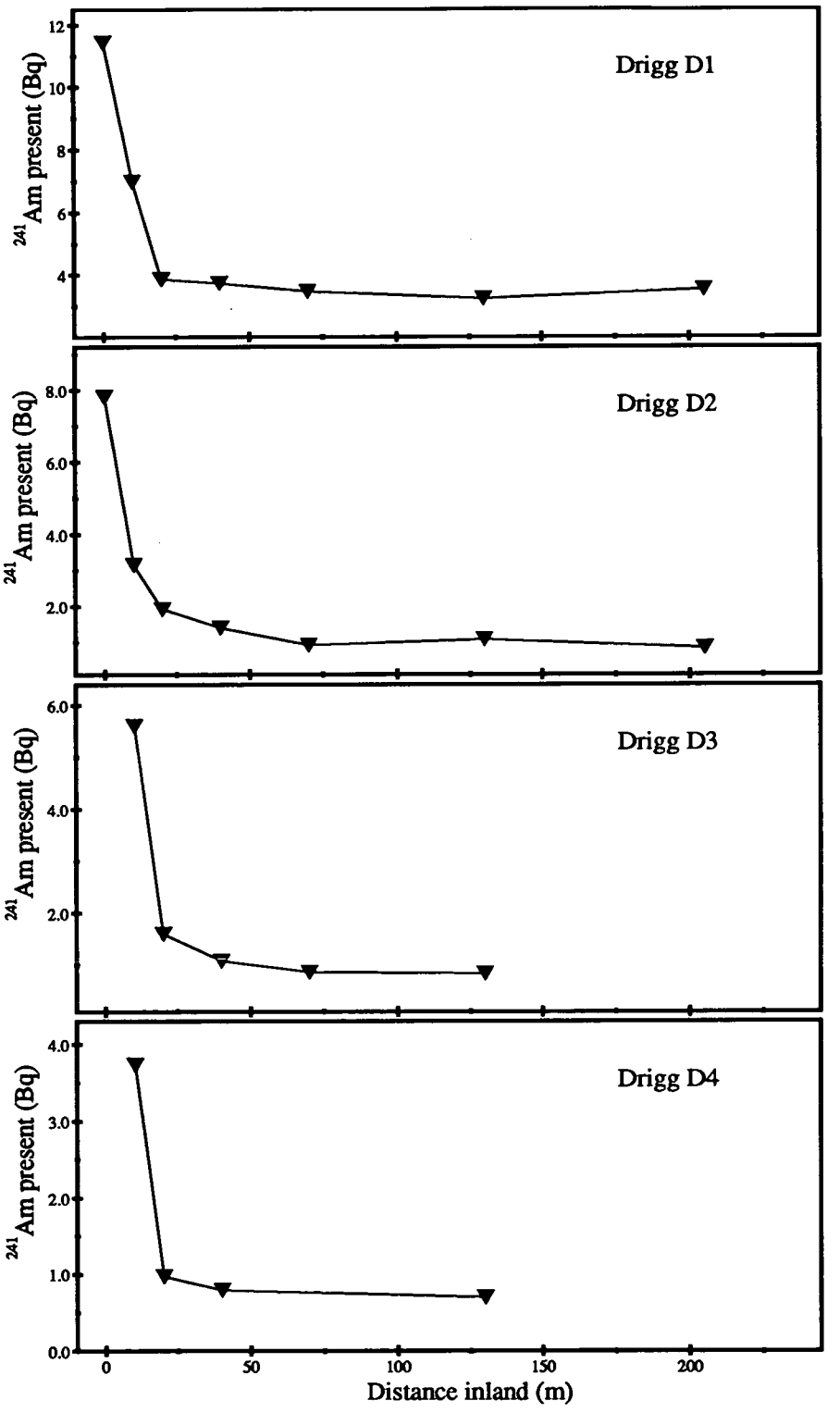

Figure 3.16: ^{241}Am collected on muslin screens exposed along transect D during exposures D1 to D4

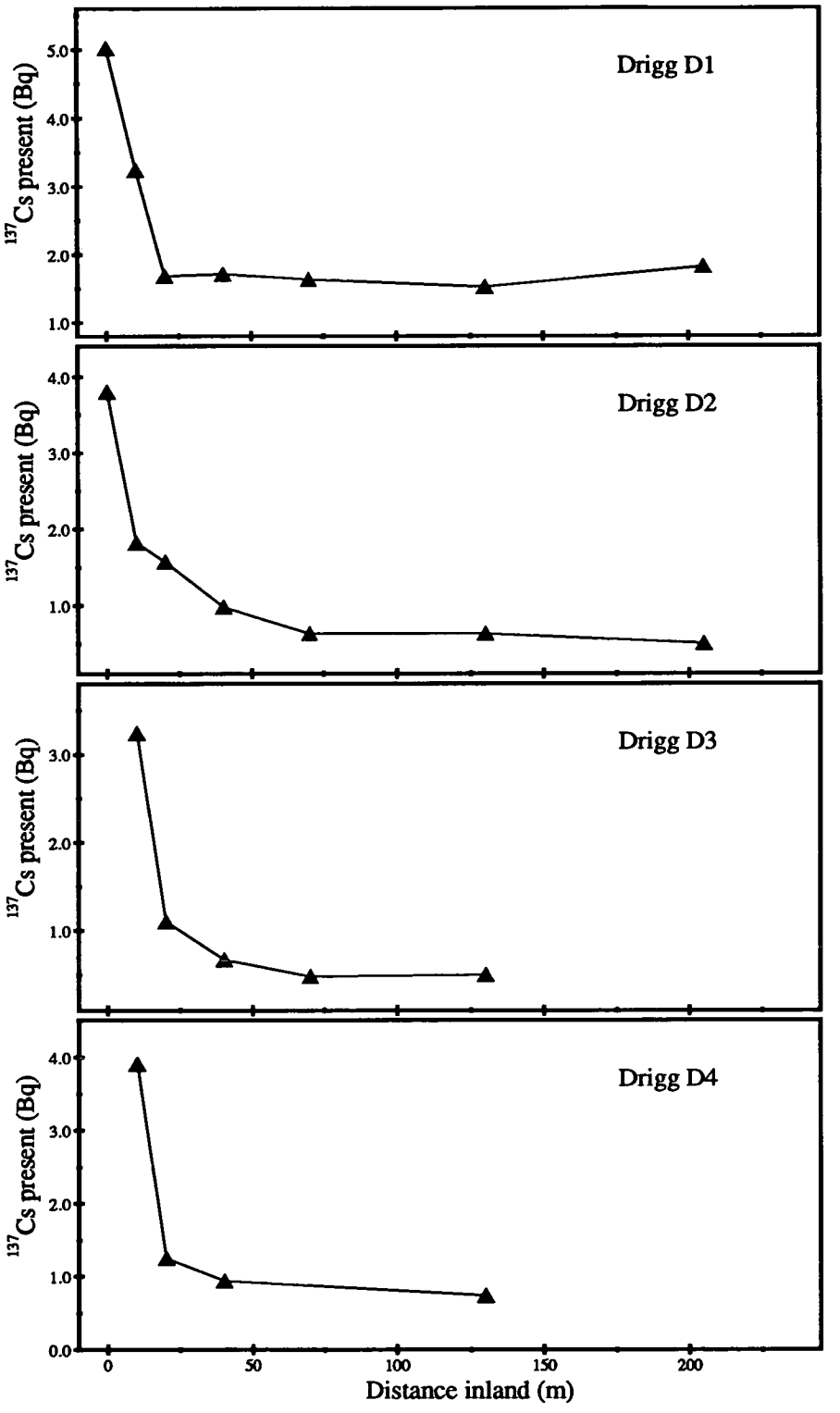

Figure 3.17: ^{137}Cs collected on muslin screens exposed along transect D during exposures D1 to D4

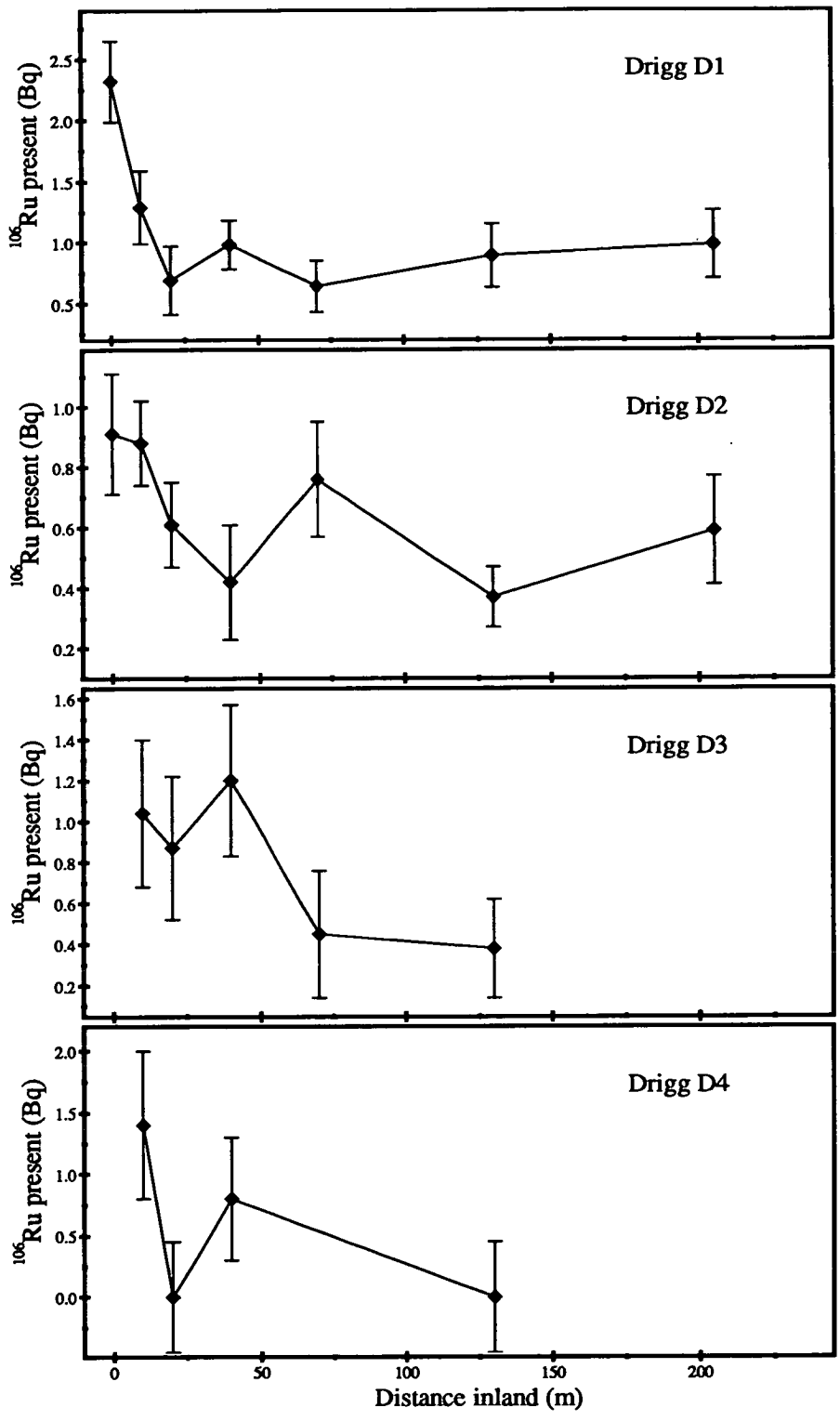

Figure 3.18: ^{106}Ru collected on muslin screens exposed along transect D during exposures D1 to D4

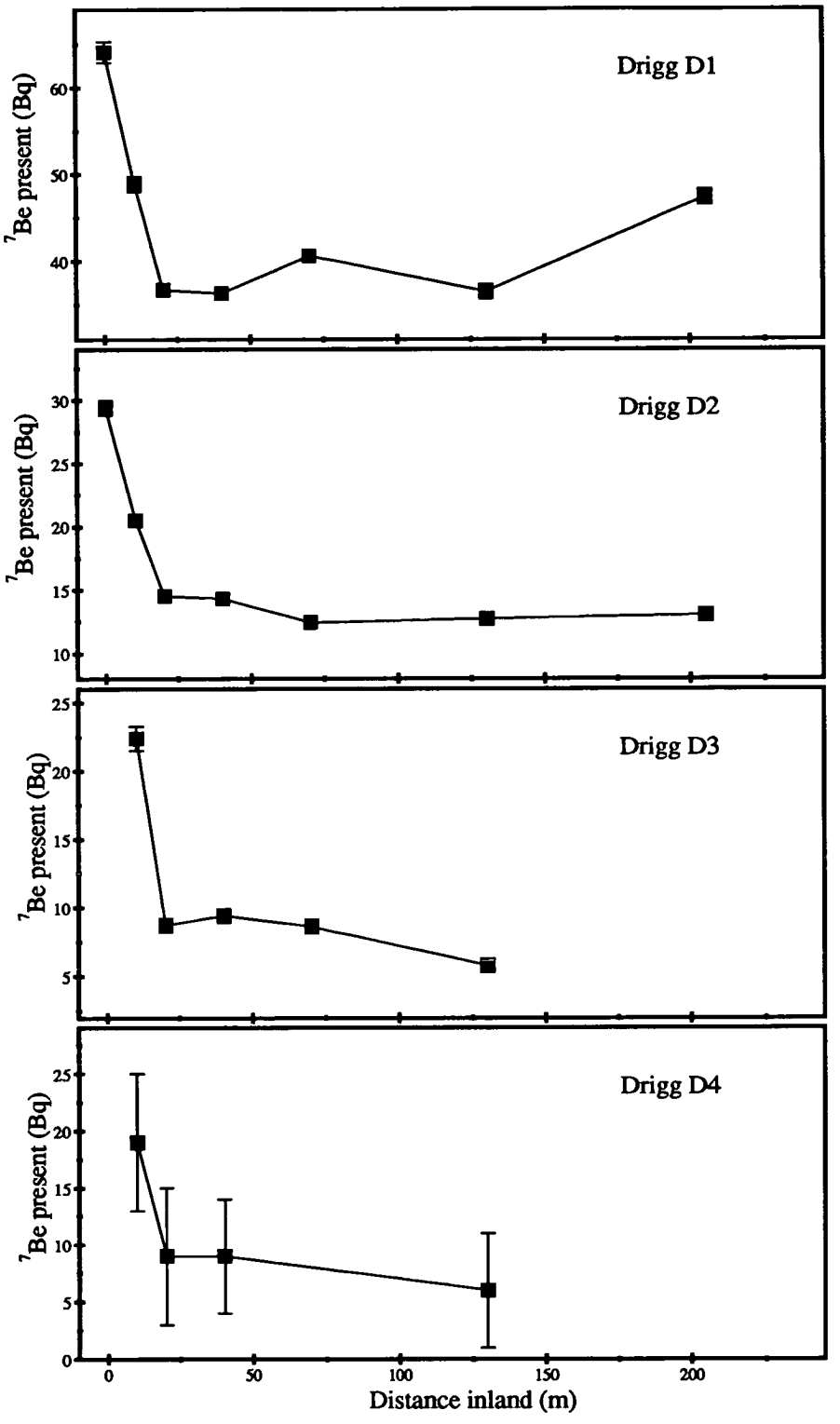

Figure 3.19: ^{7}Be collected on muslin screens exposed along transect D during exposures D1 to D4

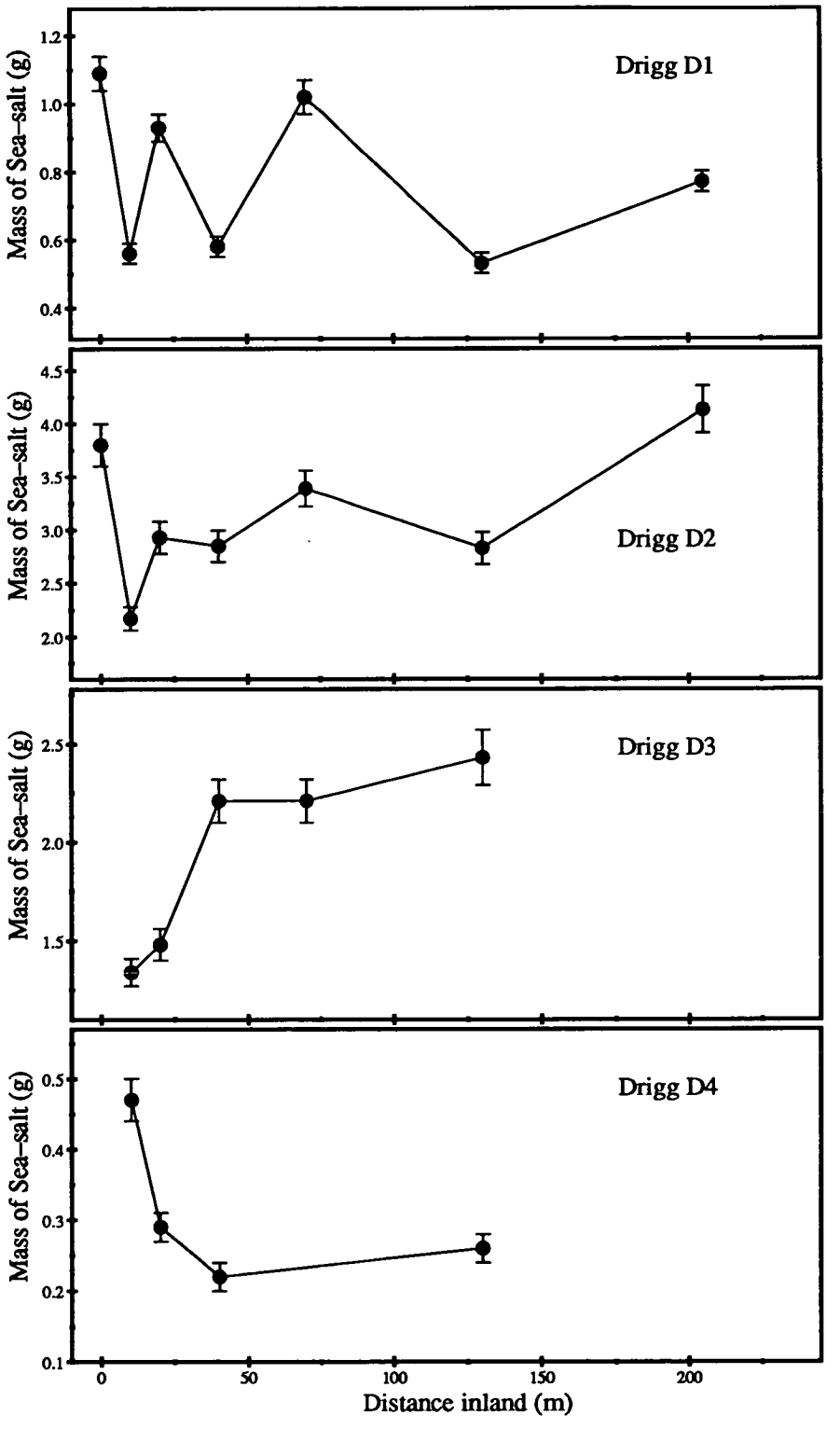

Figure 3.20: Sea-salt collected on muslin screens exposed along transect D during exposures D1 to D4

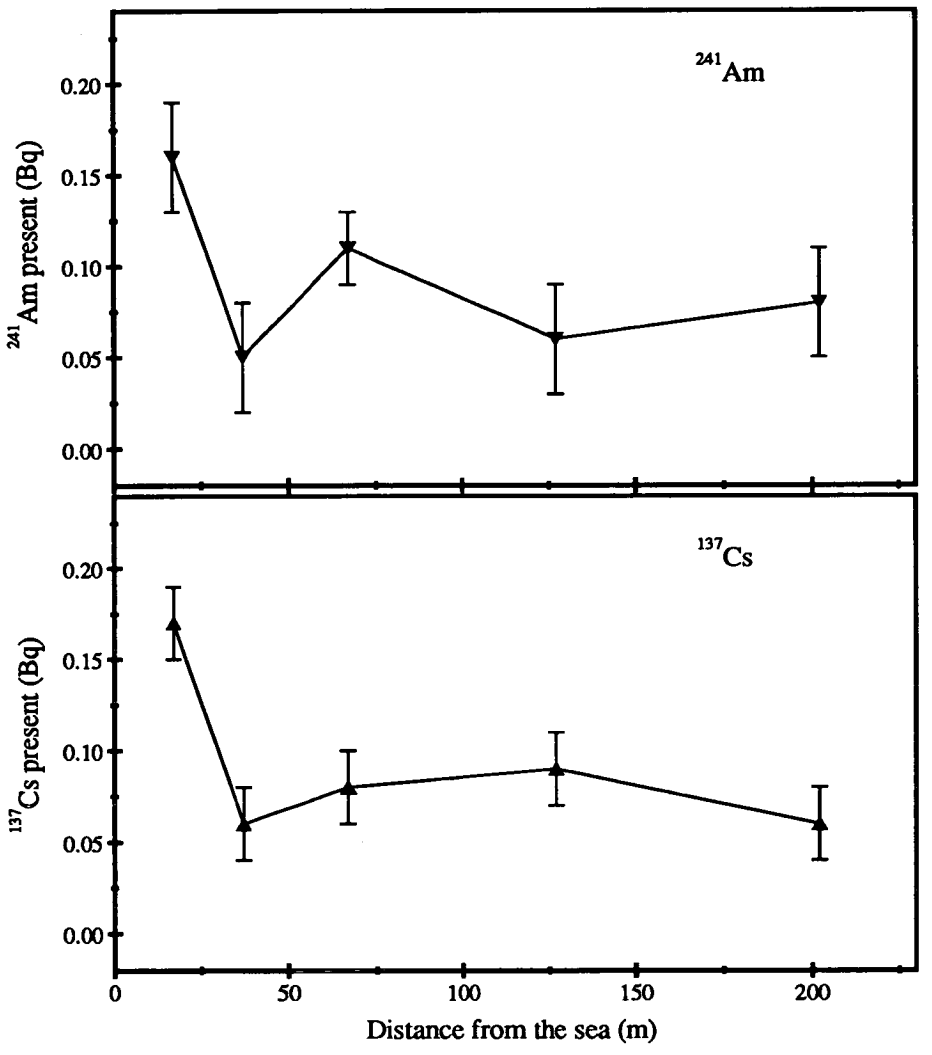

Figure 3.21: ^{241}Am and ^{137}Cs collected on muslin screens exposed along transect D during the short-term exposure S4

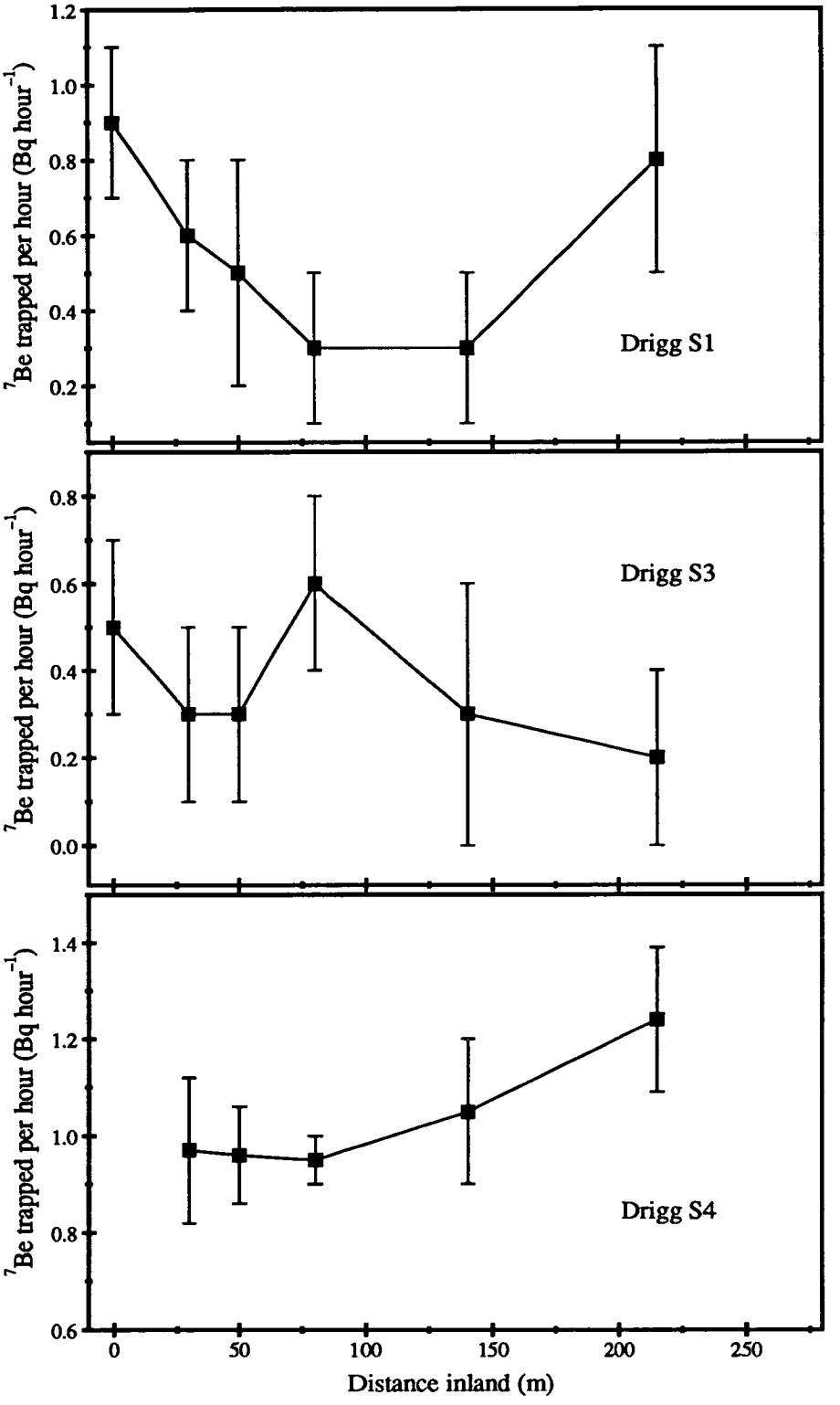

Figure 3.22: ^{7}Be collected on muslin screens exposed along transect D during the short-term exposures S1, S3 and S4

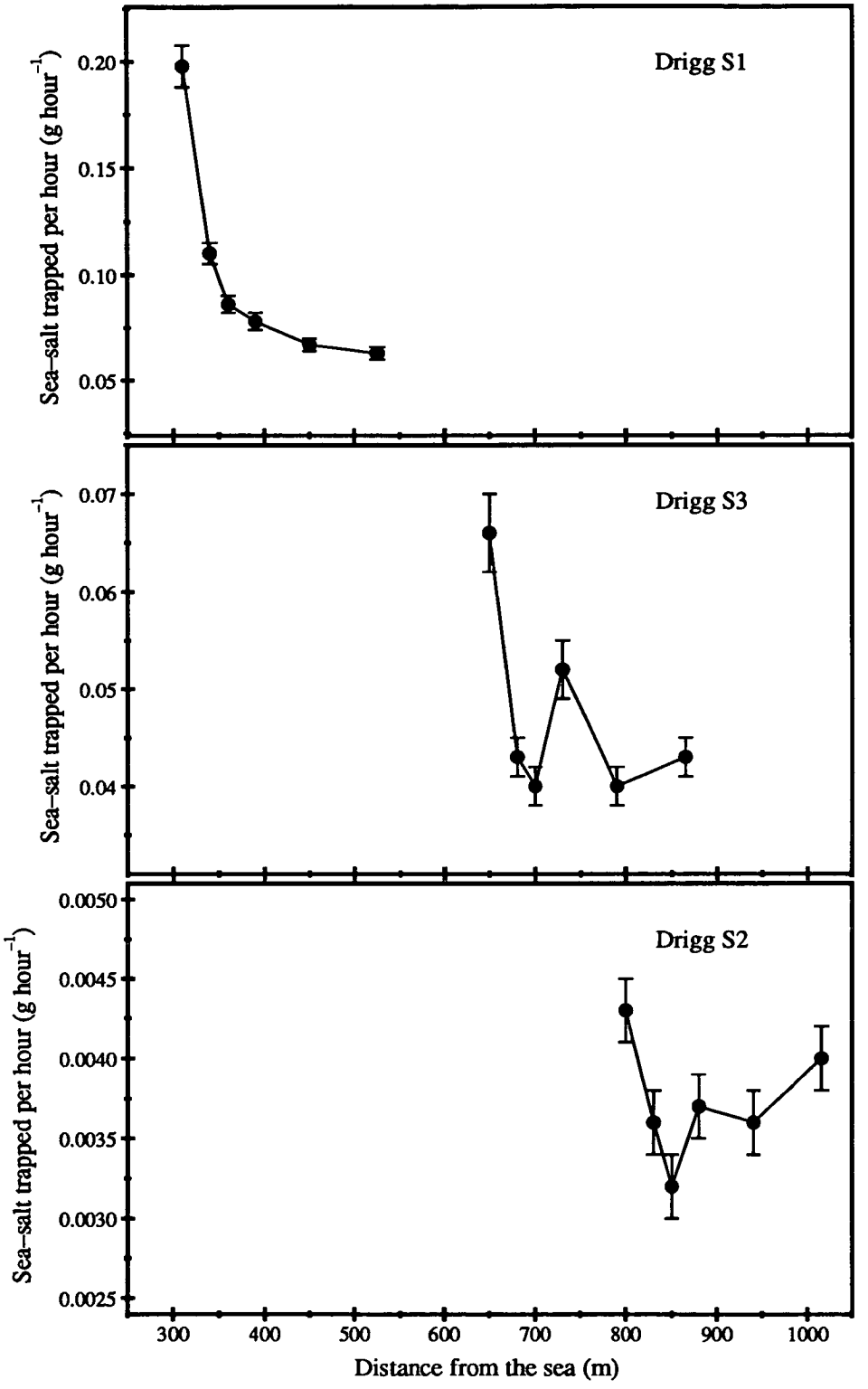

Figure 3.23: Sea-salt collected on muslin screens exposed along transect D during the short-term exposures S1, S2 and S3

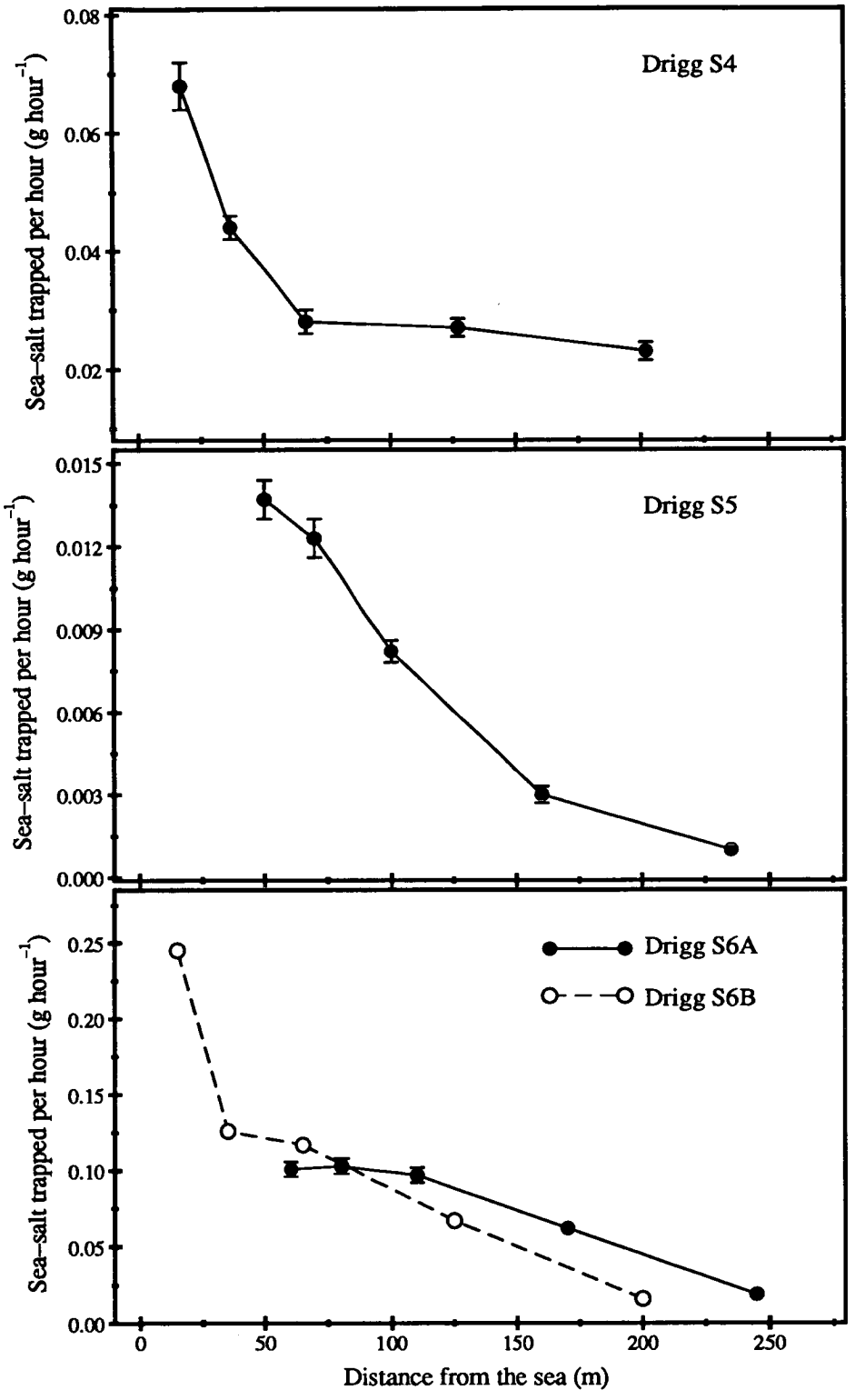

Figure 3.24: Sea-salt collected on muslin screens exposed along transect D during the short-term exposures S4, S5, S6A and S6B

3.3 Wind measurements

An analysis has been carried out on the hourly wind speed and direction data collected by the Meteorological Office at Eskmeals during the periods of the muslin screen exposures. Figures 3.25 to 3.29 illustrate the prevailing wind in this region by showing the air flux from each 10° sector during each of the long-term exposure periods. Winds from 0° are those along a compass bearing of 240°, and will have blown parallel to the Drigg transects and, therefore, perpendicularly to the exposed screens. All winds from between $\pm 90°$ in these Figures therefore came from a sea-ward direction.

Table 3.4 gives the results of a closer analysis of the wind conditions during each exposure period. The mean wind speeds recorded during each period are given in column 2. The mean *seawind* speeds, calculated by considering only winds between the compass bearings of 150° and 330°, are listed in column 5. Column 3 in Table 3.4 gives the potential wind flux through the screens exposed in each period, i.e. the total volume of air that would have passed through the $0.5\,m^2$ area occupied by a screen, set up perpendicularly to 240° winds, if the screen had not been in place. This calculation involves using different screen projections for winds from different directions. A similar process, but calculating the potential air flux through the screens only during periods when the wind was from the sea-ward direction has also been performed. In Table 3.4 these onshore wind fluxes are given in column 4 as percentages of the total fluxes in column 3.

Table 3.5 gives the details of the wind data recorded at Eskmeals at the times of the short-term screen exposures. Also given here are the mean distances from the edge of the sea to the most sea-ward screen during the course of these short-term exposures.

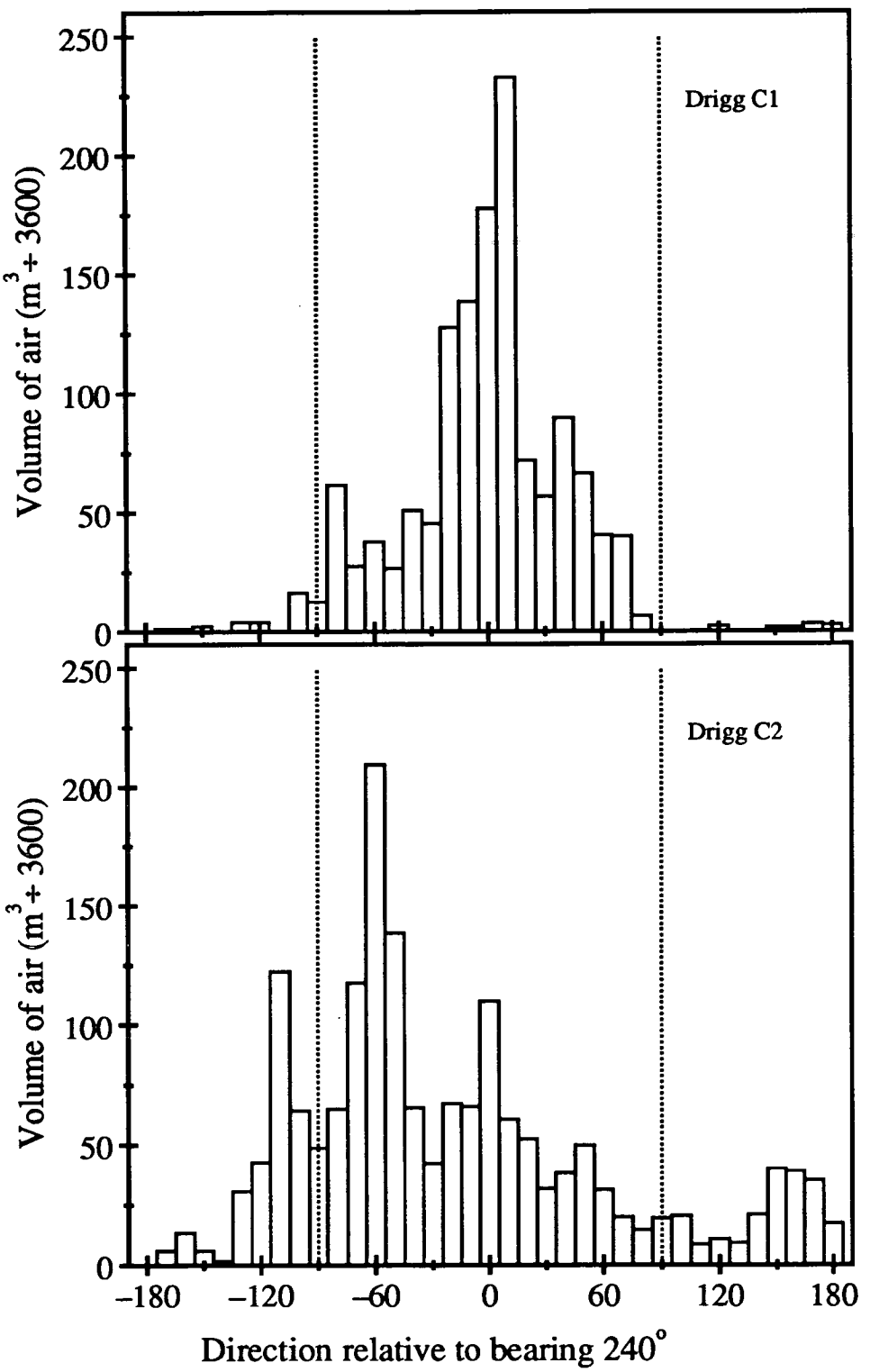

Figure 3.25: The air flux from each 10° sector during the muslin screen exposures C1 and C2. Winds from 0° were parallel to the line along the exposure transect

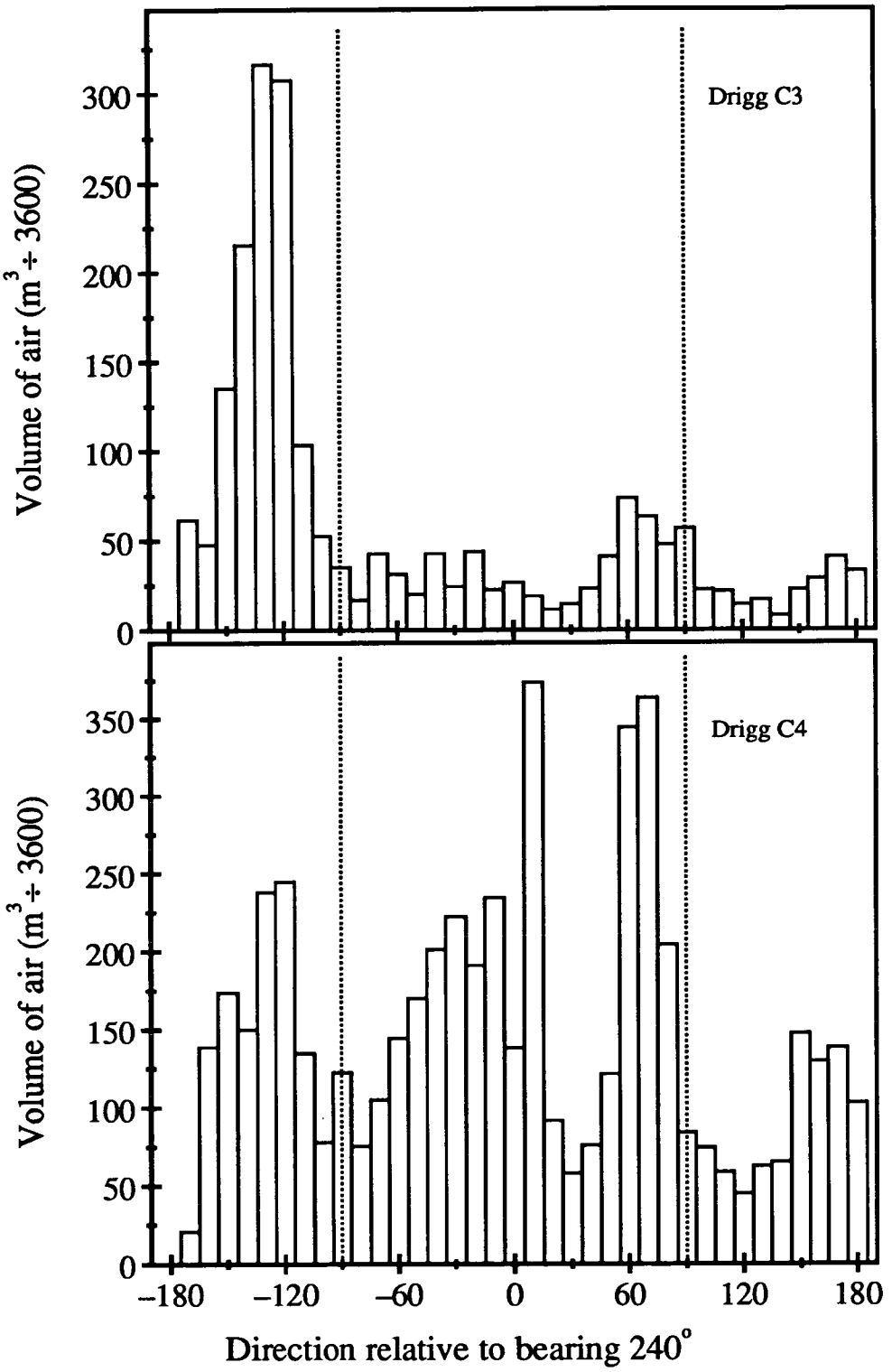

Figure 3.26: The air flux from each 10° sector during the muslin screen exposures C3 and C4. Winds from 0° were parallel to the line along the exposure transect

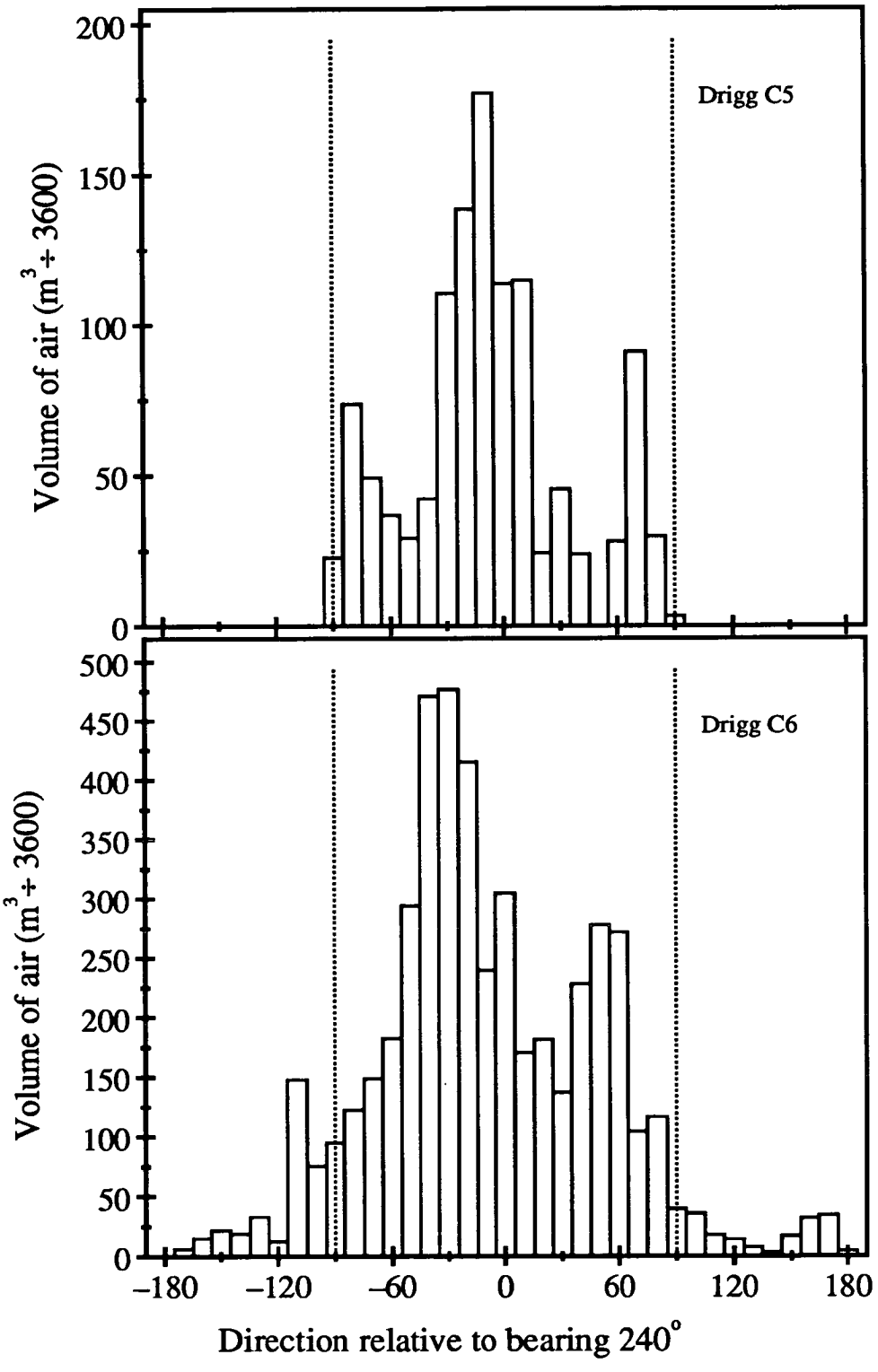

Figure 3.27: The air flux from each 10° sector during the muslin screen exposures C5 and C6. Winds from 0° were parallel to the line along the exposure transect

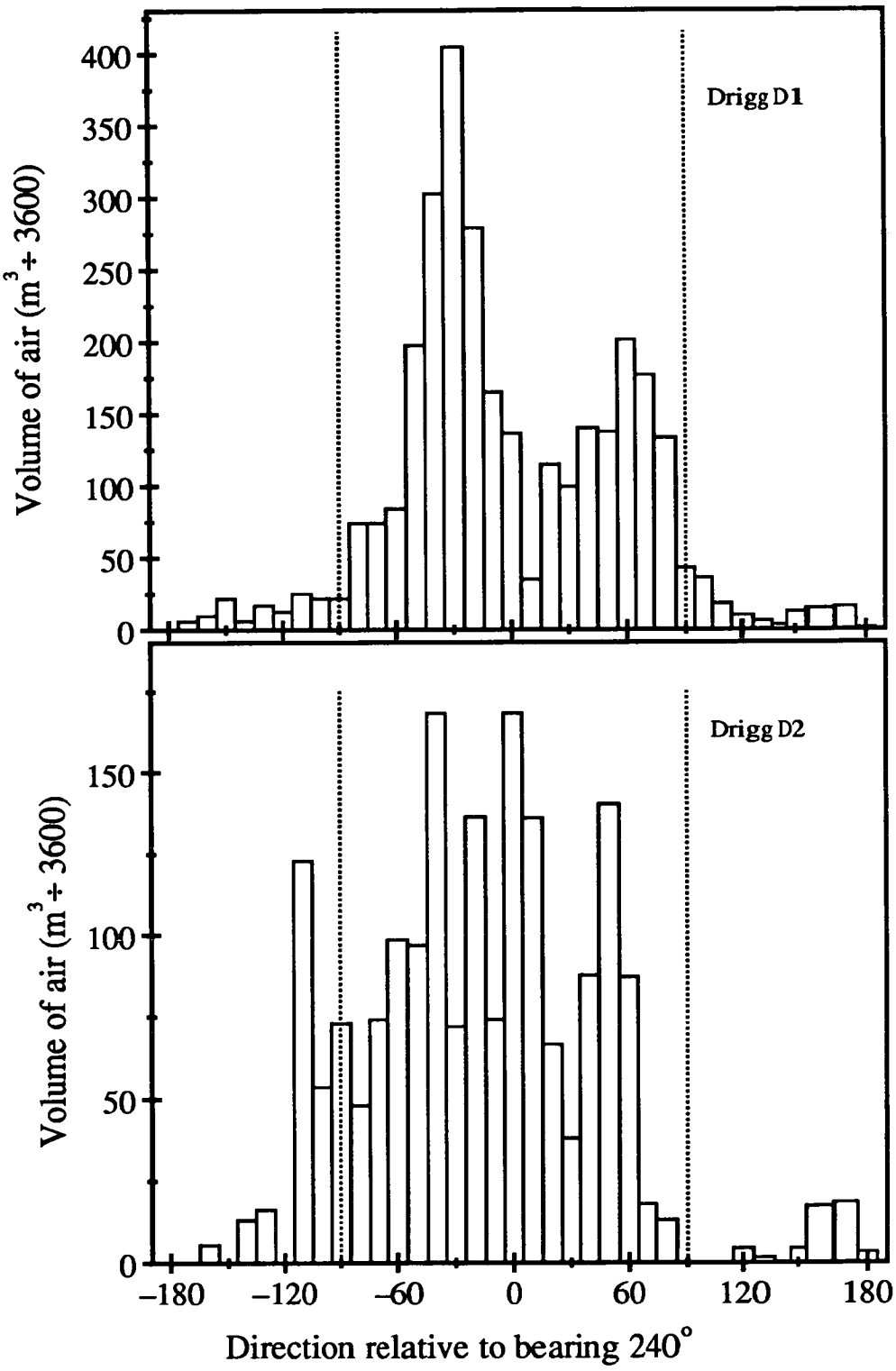

Figure 3.28: The air flux from each 10° sector during the muslin screen exposures D1 and D2. Winds from 0° were parallel to the line along the exposure transect

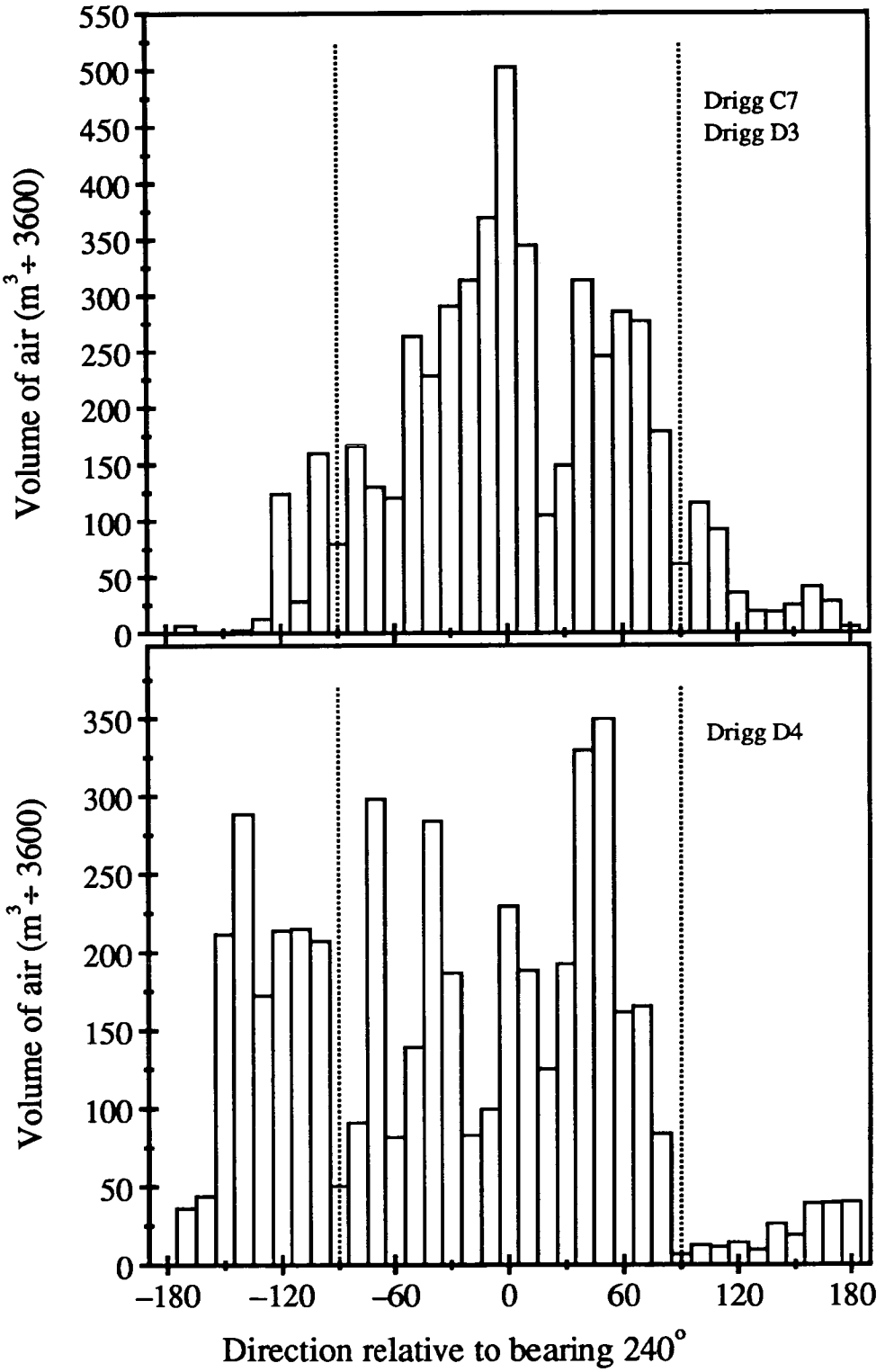

Figure 3.29: The air flux from each 10° sector during the muslin screen exposures C7, D3 (which were simultaneous) and D4. Winds from 0° were parallel to the line along the exposure transects

Exposure name	All winds		Winds from sea $150° \leq \theta \leq 330°$	
	Mean wind speed ($m\,s^{-1}$)	Volume of air through $0.5\,m^2$ ($m^3 \div 10^6$)	Volume of air as % of total flux	Mean wind speed ($m\,s^{-1}$)
C1	6.25±0.18	1.95	98.0	6.62±0.18
C2	3.45±0.10	1.93	74.1	3.81±0.12
C3	4.39±0.11	2.32	26.6	3.57±0.14
C4	3.82±0.06	6.26	60.3	4.02±0.07
C5	6.87±0.15	1.54	99.9	6.92±0.15
C6	5.84±0.11	5.96	92.3	6.46±0.12
C7	5.78±0.10	6.17	91.1	6.50±0.11
D1	6.06±0.15	3.76	93.7	6.80±0.15
D2	5.52±0.16	2.28	90.4	5.90±0.17
D3	5.78±0.10	6.17	91.1	6.50±0.11
D4	6.81±0.14	5.60	68.5	8.00±0.19

Table 3.4: Details of the wind conditions at Eskmeals during the long-term muslin screen exposures

Exposure name	Mean sea to front screen distance (m)	Mean wind speed (ms^{-1})	Wind compass bearing
S1	310	6.5	250°
S2	800	3.8	215°
S3	650	5.7	195°
S4	17	11.1	210°
S5	50	6.0	140°
S6A	60	10.8	155°
S6B	15	10.3	160°

Table 3.5: Details of the sea to screen distance and wind conditions during the short-term muslin screen exposures at Drigg D

Chapter 4

Modelling the sea-to-land transfer

The results obtained from the muslin screen exposures define the decrease in radionuclide air concentrations with distance inland from the sea. In this Chapter details of a model developed to simulate the sea-to-land transfer of sea spray are described. The Sea-to-Land Transfer Model calculates how droplets produced by the breaking waves along the shoreline behave as they are carried inland by the wind. Variation of the parameters included in the model highlights the mechanisms which have the major effect on how the air concentration of sea spray decreases with distance inland.

4.1 Description of the model

A rectilinear co-ordinate system (x,y,z) is used, with the wind blowing parallel to the x-axis with a speed $u\,m\,s^{-1}$. The spray droplets are considered to be produced above a ground-level line source lying along x=1 m, parallel to the y-axis and set at right angles to the direction of the wind flow. The height above the ground is measured along the z-axis. The air concentrations are calculated only at small distances from the source when compared to the extent of the source in the y-direction. Thus the lateral spread of the produced material with distance can be ignored, and the reduction in airborne concentration is considered

to be independent of the position on the y-axis. In the following analysis I will consider the dispersion and deposition of the droplets produced by the source between y= -0.5 m and y= $+0.5$ m, and all this material is considered to remain in the corridor, parallel to the wind flow, defined by the these y-coordinates.

The concentration of droplets present downwind of the source is calculated by solving the continuity equation, which states that the droplets produced by the source at any time t must either still be suspended at X=uT+1 m downwind at a time T s later, or have been deposited at some point between the source and X. Consider the situation where the source along x=1 m releases N droplets per metre of its length per second, and let us concentrate on the Q=N dt droplets released per unit length of source between t=0 and t=dt. The continuity equation states that, at time T:

$$\int_{-0.5}^{+0.5} Q\,dy = \int_0^{\infty}\int_{-0.5}^{+0.5}\int_1^X n(x,y,z,T)\,dx\,dy\,dz + \int_0^T\int_{-0.5}^{+0.5}\int_1^X v_g\,n(x,y,0,t)\,dx\,dy\,dt \qquad (4.1)$$

where n(x,y,z,t) is the number of the droplets released between t=0 and t=dt present per unit volume at (x,y,z) at time t. The first term on the right-hand side of Equation 4.1 integrates the number of droplets still suspended in the air at time T. The second term integrates the number of droplets which have been deposited between the source and X. The parameter v_g is the deposition velocity of the particles to the ground, using the definition of Chamberlain [11].

Equation 4.1 is satisfied by an expression of the form:

$$n(x,y,z) = \frac{Q}{u\,z_x} exp\left(\frac{v_g}{u(1-p)z_0}\right) exp\left(-\frac{v_g\,x}{u(1-p)z_x}\right) exp\left(-\frac{z}{z_x}\right) \qquad (4.2)$$

where n(x,y,z), with units of m^{-3} s, is the time integrated concentration of the droplets at (x,y,z) over the time T:

$$n(x,y,z) = \int_0^T n(x,y,z,t)\,dt \qquad (4.3)$$

The representation of the concentration downwind of the source in Equation 4.2 was calculated from a consideration of the instantaneous release of droplets between t=0 and t=dt. A similar expression is valid for extended or

continuous releases. The steady-state air concentration downwind of a source emitting N droplets per unit length per second is given by:

$$n(x,y,z) = \frac{N}{u\,z_x} exp(\frac{v_g}{u(1-p)z_0}) exp(-\frac{v_g\,x}{u(1-p)z_x}) exp(-\frac{z}{z_x}) \qquad (4.4)$$

where n(x,y,z) now has units of m^{-3}.

At all distances downwind of the source the droplet concentration, from Equation 4.4, decreases exponentially with height. The droplets are spread to greater heights by the action of atmospheric turbulence as they are transported away from the source. Thus the concentration in the air at a distance (x−1) m from the source is given by:

$$n(x,y,z) = n(x,y,0)\, exp(-\frac{z}{z_x}) \qquad (4.5)$$

where z_x , the mean height of the aerosol, is a function of the distance travelled, with the form:

$$z_x = z_o\, x^p \qquad (4.6)$$

Directly above the source, at x=1, the droplet concentration decreases with a mean height of z_0 m. The parameter p in Equation 4.4 is that defined in Equation 4.6, and determines the efficiency with which the material is dispersed to greater altitudes by the atmospheric turbulence. This procedure of maintaining the same distribution of droplets in the air and increasing the mean height with distance to model the effects of turbulent mixing, is consistent with the suggestions of the NRPB Working Group on Atmospheric Dispersion Modelling [12].

In this simulation of the transport of airborne droplets, the droplets sediment at all heights against the effective uplift caused by the mixing action of the atmospheric turbulence. The vertical velocity at any point (x,y,z) downwind of the source is a resolution of the sedimentation of the droplets and the tendency of the turbulence to mix the suspended particles to greater altitudes. The resultant downward velocity at a point (x,y,z) is given by:

$$w_{res}(x,y,z) = v_g - \frac{u\,p\,z}{x} \qquad (4.7)$$

At ground level, z=0 m, there is a downward velocity of v_g at all values of x in all turbulence conditions. Equation 4.4, which satisfies the continuity equation,

also ensures that the droplets are deposited from the suspended plume to the ground at the rate determined by their deposition velocity.

In the absence of atmospheric turbulence, the plume would not be spread to greater heights with distance, and the parameter p, which determines the rate of mixing with distance in Equation 4.6, would have a value of 0. In such conditions the suspended particles would deposit at all points at their settling velocity and would travel a distance determined entirely by their initial height and the wind speed.

The NRPB Working Group on Atmospheric Dispersion suggested techniques whereby particle deposition can be included in models of the dispersion of radionuclides in the atmosphere [43]. This can be done by using a "source depletion" technique. Particles lost from the plume by deposition to the ground are accounted for by reducing the apparent strength of the source. Following the procedure suggested by the Working Group, and considering the diffusion from a ground level source whilst maintaining an exponential decrease in droplet concentration with height, produces an expression for the depleted source strength $Q^*(x)$ downwind of the source of the form:

$$Q^*(x) = Q exp(-\frac{v_g x}{u(1-p)z_x}) \tag{4.8}$$

This procedure fully reproduces the $exp(-\frac{v_g x}{u(1-p)z_x})$ term in Equation 4.4 which accounts for the deposition of the suspended droplets in the Sea-to-Land Transfer Model developed here as a solution of the continuity equation 4.1.

It is necessary to discuss the value that the deposition velocity of the different sized droplets should take in this Sea-to-Land Transfer Model. For larger droplets, greater than $10\,\mu$m diameter, the deposition mechanism tends to be dominated by gravitational sedimentation, and v_g will have a value equal to the terminal velocity of the droplets. The terminal velocity of a particle of diameter D, $v_s(D)$, is calculated from Stokes Law to be:

$$v_s(D) = G\,D^2 \tag{4.9}$$

This relationship is strictly only valid for particles of diameter below $60\,\mu$m and will over-estimate for larger droplets by ignoring the form drag on the sedimenting

droplets [55]. The value of G in Equation 4.9 used to determine the terminal velocity of the droplets is $6.4\times10^{7}\,m^{-1}s^{-1}$ and will give the terminal velocity in $\mathrm{m\,s^{-1}}$ when D is measured in m. This value of G is calculated by considering the sedimentation of spherical particles of density $2\,\mathrm{g\,cm^{-3}}$ [24][73].

For smaller droplets, the possibility that they can be moved downwards to the surface by the action of the turbulence increases the rate of deposition over that determined by their gravitational sedimentation velocity. Thus v_g in Equation 4.4 will have a value v_T, greater than the particle settling velocity. This matter is discussed in more detail the next Section.

It is necessary to develop the model to represent more fully the transfer of sea spray inland from the surf zone. The spray droplets produced in the surf zone along the coastline will have a range of diameters, from D_{min} to D_{max}. The shape of the droplet size distribution was discussed in Section 1.4.1. The volume of sea spray droplets per unit volume of air at (x,y,z) downwind of the source along x=1 m is calculated by integrating over the droplet size range to give:

$$V(x,y,z) = \int_{D_{min}}^{D_{max}} \frac{N}{u\,z_x} F(x,z) \frac{A_3\pi}{6} S(D)\,dD \qquad (4.10)$$

where F(x,z) is defined as:

$$F(x,z) = exp(\frac{v_g}{u(1-p)z_0})exp(-\frac{v_g\,x}{u(1-p)z_x})exp(-\frac{z}{z_x}) \qquad (4.11)$$

and $A_3\frac{\pi}{6}$ S(D) dD gives the volume of spray contained in droplets with diameter between D and D+dD, as defined in Equations 1.3 and 1.4. In this case the source is considered to produce $\mathrm{N}\,A_3\,exp(-(log\frac{D}{D_0})^2)$ dD droplets of diameter between D and D+dD per unit length per second over the period of the release.

Equation 4.10 gives a calculation of the spray volume per unit volume of air downwind of the line source at x=1 m. It is of interest here to simulate the collection of the released spray by several different collection techniques at different distances from the source. The basic model of the dispersion and deposition of spray droplets can be developed to perform such calculations.

For example, it is of interest to calculate the volume of spray droplets which will pass through the area covered by muslin screens exposed downwind of the source. If the screen exposed a distance (x−1) m from the source has its bottom

left and top right corners at co-ordinates (x, y_1, z_1) and (x, y_2, z_2) when looked at in the direction of the wind flow, then the total spray volume that will pass through it in the time between t=0 and t=T s is given by C(x), calculated from:

$$C(x) = \int_0^T \int_{y_1}^{y_2} \int_{z_1}^{z_2} u\, V(x, y, z)\, dz\, dy\, dt \tag{4.12}$$

It is also of interest to determine the volume of spray that will be deposited to the ground at different distances downwind of the source. The volume of spray deposited per unit ground area is calculated from:

$$L(x, y) = \int_0^T \int_{D_{min}}^{D_{max}} v_g \frac{N}{u\, z_x} F(x, 0) \frac{A_3 \pi}{6} S(D) dD\, dt \tag{4.13}$$

where it is necessary to include v_g in this integration as it is a function of droplet diameter D.

It is also possible to develop the Sea-to-Land Transfer Model to simulate the situation of extended releases from a source which moves relative to the collection sites. (The surf zone will have moved over a large distance between low and high tides in the course of the long-term muslin screen exposures). This situation is modelled here by integrating the volume of spray at (x,y,z) released from a series of thin area sources, of width dx, positioned between x=1 m, the low-tide mark, and x=W m, the high-tide mark. This will realistically model the falloff in air concentration with distance downwind from a source which moves a distance (W-1) m from low to high tide over the course of the release of the spray droplets. The total volume of spray at (x,y,z) from such a moving source is given by:

$$V_W(x, y, z) = \int_0^{W-1} V(x - x', y, z)\, dx' \tag{4.14}$$

where V(x,y,z) is that defined in Equation 4.10. The source is now required to be considered as a thin strip, and not as a line, as in Equation 4.10. The parameter N used to calculate V(x,y,z) in Equation 4.10 and subsequently to calculate V_W(x,y,z) must now, therefore, be the number of particles released from an area of source of length 1 m and width dx′ per second; i.e. N must have units of $m^{-2}s^{-1}$. V_W(x,y,z) calculated from Equation 4.14 will then give the spray volume concentration downwind of the source as it moves between the distances of (x−1) and (x−W) m from the collection site at x.

4.2 Model input parameter values

If the model described above is to simulate the inland transfer of sea spray in a physically realistic fashion, the values which the different input parameters can take must be constrained. In this section, from a review of the relevant literature, the range of values reasonable for each of the parameters will be discussed. The necessity of using values far from the expected ranges to produce good fits to the experimental data will expose inadequacies in the model.

The first points to consider are the details of the aerosol plume likely to be produced by local breaking waves. The shape of the aerosol spectrum produced by the source used in this model is that introduced in Section 1.4.1. The size distribution S(D) used is that defined in Equation 1.4. The size range of aerosols produced by breaking waves is considered to begin at a diameter of $1\,\mu$m. Droplets of size smaller than this are considered not to be collected by the muslin screens. The upper limit of the distribution of droplets produced by bubble bursting is in the range 100–200 μm.

Few measurements investigating the droplet distribution with height above breaking waves have been reported. From laboratory measurements, it has been stated that droplets produced by breaking waves can be thrown up to a height of 0.2 m above the surface [3]. De Leeuw discusses the existence of a wind-induced upward air motion close above the sea surface which can carry the aerosol from the production zone to higher altitudes [16]. In the absence of any real data on the distribution of locally produced droplets above the sea, the assumption of an exponential decrease with height is reasonable. Values of z_0 in the range 0.2 to 0.4 m seem to give realistic estimates of the distribution of the sea spray in the air before it is blown inland.

The value of W, the distance between low and high tides, will obviously vary at different sites. At a single site it will also change over the tidal cycle and with time of year. On the beach at Drigg used in the present study it is of the order of 1 km.

Considering the expected vertical mixing of the plume by atmospheric turbulence, Pasquill & Smith give estimates of the vertical spreads from surface sources

in a range of atmospheric conditions [61]. With the vertical spread increasing with x^p, the parameter p typically changes from 0.65 to 0.95 in going from stable to unstable atmospheric conditions, with a value of 0.8 reasonable for neutral conditions. Values of p in this range can also be obtained by fitting equations of the form $\sigma_z = a\,x^p$ to plots of vertical mixing with distance for Gaussian plumes suggested for use in dispersion models by the NRPB Working Group [12].

Smith et al. discuss the loss mechanisms for spray droplets from the air at a coastal site [73]. For particles of diameter between 1 and 10 μm the deposition velocity is expected to be dominated by turbulence and is not size dependent. Smith et al. estimate a typical v_g of 0.5 cm s^{-1} for the smaller aerosol. This is reasonably consistent with the conclusions of Slinn & Slinn [70], who stated that the deposition velocity of particles with diameter close to 2 μm is expected to be independent of size and equal to a limiting value set by the atmospheric turbulence. In winds of the order of 5 ms^{-1} this turbulent velocity, v_T, is estimated to be 0.6 cm s^{-1}, equal to the sedimentation velocity of 10 μm droplets as calculated from Equation 4.9. In this model all droplets of diameter between 1 and 10 μm are considered to deposit at a velocity of 0.6 cms^{-1}, to allow the possibility of their being dumped onto the ground by turbulence. For larger droplets the deposition velocity is dominated by their terminal velocity, and is given a value equal to v_s(D) m s^{-1} calculated from Equation 4.9.

The wind speed is normally expected to increase with height above the ground, but in this model it is assumed to be constant with height. This is again consistent with the advice of the Working Group on Atmospheric Dispersion [12]. The value of the mean wind speed measured by the Meteorological Office at Eskmeals at a height of 10 m during the course of the muslin screen exposures is used at all heights in making fits to these data sets.

The default values of the different input parameters used in the Sea-to-Land Transfer Model, as discussed in this section, are given in Table 4.1. Unless explicitly stated, these values have been ascribed to each input parameter to produce the model outputs in the subsequent discussions of model sensitivity and fits to the experimental data.

Input Parameter	Description	Default Value
G	Terminal velocity constant (Equation 4.9)	$6.4\times10^{7}\,\mathrm{m^{-1}s^{-1}}$
v_T	Turbulent deposition velocity	$0.6\,\mathrm{cm\,s^{-1}}$
D_0	Mode diameter in aerosol spectrum	$4\,\mu\mathrm{m}$
D_{min}, D_{max}	Range of droplet sizes	$1\text{–}150\,\mu\mathrm{m}$
z_0	Initial droplet distribution with height	0.3 m
W	Inter-tidal distance	1 km
x_0	Minimum sea to collection site distance	10 m
z_1, z_2	Screen collection heights	0.8, 1.4 m

Table 4.1: Default values of the input parameters in Sea-to-Land Transfer Model.

4.3 Model sensitivity to input parameters

In this section outputs from the Sea-to-Land Transfer Model produced by using a range of input parameters are discussed and contrasted. This allows an elucidation of the mechanisms which most affect the dispersion and deposition of the sea spray sized droplets, and which are therefore most significant in determining the shape of the reduction in droplet concentration with distance from the source.

In this discussion the collection of spray by the muslin screens exposed along the Drigg C transect has been simulated by calculating the volume of spray present between the heights of 0.8 and 1.4 m at different distances downwind of the source. To begin, the falloff patterns from stationary sources are discussed. Later the reduction in airborne concentration downwind of sources which move relative to the collection sites is considered.

It is of interest to compare the behaviour of different sized droplets. This is done by considering sources which emit droplets of a single diameter. Figure 4.1 plots the decrease in aerosol concentration downwind of stationary sources producing mono-disperse plumes of 5, 50 and 100 μm diameter droplets. The values of the other parameters are held constant. The source was positioned 10 m upwind of the first collection site. The concentration reduces more rapidly for the larger droplets, as may be expected because they sediment from the plume more rapidly.

Figure 4.2 shows the decrease downwind of a source producing only 100 μm diameter droplets in a range of wind conditions. The concentration decreases less rapidly in higher wind speeds, as would be expected if deposition of droplets from the plume is a significant loss mechanism. By contrast, the falloff of these 100 μm droplets changes only slightly over the whole range of atmospheric turbulence conditions (Figure 4.3). The conclusion to be drawn here is that the reduction in concentration of 100 μm diameter droplets with distance is caused by the droplets depositing to the ground out of the plume. The tendency of turbulence to mix the droplets to greater heights has very little effect in reducing the air concentration downwind of the source.

In contrast, the falloff of the smallest droplets produced in the source is

determined almost totally by turbulent processes, as illustrated in Figures 4.4 and 4.5 for droplets of diameter of 5 μm. The reduction with distance remains unchanged over a wide range of wind speeds but is very sensitive to the intensity of atmospheric turbulence. The major part of the reduction in air concentration near ground level therefore appears to be caused by the droplets being mixed to increased heights with distance. Droplet deposition has little effect in reducing the concentration of these small sized droplets at increased distances from the source.

It is now time to consider the shape of the reduction in air concentration downwind of a stationary source which produces droplets with a size spectrum typical of sea spray from breaking waves. Figure 4.6 shows the falloff in two contrasting wind conditions. Figure 4.7 plots how the reduction pattern changes in a range of turbulence conditions. The pattern is affected by both wind speed and turbulence changes, as may be expected for a plume which contains both small and large droplets.

The effect on the falloff pattern of changing z_0, the parameter which determines the distribution of the droplets in the air above the source, is shown in Figure 4.8. There is a significant change in the falloff shape caused by changing z_0 from 0.1 to 0.2 m. The output appears to be much less sensitive to further increases in z_0. The reason for the initially increasing concentration in the output with z_0=0.1 m is that at any height H, the concentration will increase with distance as long as z_x<H. The concentration will begin to decrease beyond the distance downwind of the source where $z_x \simeq$H.

Consider how the airborne droplet concentration decreases downwind of a source which moves relative to the collection sites. The falloff pattern is flattened by allowing the source to move to greater distances (Figures 4.9 and 4.10). Allowing the source to come closer to the collection sites will make the decrease with distance more rapid.

The model outputs from a source moving between 10 and 1000 m from the front collection site in different wind speed and atmospheric turbulence conditions are illustrated in Figures 4.11 and 4.12. More intense turbulence significantly increases the rate at which the aerosol concentration decreases with distance.

Decreasing p from 0.95 to 0.8, which is equivalent to changing the atmospheric stability from unstable to neutral, increases the airborne concentration at 350 m relative to that at the site nearest the source, by 25%. By contrast, large variations in wind speed only slightly change the falloff pattern. Doubling u from $5\,ms^{-1}$, (typical of the mean wind speed during the muslin screen exposures), to $10\,ms^{-1}$ increases the concentration at 350 m by only 4%. The falloff pattern downwind of a moving source producing a droplet spectrum similar to that expected from a surf zone is thus apparently more dependent on the turbulence condition of the atmosphere than on the wind speed.

Figure 4.13 illustrates how loading the spray spectrum towards larger droplet sizes, by increasing the mode diameter of the distribution D_0, increases the falloff rate. Increasing D_0 from 4 to 8 μm decreases the concentration at 350 m by 12%. This also has the effect of making the spray dispersion more dependent on the wind speed and less dependent on the intensity of turbulence.

Figure 4.14 shows how the droplet concentration downwind of a moving source is affected by changes in the z_0 parameter. Increasing z_0 from 0.3 to 0.7 m has little effect on the falloff pattern. However, the model output is sensitive to changes in z_0 below 0.2 m.

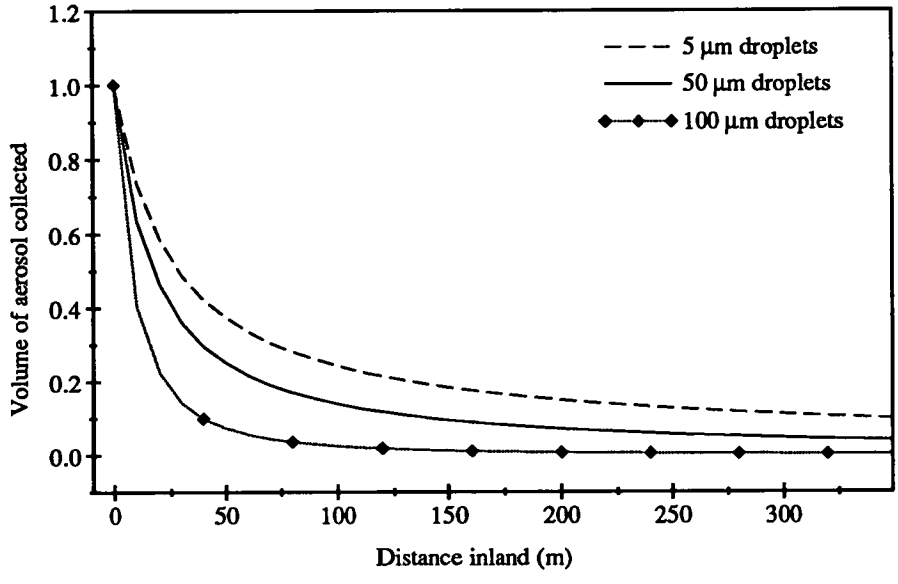

Figure 4.1: Output of the Sea-to-Land Transfer Model. Sources producing monodisperse plumes of droplets of diameter 5, 50 and 100 μm. Source to front site=10 m. p=0.8, u=5 ms^{-1}, z_0=0.3 m.

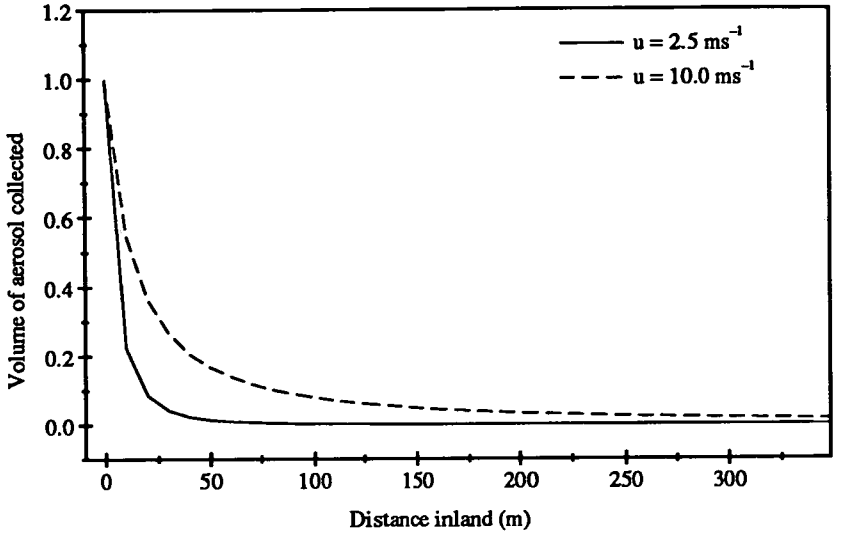

Figure 4.2: Output of the Sea-to-Land Transfer Model. Source producing mono-disperse plume of droplets of diameter 100 μm. Source to front site=10 m. p=0.8, u=2.5 and 10.0 ms^{-1}, z_0=0.3 m.

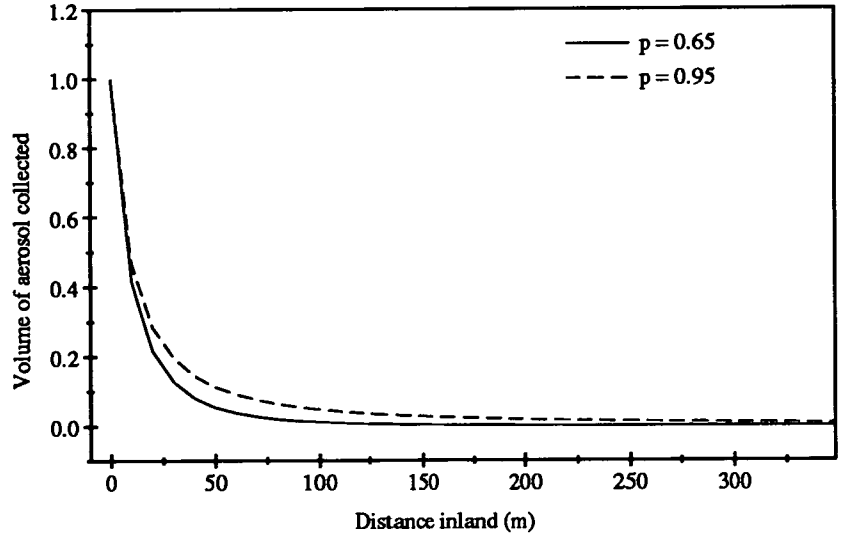

Figure 4.3: Output of the Sea-to-Land Transfer Model. Source producing mono-disperse plume of droplets of diameter 100 μm. Source to front site=10 m. p=0.65 and 0.95, u=5.0 ms^{-1}, z_0=0.3 m.

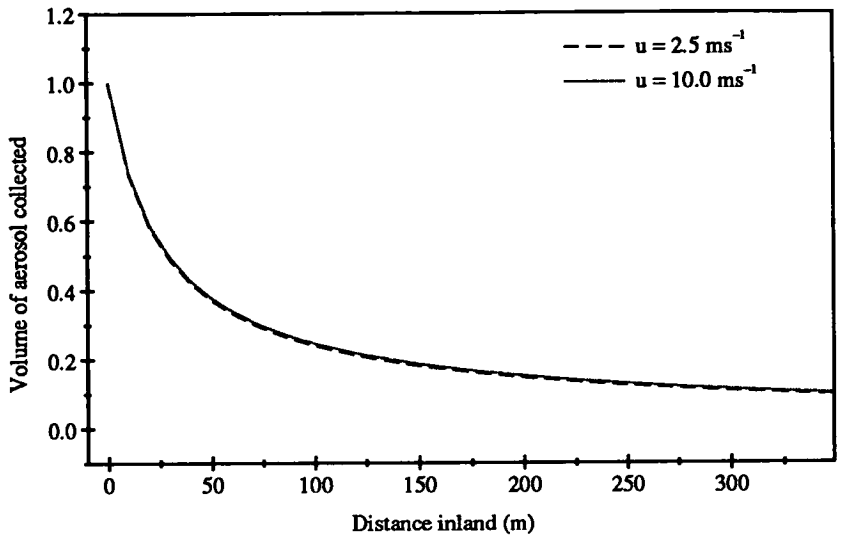

Figure 4.4: Output of the Sea-to-Land Transfer Model. Source producing mono-disperse plume of droplets of diameter 5 μm. Source to front site=10 m. p=0.8, u=2.5 and 10.0 ms^{-1}, z_0=0.3 m.

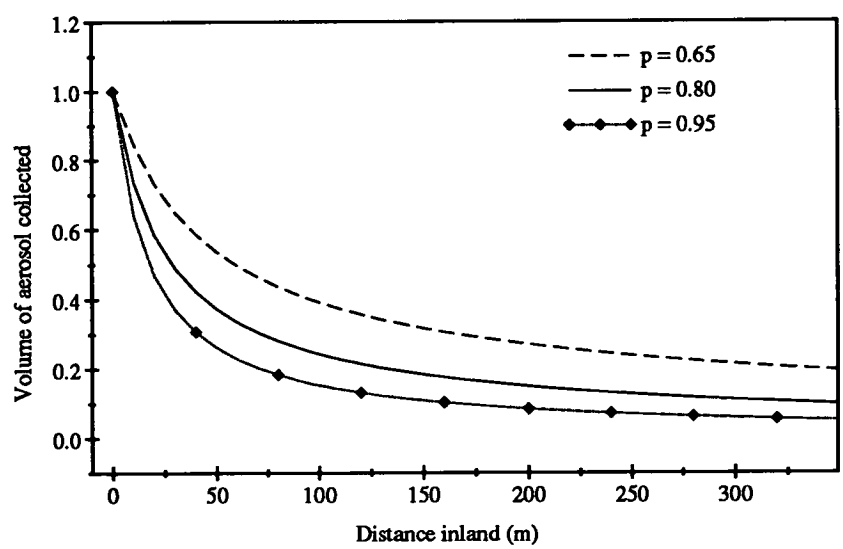

Figure 4.5: Output of the Sea-to-Land Transfer Model. Source producing mono-disperse plume of droplets of diameter 5 μm. Source to front site=10 m. p=0.65, 0.80 and 0.95, u=5.0 ms^{-1}, z_0=0.3 m.

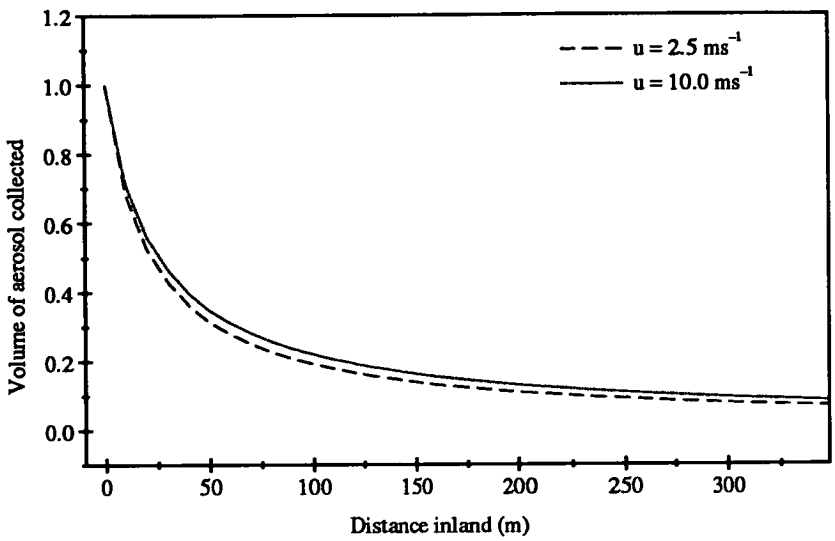

Figure 4.6: Output of the Sea-to-Land Transfer Model. Source producing spectrum of spray droplets of diameter 1–150 μm, D_0=4 μ (See Equation 1.4). Source to front site=10 m. p=0.8, u=2.5 and 10.0 ms^{-1}, z_0=0.3 m.

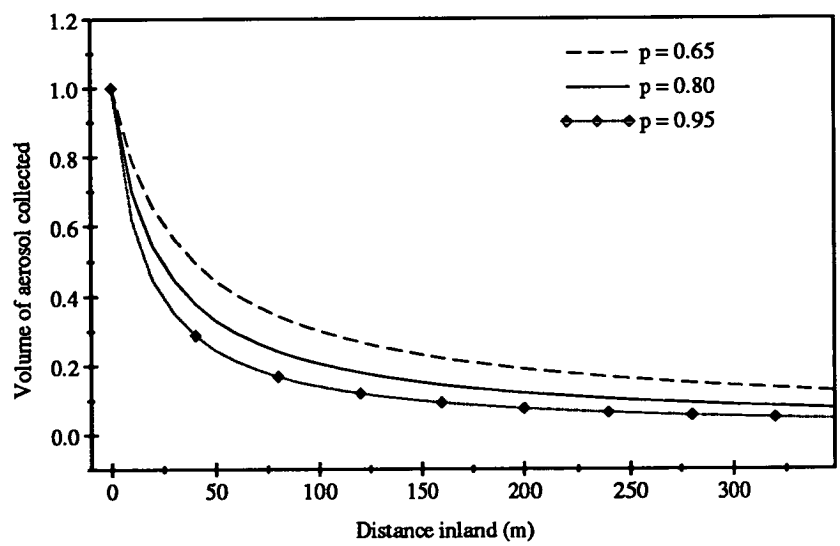

Figure 4.7: Output of the Sea-to-Land Transfer Model. Source producing spectrum of spray droplets of diameter 1–150 μm, D_0=4 μ (See Equation 1.4). Source to front site=10 m. p=0.65, 0.8 and 0.95, u=5.0 ms^{-1}, z_0=0.3 m.

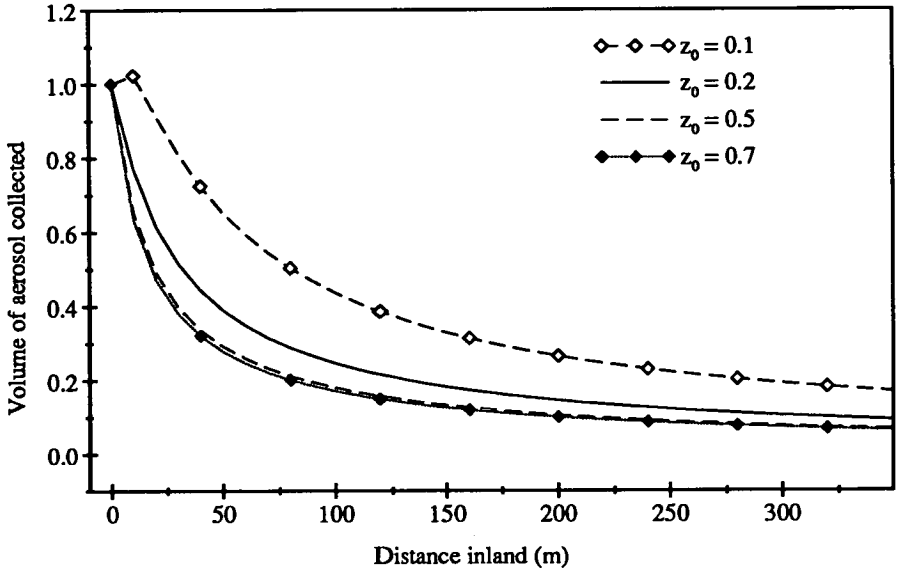

Figure 4.8: Output of the Sea-to-Land Transfer Model. Source producing spectrum of spray droplets of diameter 1–150 μm, D_0=4 μ (See Equation 1.4). Source to front site=10 m. p=0.8, u=5.0 ms^{-1}, z_0=0.1, 0.2, 0.5 and 0.7 m.

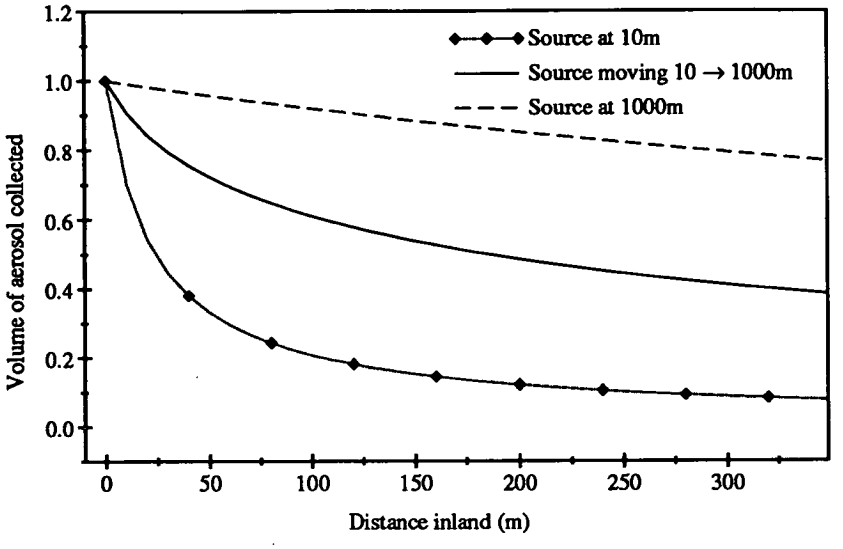

Figure 4.9: Output of the Sea-to-Land Transfer Model. Source producing spectrum of spray droplets of diameter 1–150 μm, D_0=4 μ (See Equation 1.4). Source to front site=10 and 1000 m, and moving between these extremes. p=0.8, u=5.0 ms^{-1}, z_0=0.3 m.

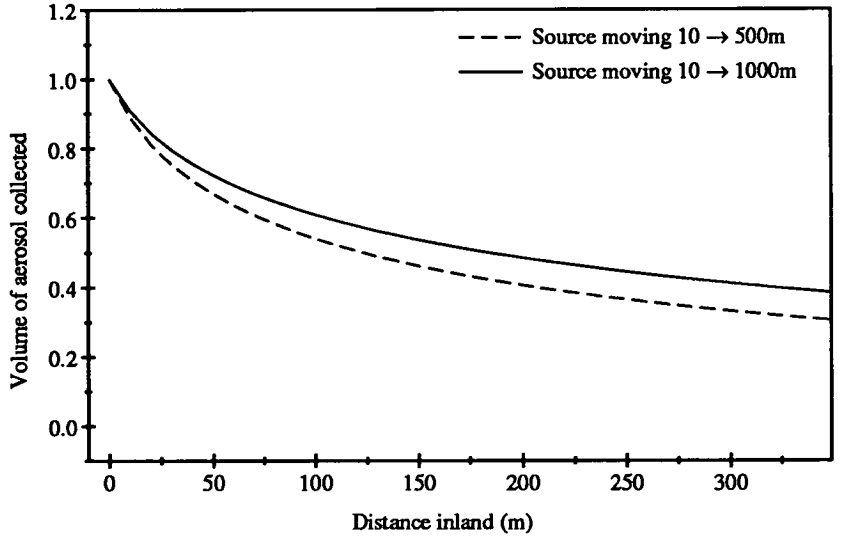

Figure 4.10: Output of the Sea-to-Land Transfer Model. Source producing spectrum of spray droplets of diameter 1–150 μm, D_0=4 μ (See Equation 1.4). Moving source from 10 to 500 m and 10 to 1000 m from the front site. p=0.8, u=5.0 ms^{-1}, z_0=0.3 m.

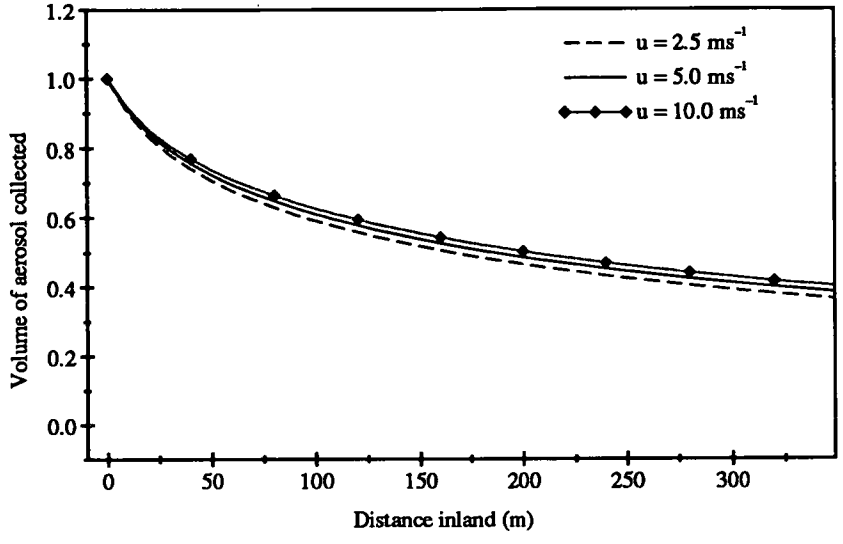

Figure 4.11: Output of the Sea-to-Land Transfer Model. Source producing spectrum of spray droplets of diameter 1–150 μm, D_0=4 μ (See Equation 1.4). Moving source from 10 to 1000 m from the front site. p=0.8, u=2.5, 5.0 and 10.0 ms^{-1}, z_0=0.3 m.

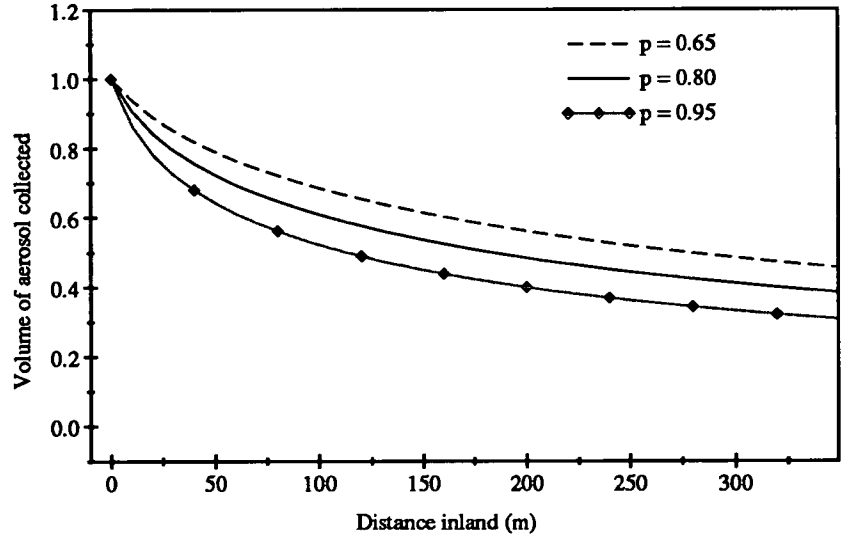

Figure 4.12: Output of the Sea-to-Land Transfer Model. Source producing spectrum of spray droplets of diameter 1–150 μm, D_0=4 μ (See Equation 1.4). Moving source from 10 to 1000 m from the front site. p=0.65, 0.8 and 0.95, u=5.0 ms^{-1}, z_0=0.3 m.

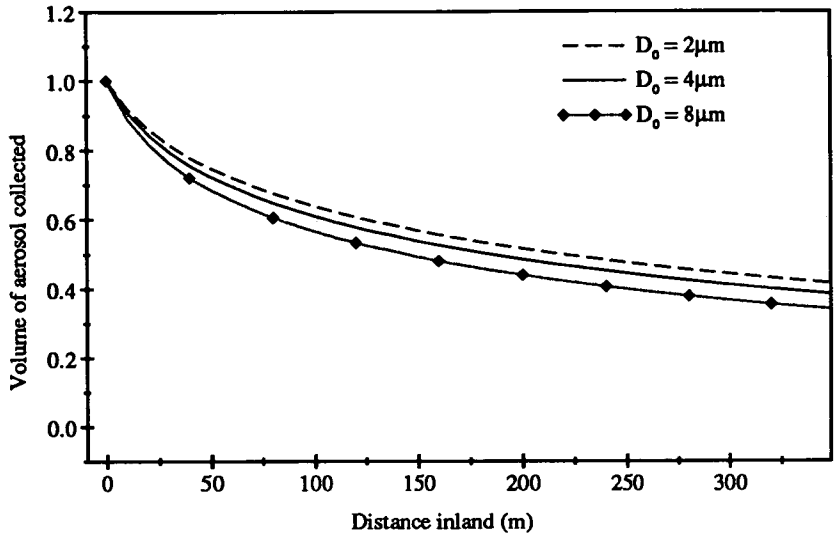

Figure 4.13: Output of the Sea-to-Land Transfer Model. Source producing spectrum of spray droplets of diameter 1–150 μm, D_0=2, 4 and 8 μ (See Equation 1.4). Moving source from 10 to 1000 m from the front site. p=0.8, u=5.0 ms^{-1}, z_0=0.3 m.

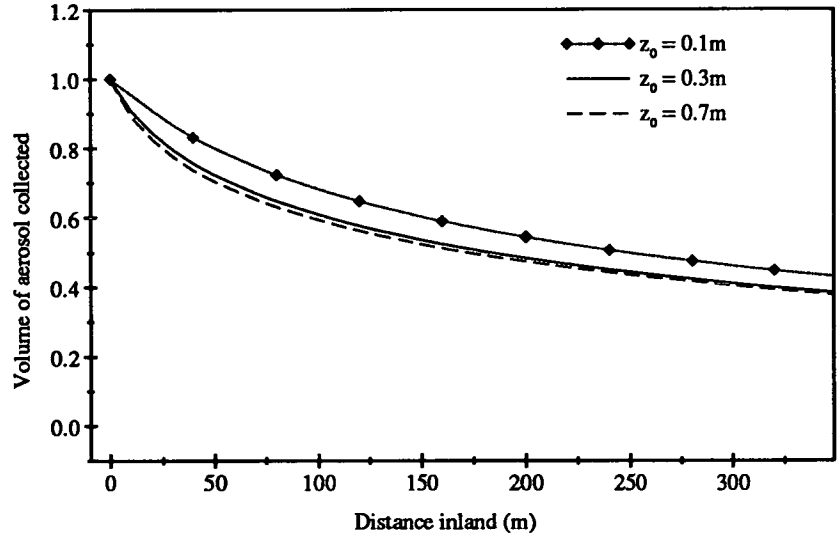

Figure 4.14: Output of the Sea-to-Land Transfer Model. Source producing spectrum of spray droplets of diameter 1–150 μm, D_0=4 μ (See Equation 1.4). Moving source from 10 to 1000 m from the front site. p=0.8, u=5.0 ms^{-1}, z_0=0.1, 0.3 and 0.7 m.

4.4 Applying the model to other datasets

The Sea-to-Land Transfer Model has been applied to measurements of the inland transfer of sea spray and marine discharged radioactivity made by other workers. The aim of this is to see if the reduction patterns with distance inland observed in these measurements can be explained by considering the dispersion and deposition of spray droplets as they are transported from the sea.

These data fits have been obtained using the typical sea spray size distribution described in Section 1.4.1, with droplets of diameter 1 to 150 μm and a mode diameter of 4 μm. The parameter determining the initial distribution of spray droplets with height, z_0, has been given a value of 0.3 m. The parameter p has been given a value of 0.8, typical of neutral atmospheric stability conditions. In the fits to the data collected over short time periods a stationary source is used. The wind speed reported by the authors for the collection period is used in fitting the data. In producing fits to data obtained from radioactivity levels in coastal vegetation and soil, when collection will have been over extended periods, an inter-tidal range of 1000 m has been assumed. A typical mean wind speed of 5 ms^{-1} has been used.

Figure 4.15 shows the output of the model to fit the data obtained by Fujiwara & Umejima [28]. These workers exposed screens of cotton gauze along a line extending to over 1 km from the sea on several occasions. The data in Figure 4.15 shows the mean mass of sea-salt present on the inland screens relative to the most sea-ward screen, from the exposures named A1 to A6. As the exposures were only for short periods the fit to the data has been produced by using a stationary source positioned 5 m from the front collection site. The collection of the exposed screens was simulated by calculating the spray volume between the heights of 1.0 and 1.25 m from the ground at distances from the source. The model simulates the initial rapid reduction in sea spray concentration and then the much flatter change with distance further inland.

Fraizier et al. measured the $^{239+240}$Pu concentration in vegetation samples collected along a transect inland from the sea in Normandy [26]. Samples were collected between 5 and 1200 m from the high water mark and the data are

illustrated in Figure 4.16. The fit has been produced by allowing the source of the spray droplets to move between 5 and 1000 m from the front collection site, and closely follows the reduced concentration in the vegetation with increasing distance inland.

Martin et al. measured the activity levels of ^{106}Ru, ^{134}Cs, ^{137}Cs, ^{144}Ce, ^{238}Pu and $^{239+240}$Pu in 4 vegetation samples collected up to 1000 m inland from the sea in the same region as Fraizier et al. [49]. The mean activity concentrations in the inland samples relative to the most sea-ward, are illustrated in Figure 4.17 along with the output from the model. The air concentration between the ground and a height of 0.5 m, assumed to be typical of the vegetation, has been calculated. Again the model gives a similar reduction with distance from the high-water mark to that plotted by the results of the vegetation analyses.

Cambray & Eakins measured the radionuclides present in soil cores collected along two transects inland from the sea in Cumbria [8]. These authors found the radionuclide content from the sea spray to decrease at different rates with distance for $^{239+240}$Pu, ^{241}Am and ^{137}Cs. The expected levels of sea spray depostion at different distances inland from the model are shown in Figure 4.18, along with the $^{239+240}$Pu and ^{241}Am concentrations in the soil cores collected along the Nethertown to Newlands transect, relative to the activity concentration of the most sea-ward sample which was collected 50 m from the high-water mark. This calculation determined the spray volume deposited on the ground and was obtained by moving the source between 50 and 1000 m from the front site. As can be seen the model output fits the falloff in ^{241}Am inventory in the soil very closely up to a distance greater 10 km inland. The $^{239+240}$Pu results illustrate a less rapid reduction in concentration with distance than that plotted by the ^{241}Am data and the model output. The ^{137}Cs soil concentrations decreased more slowly with distance inland than the $^{239+240}$Pu.

Pattenden et al. measured radionuclide deposition along a transect inland from the sea [63]. These authors found that the $^{239+240}$Pu and ^{241}Am deposits reduced at an almost identical rate with distance inland, but that ^{137}Cs and ^{106}Ru present in the deposit decreased more rapidly. Figure 4.19 shows the fit to the Pattenden et al. actinide data produced by the Sea-to-Land Transfer Model,

using an inter-tidal distance of 600 m, as quoted for this site by the authors. This simulation was performed by calculating the volume of spray deposited on the ground with distance inland. This plot also illustrates a reasonably good fit by the model to the measured results.

Eakins & Lally report on a short-term exposure of muslin screens simultaneously at five sites up to 8.6 km from the sea in Cumbria [19]. The model output, showing the changing air concentration between 1 and 2 m from the ground between the distances of 5m and 10 km from a stationary source is given in Figure 4.20, and closely fits the reduction in airborne radionuclide concentration with distance inland measured by the screens.

The examples of applying the Sea-to-Land Transfer Model to published results of the inland transport of spray borne radioactivity have shown that the model successfully explains the measured results by considering the dispersion and deposition of the spray droplets. These data-sets were obtained by different collection techniques, including measurement of the radionuclide inventories in coastal soil and vegetation, and from collections of airborne and depositing particulate material. There is thus justification for the belief that this model can be used to give predictions of the extent of the inland transfer of spray borne pollutants and that it will be of use in estimating the radiation exposure of members of the public arising from this pathway.

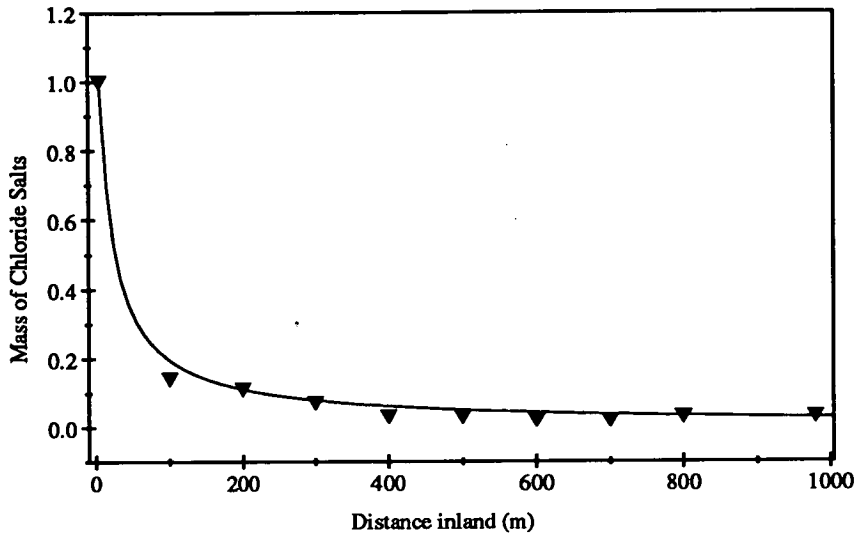

Figure 4.15: Output of the Sea-to-Land Transfer Model to fit the sea spray data of Fujiwara & Umejima [28].
Default input parameters (See Table 4.1 Source to front screen=5 m. u=5.4 ms^{-1})

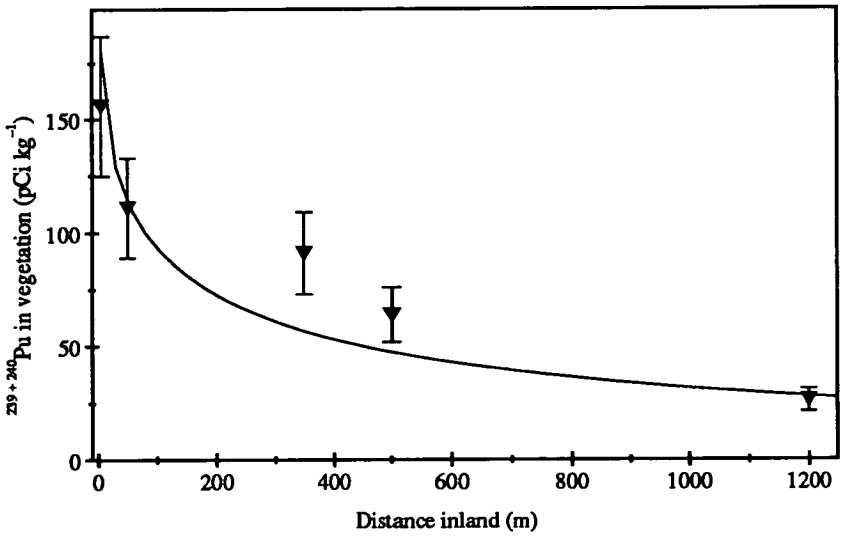

Figure 4.16: Output of the Sea-to-Land Transfer Model to fit the $^{239+240}$Pu in coastal vegetation data of Fraizier et al. [26].
Default input parameters (See Table 4.1 Source to front site=5 to 1000 m. u=5.0 ms^{-1})

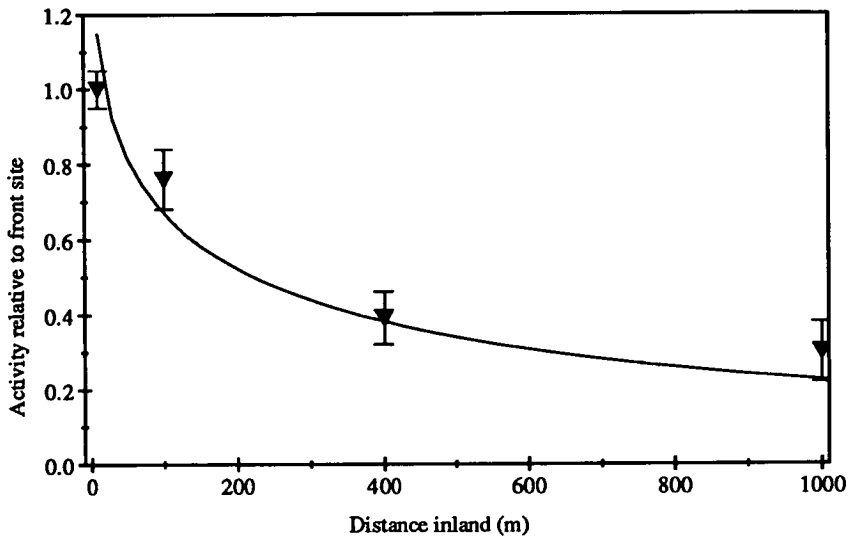

Figure 4.17: Output of the Sea-to-Land Transfer Model to fit the radionuclides in coastal vegetation data of Martin et al. [49].
Default input parameters (See Table 4.1 Source to front site=10 to 1000 m. u=5.0 ms^{-1})

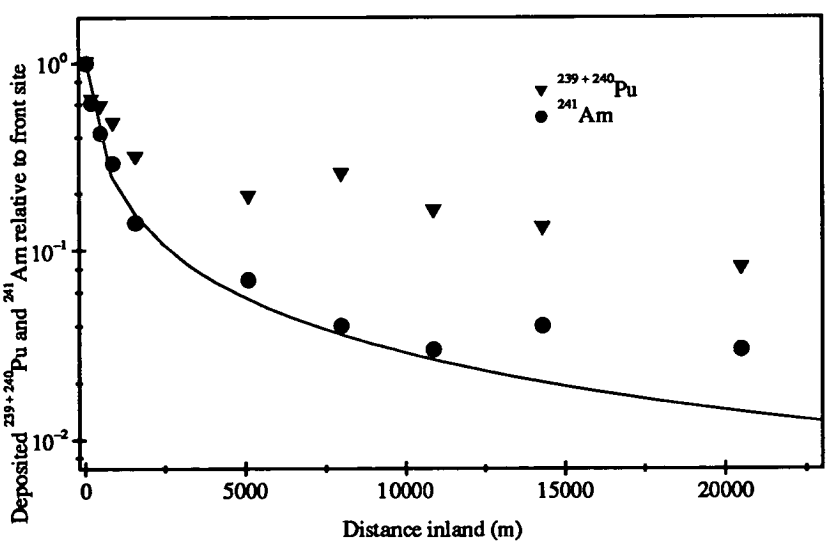

Figure 4.18: Output of the Sea-to-Land Transfer Model to fit the radionuclides in coastal soil data of Cambray & Eakins [8]. Default input parameters (See Table 4.1 Source to front site =50 to 1000 m. u=5.0 ms^{-1})

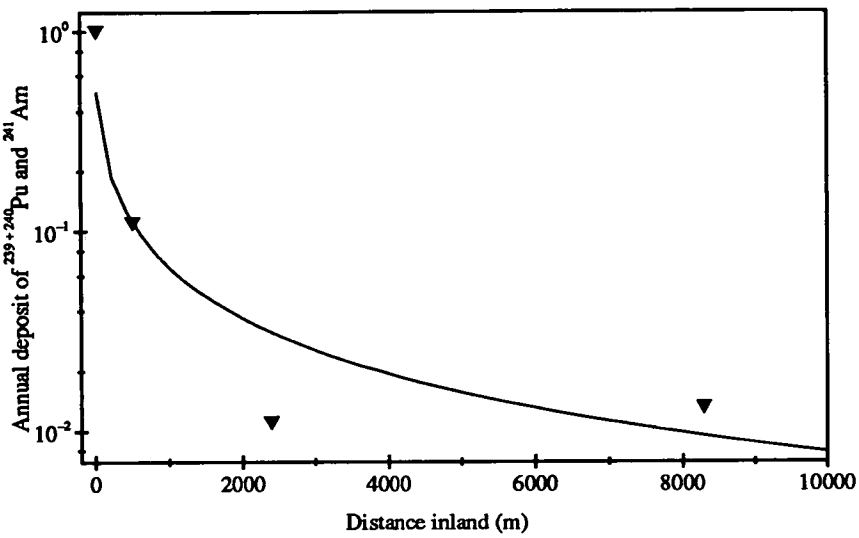

Figure 4.19: Output of the Sea-to-Land Transfer Model to fit the measurements of depositing radionuclides by Pattenden et al. [63].
Default input parameters (See Table 4.1 Source to front site =20 to 620 m. u=5.0 ms^{-1})

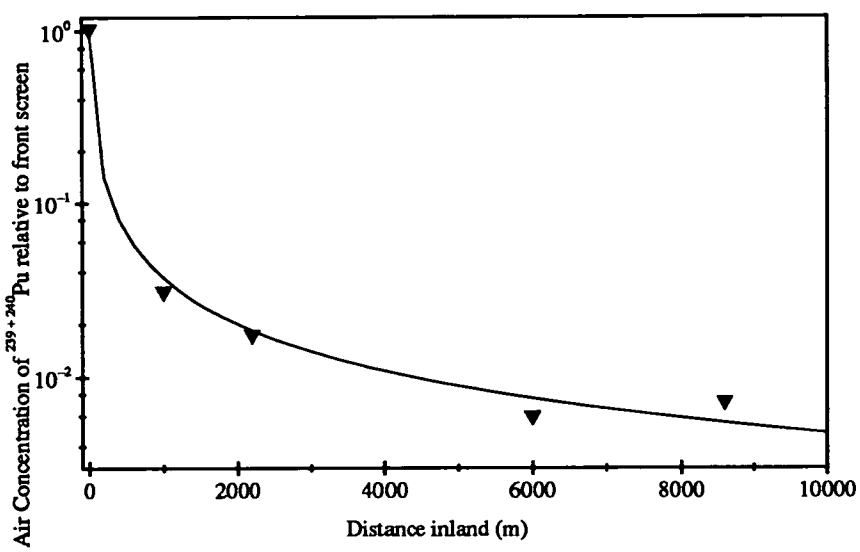

Figure 4.20: Output of the Sea-to-Land Transfer Model to fit the air concentration of $^{239+240}$Pu data of Eakins & Lally obtained by exposure of muslin screens [19].
Default input parameters (See Table 4.1 Source to front screen=5 m. u=6.0 ms^{-1})

4.5 Possible model short-comings

As discussed, the Sea-to-Land Transfer Model has been found to successfully produce fits to measurements of the inland transfer of sea spray and sea spray borne radioactivity. This model, however, obviously treats certain aspects of the transfer in a simplistic fashion. For example, the maintenance of an exponential spray distribution with height at all distances from the source is an idealisation which is unlikely to bear much similarity to reality. Other aspects of the sea-to-land transfer and the simulation of the collection of the airborne spray droplets by the muslin screens have been dealt with in an uncomplicated fashion. In some cases this is because, at this developmental stage, increased sophistication is unnecessary. In other cases there is no relevant experimental data available to merit taking certain phenomena into account in anything but a cursory way. Some possible short-comings in the model will be discussed here.

The model described here is similar in many respects to the model suggested by the NRPB Working Group on Atmospheric Dispersion. This group has reported comparisons of their models with the predictions of more physically realistic and complicated models, such as surface depletion models, which treat the dispersion and deposition of released particles in a more physical fashion [43]. Both types of models gave similar predictions, making the development of more sophisticated models unnecessary at this stage. Agreement between the different models, over a wide range of wind speed and particle sizes, was much better when simulating emissions in neutral and unstable conditions, than when modelling releases in stable conditions. Large discrepancies were found for releases from low level sources in stable conditions, especially at distances over 10 km from the source. It seems likely that the majority of sea spray is transferred inland in reasonably stormy conditions. Wind speeds greater than $5\,ms^{-1}$ are not conducive to the development of extreme stability or instability in the atmosphere (See Figure 6.10 in Pasquill & Smith 1983 [61]). Periods of intense sea spray transfer will mostly occur in neutral stability conditions, when the NRPB-type models gave similar predictions to the more physical models.

The Sea-to-Land Transfer Model, as it stands, does not take into account

the possibility that material becoming airborne at ground level can be trapped underneath a temperature inversion in the atmosphere. In reality the spray droplets will not continue to be mixed to greater heights with distance. When the value of the dispersion coefficient z_x becomes of the order of the height of the boundary layer, the material will be reflected back towards the ground. An estimate of the typical height of the mixing layer in neutral conditions and $5\,m\,s^{-1}$ winds is 800 m [12]. The parameter z_x becomes of this order at a distance of 19 km when z_0 has a value of 0.3 m and the turbulence coefficient p has a value of 0.8. This model is thus considered to be limited in applicability to distances within the order of 10–20 km from the source. Beyond these distances it will tend to under-estimate the concentration of released droplets in the air by continuing to mix them to greater altitudes than are likely in reality.

Conflicting theories as to the relationship between droplet size and its enrichment relative to the seawater in the surf zone have been proposed in the literature. Eakins & Lally found that the enrichment of a droplet appeared to increase with droplet diameter [19], while Pattenden et al. proposed the opposite to be the case [63]. In this situation it seems prudent to assume no variation of droplet enrichment with diameter. The level of radioactivity being transferred inland in a sea spray droplet is therefore assumed to be proportional to the volume of the droplet.

As discussed in Section 1.6, firm experimental data on the collection characteristics of the muslin screens are unavailable. This model assumes that droplets of all sizes over 1 μm are collected with equal efficiency, while those smaller than this are not collected at all. Although it appears likely that sub 1 μm droplets will not be collected by the screens very efficiently, it is unlikely to be the case that droplets of diameter 1 μm will be collected as efficiently as 100 μm diameter droplets. The model may therefore be expected to underestimate the decrease of concentration with distance from the source, as measured by the muslin screens, by exaggerating the influence of the smaller droplets.

The model assumes that the parameters p and z_0 are the same for droplets of all diameters. This may not be the case in reality as heavier droplets may tend to resist the uplifts caused by turbulence and so have smaller values of both

z_0 and p than very small droplets. It is considered that including a relationship between these parameters and droplets diameter is unnecessary at this time. In any case, it is unclear what form this relationship would take.

As the activity in the sand and sediment may change with position over the extent of the inter-tidal zone, the activity of the spray coming ashore may vary with the position of the surf. There is no data available on activity concentration changes over the inter-tidal zone at the sites under consideration, so this possibility is also ignored in the current model.

Chapter 5

Discussion of Results

5.1 Marram grass results

5.1.1 Removing the Chernobyl contribution

It was found that a large proportion of the ^{137}Cs, ^{134}Cs and ^{106}Ru present in the marram grass collected at Drigg was not of Sellafield origin, but was deposited from the radioactive plume released during the course of the accident at the Chernobyl nuclear reactor in the USSR in late April 1986, and which passed over the British Isles on 2^{nd} and 3^{rd} May (See Section 1.5).

Table 3.1 shows the radioactivity concentrations present in the Drigg A1 sample, collected before May 1986, and the most sea-ward of the Drigg A2 samples, collected 6 months after the Chernobyl accident, revealing that the concentrations of ^{137}Cs, ^{134}Cs and ^{106}Ru increased considerably in the vegetation in this region between these grass collections. The concentration of ^{241}Am also increased from Drigg A1 to A2, but to a much lesser extent than for the other radionuclides present. Very low actinide levels are assumed to have been deposited in the U.K. in fallout from Chernobyl [9]. The increased level of ^{241}Am is therefore not thought to be due to Chernobyl radioactivity.

Information gained from the isotopic ratio of ^{137}Cs : ^{134}Cs in the Drigg A2 samples supports the assumption that their major source was in the Chernobyl fallout. Table 5.1 gives the ratio ^{137}Cs : ^{134}Cs found in each of the Drigg A2 grass samples at the time of analysis. It can be assumed from Table 3.1 that

Sample No.	^{137}Cs : ^{134}Cs ratio
1	2.54±0.07
2	2.41±0.06
3	2.37±0.06
4	2.45±0.08
5	2.26±0.10

Table 5.1: The ^{137}Cs : ^{134}Cs ratio in the Drigg A2 samples at the time of analysis

all the ^{134}Cs in these samples is attributable to the Chernobyl fallout. Therefore the changing ratios in Table 5.1 are due to the collection of different levels of ^{137}Cs from Sellafield, and sample 5, with the lowest ratio, can be assumed to have received the smallest contribution of Sellafield material. The ^{241}Am present in this sample was below the detection limits. It therefore seems likely that it also contains very little Sellafield ^{137}Cs. Back-dating the ^{137}Cs : ^{134}Cs ratio in sample 5 to correct for the radioactive decay of ^{134}Cs, indicates a ^{137}Cs : ^{134}Cs ratio at the time of initial deposition from the Chernobyl cloud of 1.72±0.08. The ^{137}Cs : ^{134}Cs ratio in rainfall collected in Cumbria in early May 1986 is reported at 1.82 [9]. Therefore, the ^{137}Cs : ^{134}Cs ratio in the Drigg grass samples is very indicative of the presence of Chernobyl contamination.

Assuming that the ratio ^{137}Cs : ^{134}Cs in the initial deposition was 1.72±0.08 at all sites on the Drigg beach, it is possible to subtract the ^{137}Cs of Chernobyl origin present in the grass samples collected to give the ^{137}Cs originating from Sellafield (Table 5.2). The samples from Drigg A2, B1 and B2 contained very large levels of ^{137}Cs, over 90% in some instances being from Chernobyl. Estimating the Sellafield contribution to these samples required taking the relatively small difference of large numbers, resulting in large errors. The samples collected

in Drigg C1 and C2 contained a more significant fraction of Sellafield ^{137}Cs, and the uncertainties in the results are therefore much smaller.

Figure 5.1 shows the ^{137}Cs calculated to be from Sellafield in the Drigg C2 samples plotted against the ^{241}Am present, all of which can be considered to have originated from Sellafield. The line drawn is a best fit through the points and shows excellent correlation (r=0.946). It can be concluded that the mechanism whereby the ^{241}Am was transferred inland to be collected by the marram grass along the transect also transferred the Sellafield ^{137}Cs inland. There is no evidence of an offset from the origin in the fit to the data points in Figure 5.1. This implies that the input of ^{137}Cs to this vegetation from bomb fallout is of an insignificant level and that the great majority of the ^{137}Cs is of Sellafield origin.

Figure 5.2 shows the levels of ^{106}Ru and ^{134}Cs measured in the Drigg A2 grass samples. The similarity in the shape of these lines is evidence for the Chernobyl origin of a significant fraction of the ^{106}Ru. Subtracting the expected Sellafield contribution of ^{106}Ru, as found in the pre-Chernobyl Drigg A1 sample, from the ^{106}Ru in the Drigg A2 Sample 1, and correcting for radioactive decay, estimates the ratio ^{106}Ru : ^{134}Cs in the Chernobyl deposition at 0.43 ± 0.16. Cambray et al. report measurements of the ratio of ^{106}Ru : ^{134}Cs in air at Chilton in early May, quoting a mean value of 0.66 ± 0.10 [9].

5.1.2 ^{241}Am in the grass samples

Although the same vegetation species was being collected along the transects, the growing conditions of the grass being collected varied greatly at the different sites. The growing density varied between 0.15 and 1.5 kg dry weight per m^2 along the Drigg B transect. Also, the more dense samples contained large amounts of dead vegetation from previous seasons, which would have been exposed to sea spray over a much longer period than fresher grass.

Figure 3.1 shows the ^{241}Am present in the samples from collections B1 and B2. It is felt that the ^{241}Am concentration depends to a large extent on the characteristics of the sample collected, and not just to its position on the transect. For example, Figure 5.3 shows the ^{241}Am concentration in each sample from the

Site No.	Collection Name				
	A1	B1	B2	C1	C2
1	143±72	40±11	36±14	30±2	31±3
2	71±72	157±82	40±18	20±2	14±2
3	57±78	165±55	69±26	26±1	24±2
4	31±27	55±44	45±28	15±1	15±3
5	0±25	119±44	37±18	20±2	9±4
6	—	32±133	103±64	18±3	3±3
7	—	62±74	48±22	9±2	9±1
8	—	115±64	47±31	3±3	4±3
9	—	57±36	79±31	6±4	9±2
10	—	227±113	107±42	10±3	1±6
11	—	93±102	89±58	7±3	9±3

Table 5.2: The levels of ^{137}Cs calculated to be of Sellafield origin in the marram grass samples collected along the transects at Drigg

Drigg B1 collection plotted against the grass density at the site. The denser clumps have collected much more ^{241}Am from the sea spray. The variation in the collected ^{241}Am along the transect is therefore not considered to be solely due to a reduction in the sea spray intensity with distance inland from the sea.

The collection technique used along Drigg C was used specifically in an attempt to remove the effects of the changing grass characteristics along the transect. These results show the ^{241}Am falling off more uniformly with distance inland (Figure 3.1). The samples at Drigg C were collected around the sites of the muslin screen exposures and their activity concentrations change with distance in a similar way to the muslin results along this transect (eg Figures 3.6

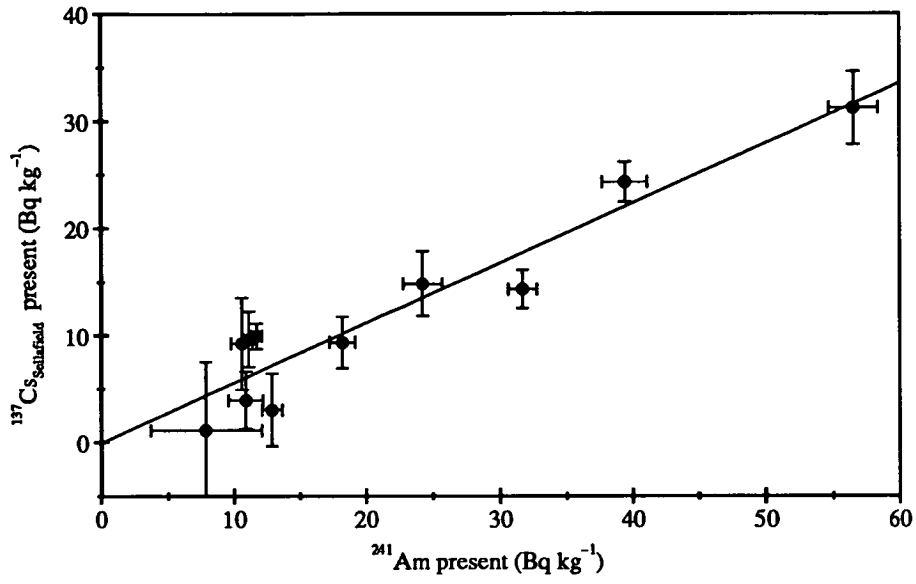

Figure 5.1: Estimated ^{137}Cs of Sellafield origin in the Drigg C2 grass samples against the ^{241}Am present

and 3.7). The ^{241}Am activity decreases very rapidly initially and very much more slowly further inland.

The diagrams in Figure 3.1 show that the activity levels of ^{241}Am in vegetation along the Drigg B and C transects did not change significantly in the period between the different collections. The ^{241}Am concentrations in the C2 samples, collected in February 1988, are not significantly increased from those in the samples taken from these sites 3 months earlier, in the C1 collection. The ^{137}Cs activity calculated to be of Sellafield origin also did not change significantly over this period (Table 5.2). Significant levels of radionuclides would be expected to have been transferred inland in the time between these collections, as it covers the generally stormy winter months of November, December and January. There is an implication here that the marram grass must either have a very low collection efficiency for the sea spray borne radioactivity, or there must be an efficient loss mechanism whereby the ^{241}Am and ^{137}Cs, once collected, can be removed from the vegetation.

A consideration of the loss of ^{134}Cs from the marram grass along the Drigg B

transect between the two collections at that site, on 27^{th} April and 3^{rd} July, gives an estimation of the mean retention time of this isotope by marram grass of 90 ± 15 days. The loss mechanisms from vegetation are expected to be even less efficient in the winter months [10], implying an even greater retention time for the period between the Drigg C1 and C2 collections. There is no evidence, therefore, of the existence of a mechanism which rapidly removes the collected radionuclides from the marram grass leaves. It is to be concluded that marram grass is an inefficient collector of the radionuclides being transferred inland in the sea spray. This aside, the results from the grass collections indicate that there is a significant reduction in the ^{241}Am and ^{137}Cs from the sea spray collected over the extent of the transects, implying a reduction in the surface air concentration of these radionuclides over this distance.

5.1.3 ^{7}Be in the grass samples

The concentration of the atmospheric aerosol ^{7}Be (See Section 1.7) in the grass samples show a greatly differing collection rate along the transects, varying over an order of magnitude in the collections along Drigg B. This may be a result of the marram grass collection technique used along this transect. The ^{7}Be concentrations in the vegetation collected along Drigg B did not change significantly in the period between the grass collections, and the two collections show a very similar change in the ^{7}Be concentration in the vegetation with distance along the transect (Figure 3.5). The collections at Drigg C do show, however, a very significant increase in ^{7}Be concentration between November 1987 and February 1988. This could be due to an increased precipitation in this period bringing more ^{7}Be to the ground. The increased ^{7}Be concentration could also been caused by an increase in the ^{7}Be tropospheric inventory after a tropospheric folding event, although it would have been early in the year for such an occurrence [17].

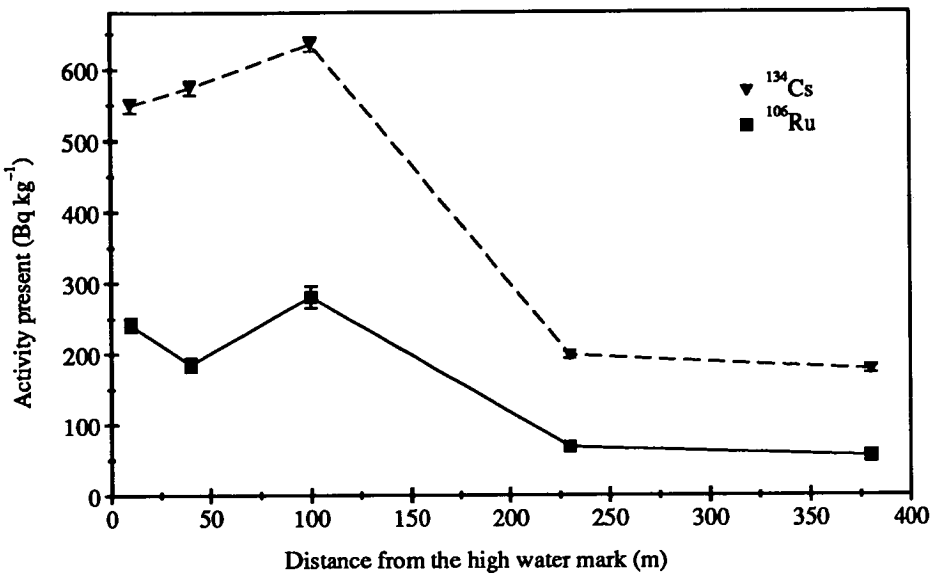

Figure 5.2: ^{106}Ru and ^{134}Cs present in the samples of grass from collection Drigg A2

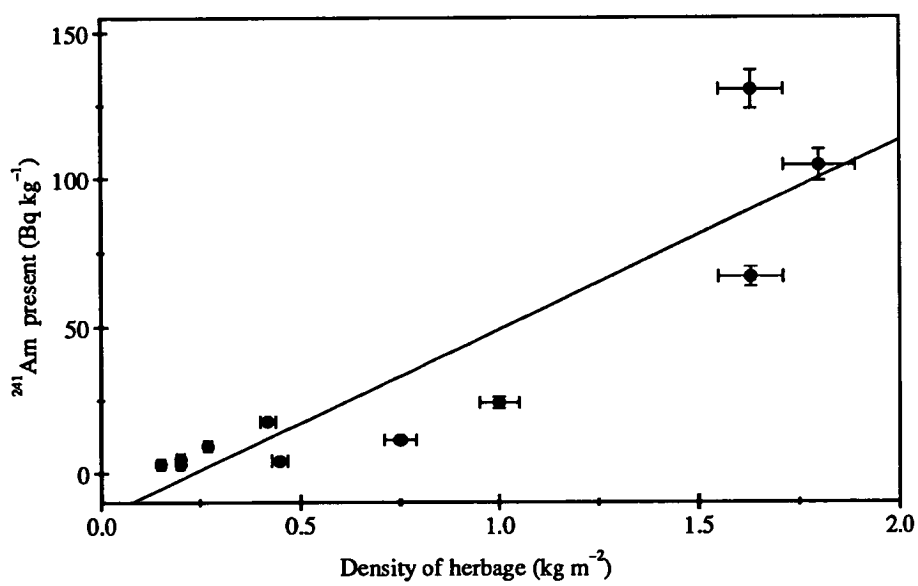

Figure 5.3: ^{241}Am activity of grass samples from the Drigg B1 collection against the grass density at the site

5.2 Muslin screen results

5.2.1 ^{241}Am, ^{137}Cs, ^{106}Ru and sea-salt correlations

In Figure 5.4 the ^{241}Am activity present on each muslin screen collector after exposure along the Drigg C transect is plotted against the mass of sea-salt collected. Also illustrated is a plot of the total ^{241}Am collected at each site during the whole exposure period against the total sea-salt collected at that site. The straight lines on the graphs are least-square best fits to each data set. Corresponding plots of the ^{137}Cs and ^{106}Ru collected against the sea-salt are given in Figures 5.5 and 5.6. The details of the fits to these data are given in Tables 5.3, 5.4 and 5.5. On the whole there is a very significant correlation between the radionuclides present on the exposed muslin screens and the collected sea-salt, clearly implicating the sea spray droplets as the carriers of the radioactive contaminants inland from the sea.

An interesting feature of these results is the very similar behaviour of ^{241}Am, ^{137}Cs and ^{106}Ru. Figure 5.7 shows the ^{241}Am collected on each screen plotted against the ^{137}Cs collected. Figures 5.8 and 5.9 show the ^{106}Ru collected against the ^{241}Am and ^{137}Cs on each occasion. Details of the best fit lines drawn to the data points are given in Tables 5.6, 5.7 and 5.8. The Sellafield radionuclides appear to be transferred inland by the same process, and the airborne concentrations are falling off at the same rate with distance travelled inland from the sea.

This conclusion contradicts that of Cambray & Eakins whose data from the analyses of soil cores collected along transects inland from the sea appear to show that the ^{137}Cs concentration in the soil decreases less rapidly with distance than the concentrations of $^{239+240}$Pu and ^{241}Am [7][8]. The ^{241}Am present in the most seaward of Cambray & Eakins' soil cores was a factor of 40 over that expected from fallout from the bomb tests, while the ^{137}Cs was only 1.5 times that expected. It seems likely that the details of the reduction of ^{137}Cs in sea spray with distance in Cambray and Eakins' work was being masked by the relatively large level of bomb fallout ^{137}Cs already present in the soil cores, and the difficulty of estimating its contribution accurately.

Figures 5.10 and 5.11 show the plots of the radionuclides collected during the exposures along the Drigg D transect. Again there is an excellent correlation between the different Sellafield radionuclides, showing that their concentrations in the air are falling off in an identical fashion.

Consider, however, the plots of the ^{241}Am collected during the exposures along Drigg D against the sea-salt, as illustrated in Figure 5.12. The ^{241}Am collected does not correlate with the sea-salt, except in the Drigg D4 data where there is a significant correlation. The details of the fits are given in Table 5.3. These data either indicate a source of the radioactivity collected by the screens which is not from the sea, or a source of sea-salt which does not transfer a concomitant level of Sellafield radionuclides to the screens. A possible source of radionuclides to the screens is in the collection of blowing sand along the transect. This sand will contain levels of ^{241}Am, ^{137}Cs and ^{106}Ru activity. There are, however, excellent inter-correlations between the radionuclides collected along the transect, implying a single source for the radioactivity. It is unlikely that all the radioactivity is collected from blowing sand.

The Ravenglass Estuary runs inland along the side of transect D (Figure 2.2). The increasing sea-salt collections at larger distances along the transect in exposures D1, D2 and D3 (Figure 3.20) may be explained by considering the possibility of sea-salt coming in from the south side of the transect. The inland screens are not at an increased distance from the surf in such conditions. These are also the exposures which have very poor ^{241}Am – sea-salt correlations, as shown in Figure 5.12. A reduced ^{241}Am : sea-salt ratio in the spray off the estuary compared to the spray coming inland off the sea would explain the poor ^{241}Am – sea-salt correlations from these exposures.

It is possible to estimate the enrichment in the radionuclide content of sea spray over that present in seawater. Seawater and sea spray contain 3.2% by weight sea-salt. The mass of sea-salt on the exposed muslin screens is thus indicative of the collection of a certain volume of seawater in the form of spray. The gradients of the lines in the plots in Figures 5.4, 5.5 and 5.6 give the activity of each radionuclide collected per unit mass of sea-salt along the Drigg C transect. The radioactivity concentration in the corresponding volume of seawater can be

calculated, as given in column 3 of Table 5.9, for comparison with measured surf zone radionuclide concentrations in this area of Cumbria, given in column 4 (See Section 1.2.2). The ratio of sea spray to seawater radionuclide concentration is the enrichment factor of the spray droplets. The mean radionuclide to sea-salt ratios from the 7 exposures along the Drigg C transect were used in these calculations.

The estimated enrichment factor for ^{137}Cs is similar to the value quoted by other workers [18][52][63]. The lower values in the range estimated for the ^{241}Am enrichment factor are also similar to those estimated by others; Eakins et al. estimated ^{241}Am enrichment factors ranging from 3 to 50 from their muslin screen exposures [18]. The upper estimates of the ^{241}Am enrichment factors from the Drigg exposures, however, are much greater than those measured by other authors. The low values of radionuclide concentrations in in-shore seawater used to calculate these very large ^{241}Am enrichment factors do not appear to be typical of the concentrations in the surf zone when the majority of the inland transfer of radioactivity is occurring at Drigg.

The poor correlation between the Sellafield radionuclides and sea-salt collected at Drigg D makes it difficult to estimate the enrichment of the sea spray bringing in the radioactive contamination at this site. Only the D4 exposure gave significant correlations between the radionuclides collected on the exposed screens and the mass of sea-salt (Tables 5.3 and 5.4). The mean ^{241}Am : sea-salt ratio on these screens was 12.9 ± 1.5 and the ^{137}Cs : sea-salt ratio was 13.1 ± 1.5, both much greater than the mean ratios from the exposures along the Drigg C transect. There is an implication here that the sea spray produced at Drigg Point, the site of transect D, is more enriched in radioactivity than the spray produced near the site of Drigg C, about 1 mile to the north. This may be a result of the proximity of Drigg D to the Ravenglass Estuary, possibly reflecting the increased silt component of the sediment in this region [34]. This smaller particulate material will have a greater specific activity and will be preferentially transferred to the spray droplets produced in the surf zone.

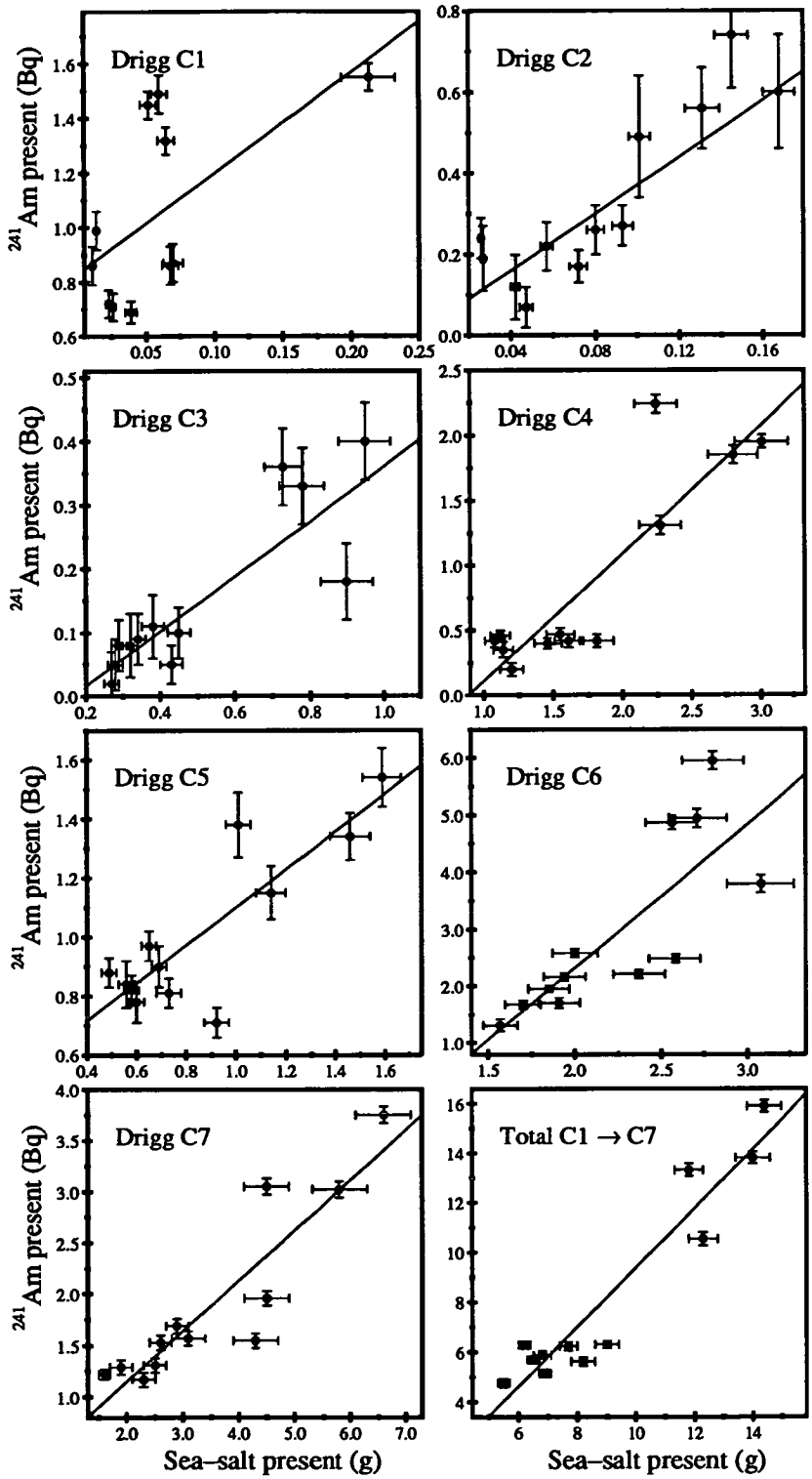

Figure 5.4: ^{241}Am on screens exposed along Drigg C against the sea-salt collected. Lines are least-square best fits to the data points. (See Table 5.3)

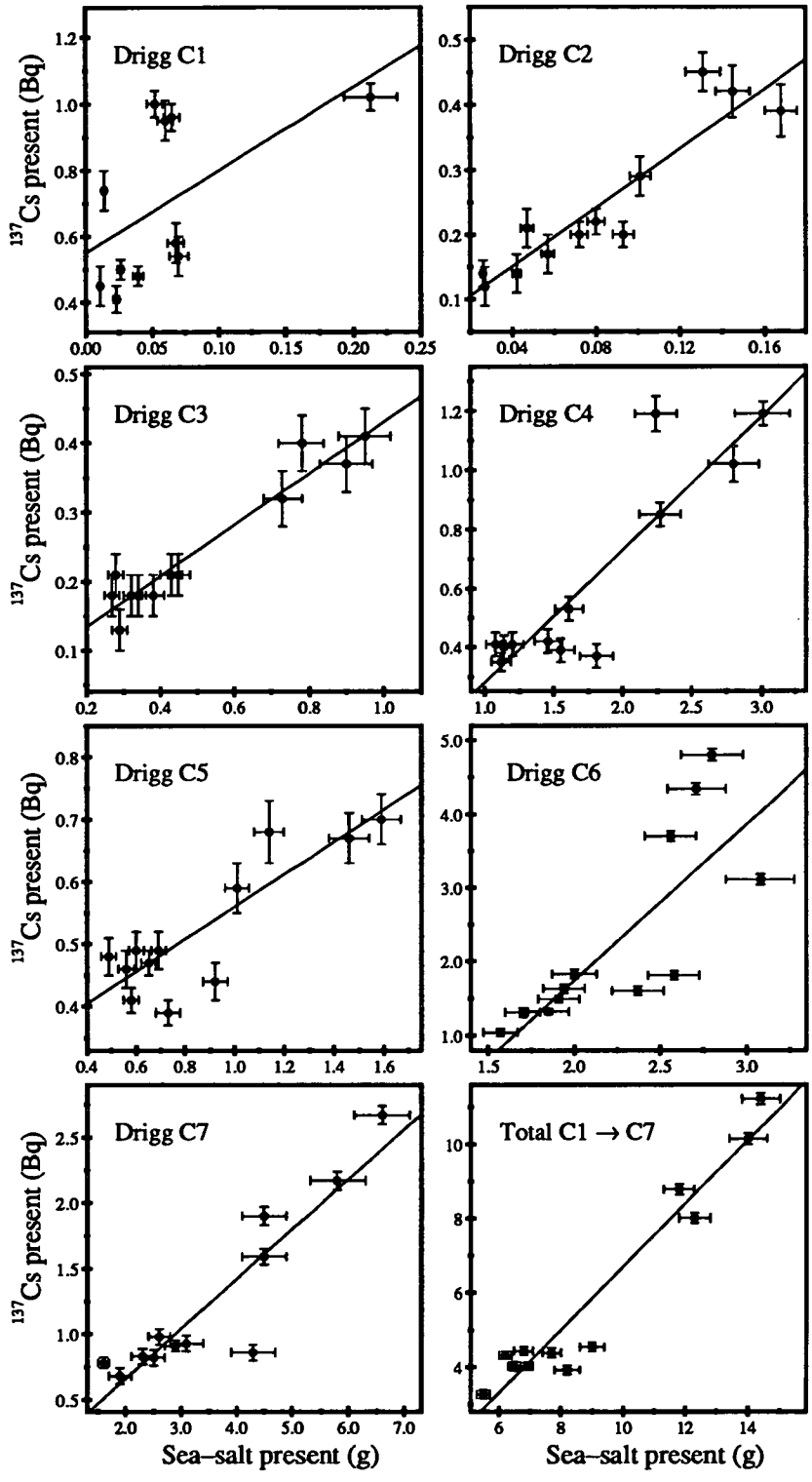

Figure 5.5: ^{137}Cs on screens exposed along Drigg C against the sea-salt collected. Lines are least-square best fits to the data points. (See Table 5.4)

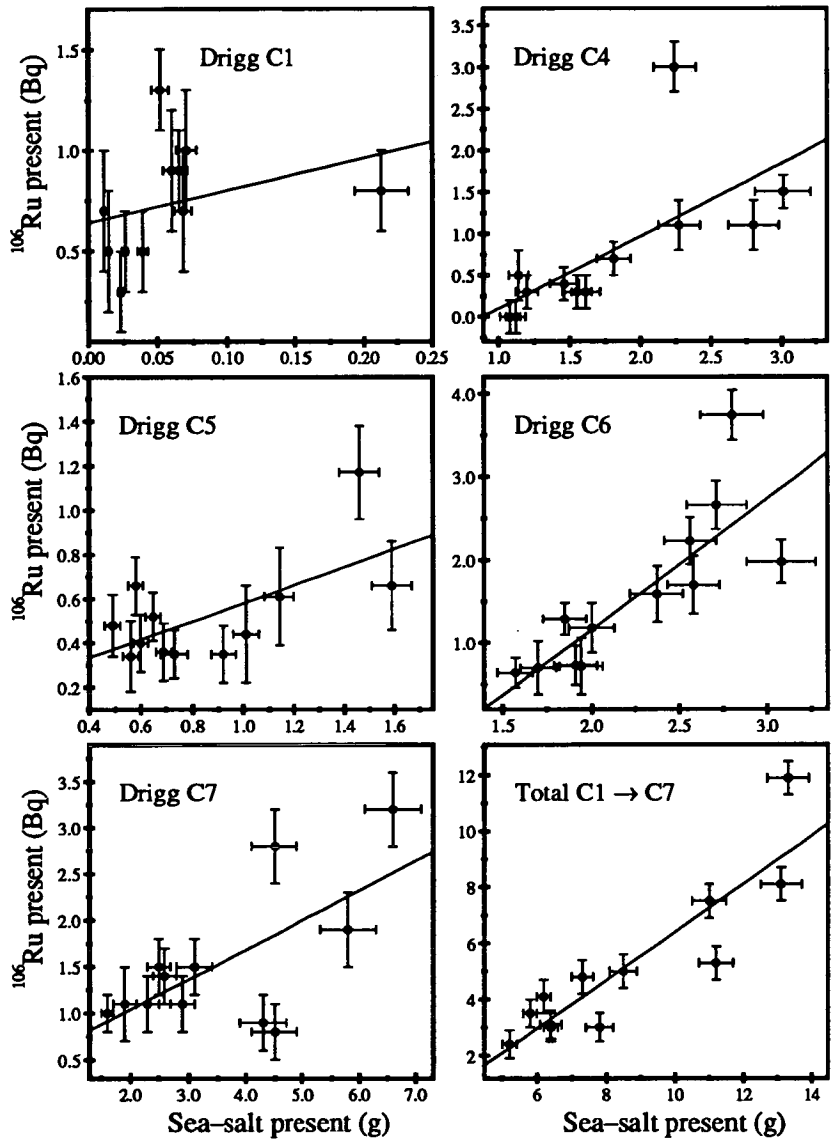

Figure 5.6: ^{106}Ru on screens exposed along Drigg C against the sea-salt collected. Lines are least-square best fits to the data points. (See Table 5.5)

Exposure	Number of points N	Correlation Coefficient r	Gradient m	Intercept c
Drigg C1	11	0.61	3.69±1.45	0.83±0.11
Drigg C2	12	0.87	3.50±0.60	0.02±0.05
Drigg C3	12	0.86	0.43±0.08	−0.07±0.04
Drigg C4	12	0.88	0.98±0.15	−0.9±0.3
Drigg C5	12	0.85	0.64±0.11	0.46±0.11
Drigg C6	12	0.80	2.51±0.54	−2.7±1.2
Drigg C7	12	0.91	0.49±0.07	0.17±0.25
C1→C7	12	0.95	1.19±0.11	−2.5±1.1
Drigg D1	7	0.41	5.3±4.5	1.0±3.0
Drigg D2	7	0.17	0.7±1.4	0.4±4.5
Drigg D3	5	−0.78	−3.2±1.2	8.0±2.0
Drigg D4	4	0.98	12.9±1.5	−2.4±0.5

Table 5.3: Details of best-fits to the ^{241}Am vs sea-salt data for the muslin screen exposures along the transects C and D at Drigg

Exposure	Number of points N	Correlation Coefficient r	Gradient m	Intercept c
Drigg C1	11	0.57	2.50±1.09	0.55±0.09
Drigg C2	12	0.92	2.27±0.27	0.06±0.03
Drigg C3	12	0.96	0.37±0.03	0.06±0.02
Drigg C4	12	0.90	0.45±0.06	−0.17±0.12
Drigg C5	12	0.86	0.26±0.04	0.30±0.04
Drigg C6	12	0.80	2.12±0.46	− 2.5±1.1
Drigg C7	12	0.92	0.38±0.05	−0.10±0.18
C1→C7	12	0.97	0.85±0.07	−1.8±0.6
Drigg D1	7	0.38	2.1±2.0	0.7±1.6
Drigg D2	7	0.09	0.16±0.66	0.9±2.1
Drigg D3	5	−0.81	−1.9±0.6	5.0±1.2
Drigg D4	4	0.98	13.1±1.5	−2.3±0.5

Table 5.4: Details of best-fits to the ^{137}Cs vs sea-salt data for the muslin screen exposures along the transects C and D at Drigg

Exposure	Number of points N	Correlation Coefficient r	Gradient m	Intercept c
Drigg C1	11	0.32	1.61±1.45	0.64±0.11
Drigg C2	—	—	—	—
Drigg C3	—	—	—	—
Drigg C4	12	0.69	0.87±0.27	−0.77±0.50
Drigg C5	12	0.64	0.41±0.14	0.17±0.13
Drigg C6	12	0.82	1.58±0.32	− 2.0±0.7
Drigg C7	12	0.66	0.32±0.10	0.40±0.40
C1→C7	12	0.89	0.86±0.12	−2.2±1.1
Drigg D1	7	0.30	0.74±0.89	0.53±0.72
Drigg D2	7	0.09	0.03±0.12	0.55±0.39
Drigg D3	5	−0.53	−0.4±0.3	1.42±0.51
Drigg D4	—	—	—	—

Table 5.5: Details of best-fits to the ^{106}Ru vs sea-salt data for the muslin screen exposures along the transects C and D at Drigg

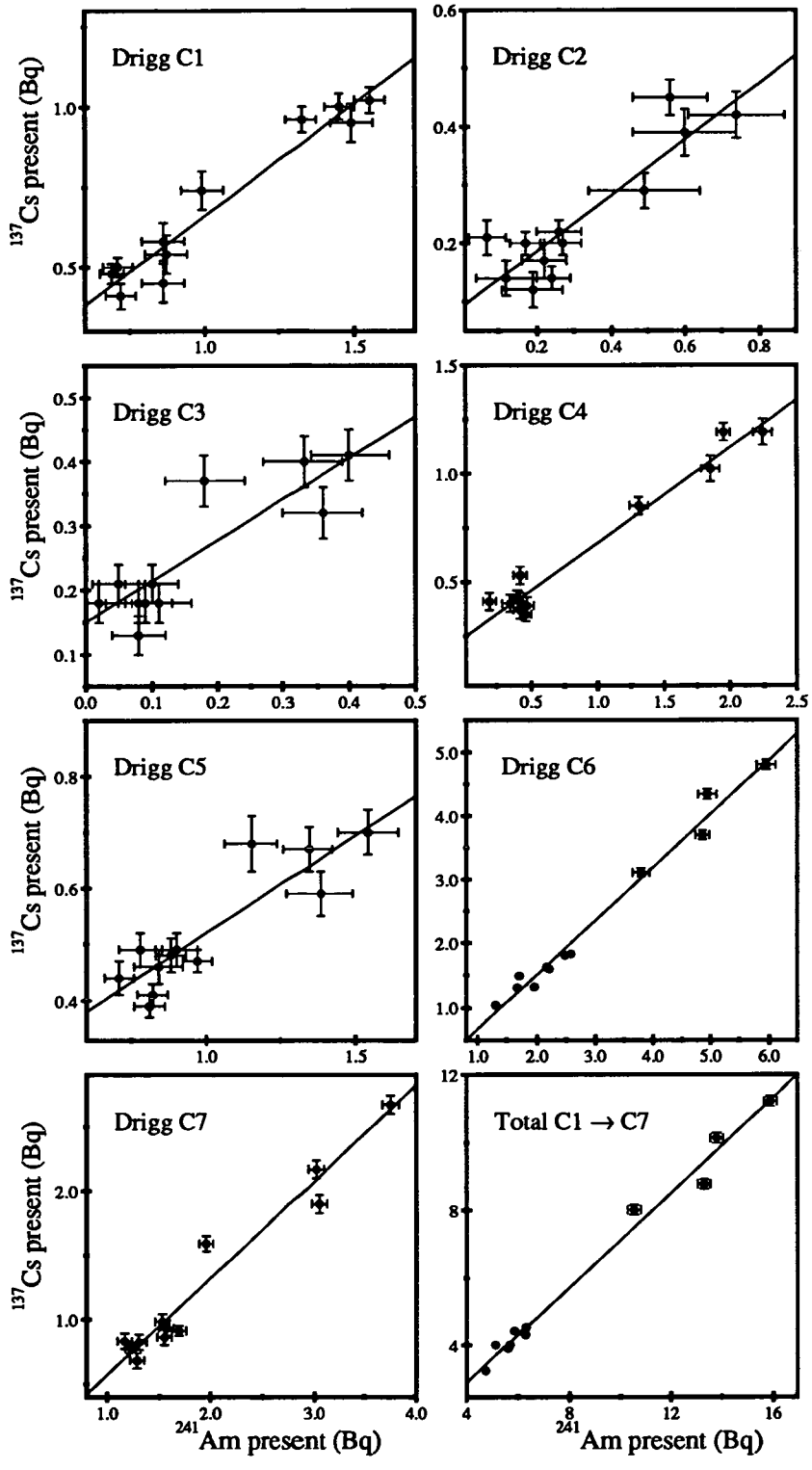

Figure 5.7: ^{241}Am on screens exposed along Drigg C against the ^{137}Cs collected. Lines are least-square best fits to the data points. (See Table 5.6)

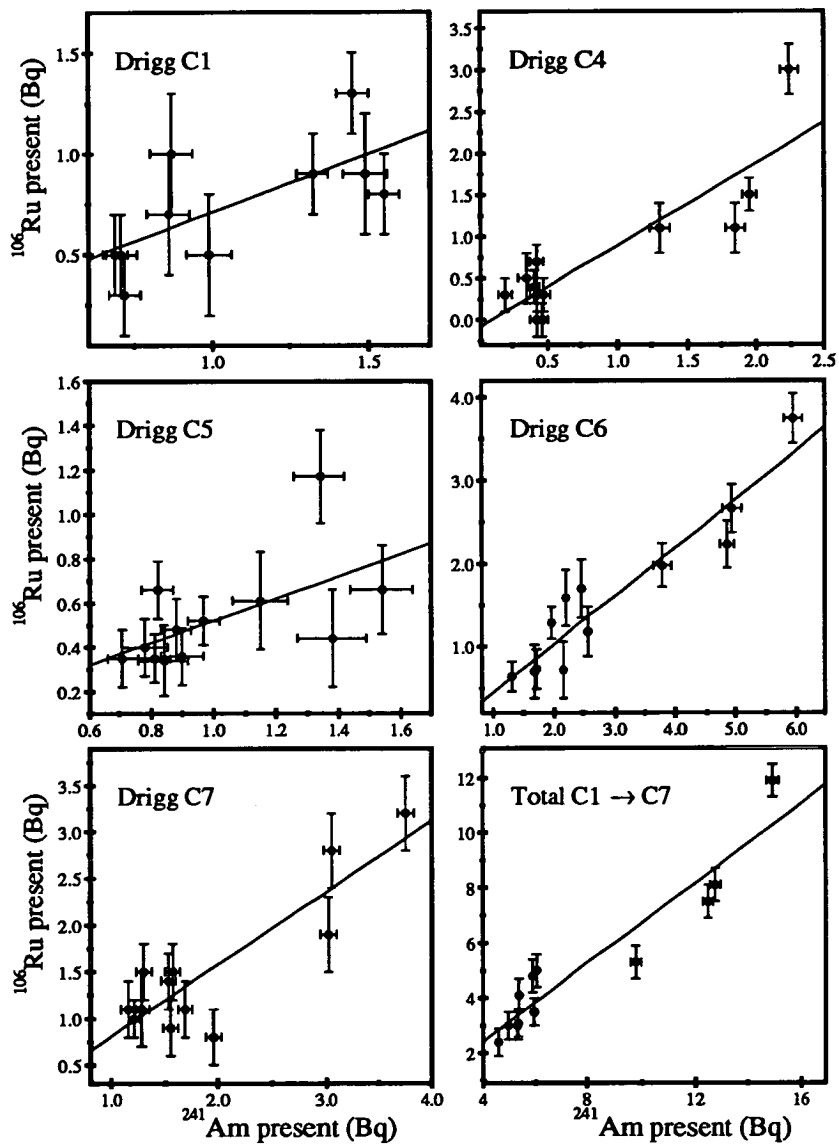

Figure 5.8: ^{241}Am on screens exposed along Drigg C against the ^{106}Ru collected. Lines are least-square best fits to the data points. (See Table 5.7)

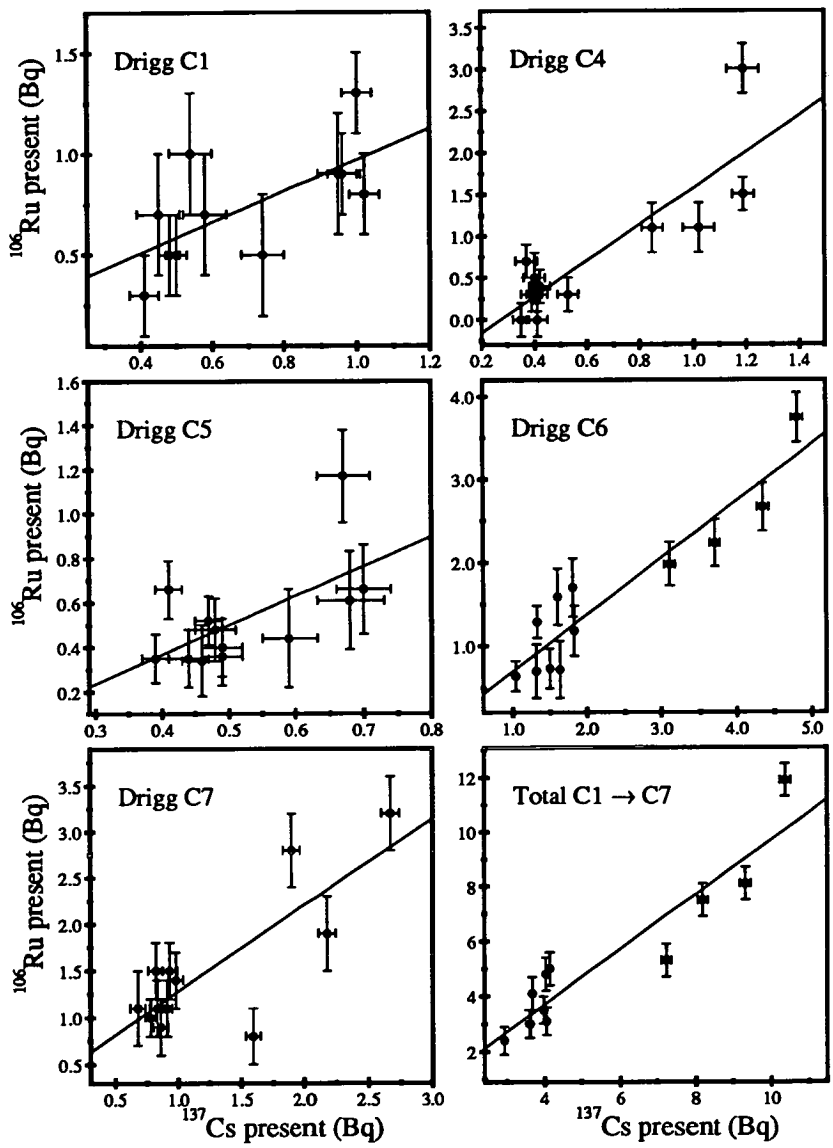

Figure 5.9: ^{137}Cs on screens exposed along Drigg C against the ^{106}Ru collected. Lines are least-square best fits to the data points. (See Table 5.8)

Exposure	Number of points N	Correlation Coefficient r	Gradient m	Intercept c
Drigg C1	11	0.97	0.70±0.05	−0.04±0.06
Drigg C2	12	0.90	0.48±0.07	0.09±0.03
Drigg C3	12	0.87	0.64±0.11	0.15±0.02
Drigg C4	12	0.98	0.44±0.02	0.24±0.03
Drigg C5	12	0.89	0.35±0.05	0.17±0.05
Drigg C6	12	0.99	0.84±0.03	−0.17±0.11
Drigg C7	12	0.98	0.75±0.05	−0.18±0.10
C1→C7	12	0.99	0.70±0.02	0.11±0.21
Drigg D1	7	1.00	0.43±0.01	0.16±0.07
Drigg D2	7	0.99	0.46±0.03	0.30±0.10
Drigg D3	5	1.00	0.57±0.02	0.06±0.05
Drigg D4	4	1.00	1.01±0.03	0.14±0.07

Table 5.6: Details of best-fits to the ^{137}Cs vs ^{241}Am data for the muslin screen exposures along the transects C and D at Drigg

Exposure	Number of points N	Correlation Coefficient r	Gradient m	Intercept c
Drigg C1	11	0.69	0.58±0.18	0.13±0.20
Drigg C2	—	—	—	—
Drigg C3	—	—	—	—
Drigg C4	12	0.88	0.99±0.16	−0.10±0.18
Drigg C5	12	0.58	0.50±0.20	0.02±0.20
Drigg C6	12	0.94	0.58±0.06	−0.13±0.19
Drigg C7	12	0.87	0.77±0.12	0.04±0.26
C1→C7	12	0.95	0.72±0.07	−0.47±0.61
Drigg D1	7	0.96	0.18±0.02	0.17±0.12
Drigg D2	7	0.67	0.06±0.02	0.51±0.08
Drigg D3	5	0.46	0.08±0.07	0.58±0.18
Drigg D4	—	—	—	—

Table 5.7: Details of best-fits to the ^{106}Ru vs ^{241}Am data for the muslin screen exposures along the transects C and D at Drigg

Exposure	Number of points N	Correlation Coefficient r	Gradient m	Intercept c
Drigg C1	11	0.66	0.77±0.26	0.20±0.19
Drigg C2	—	—	—	—
Drigg C3	—	—	—	—
Drigg C4	12	0.86	2.16±0.37	−0.59±0.26
Drigg C5	12	0.61	1.32±0.49	−0.16±0.26
Drigg C6	12	0.93	0.68±0.08	0.02±0.20
Drigg C7	12	0.81	0.93±0.20	0.35±0.28
C1→C7	12	0.94	1.00±0.11	−0.29±0.66
Drigg D1	7	0.97	0.42±0.04	0.11±0.12
Drigg D2	7	0.67	0.12±0.05	0.47±0.09
Drigg D3	5	0.48	0.14±0.11	0.57±0.18
Drigg D4	—	—	—	—

Table 5.8: Details of best-fits to the ^{106}Ru vs ^{137}Cs data for the muslin screen exposures along the transects C and D at Drigg

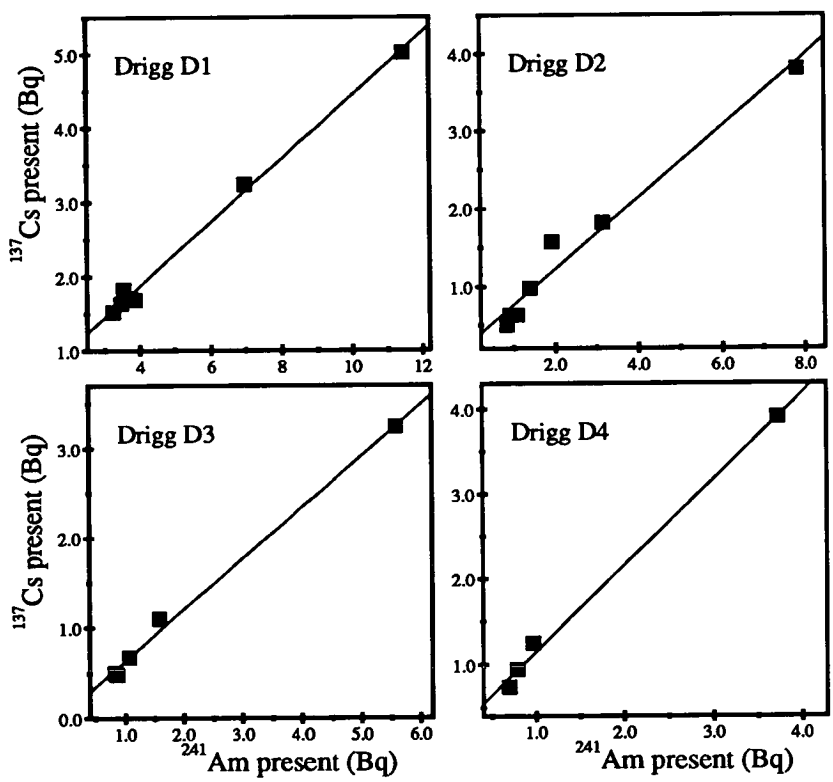

Figure 5.10: ^{241}Am on screens exposed along Drigg D against the ^{137}Cs collected. Lines are least-square best fits to the data points. (See Table 5.6)

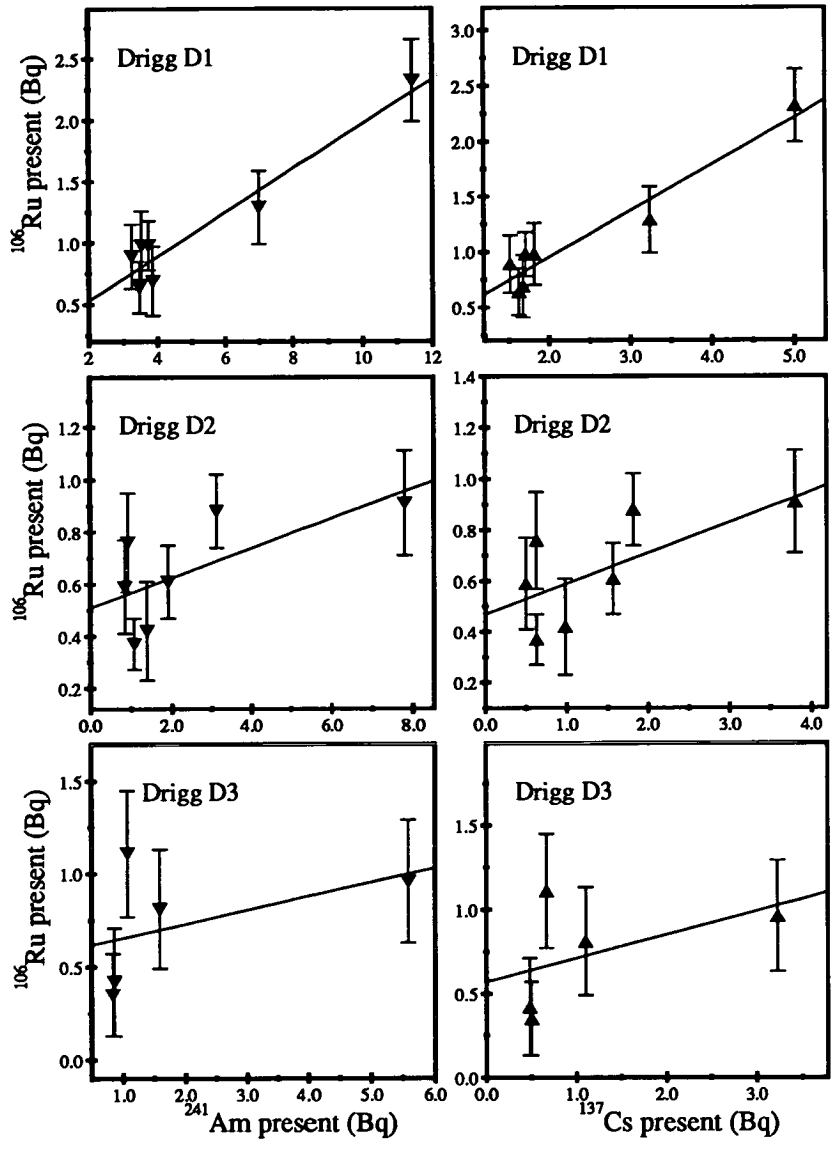

Figure 5.11: ^{241}Am and ^{137}Cs on screens exposed along Drigg D against the ^{106}Ru collected. Lines are least-square best fits to the data points. (See Tables 5.7 and 5.8)

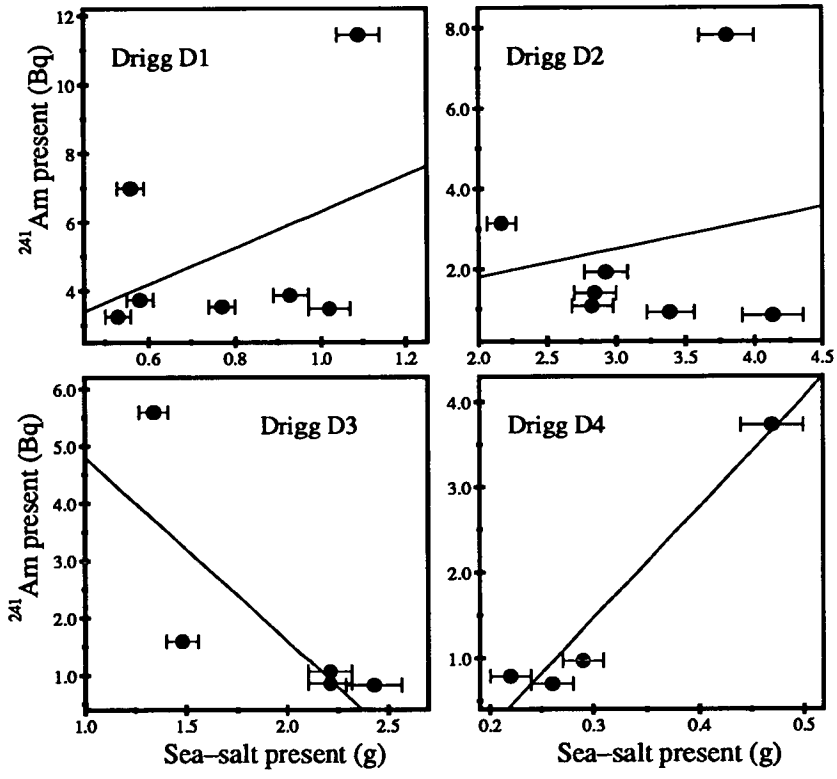

Figure 5.12: ^{241}Am on screens exposed along Drigg D against the sea-salt collected. Lines are least-square "best" fits to the data points. (See Table 5.3)

Radionuclide	$Bq\,g^{-1}$ of sea-salt	$Bq\,l^{-1}$ of spray	$Bq\,l^{-1}$ in seawater	Enrichment factor
^{241}Am	1.19±0.11	38±4	0.2–1.5 [18] 0.06–3.7 [52]	25–190 10–633
^{137}Cs	0.85±0.07	27±2	6.8–15.2 [18] 3.0–47.9 [52]	1.8–4.0 0.6–9.0
^{106}Ru	0.86±0.12	27±4	—	—

Table 5.9: The enrichment factor of sea spray relative to seawater for the Sellafield radionuclides collected on the muslin screens exposed along Drigg C. The enrichments are estimated using typical levels of radioactivity in in-shore seawater.

5.2.2 ^{7}Be collected on the exposed screens

As illustrated in Figures 3.12, 3.13, 3.19 and 3.22, measurable levels of the atmospheric aerosol ^{7}Be were present on the muslin screens after their exposure on the beach at Drigg. The ^{7}Be will have been collected in one or both of the following ways:

- In rainfall deposited onto the screens.
- By impaction of the ^{7}Be-bearing aerosol on the screen fibres. This must be a possible collection mechanism, as there was no rain during the short-term exposures S1 and S3, and ^{7}Be was later found on the cloth.

From the discussion of the collection characteristics of the muslin screens in Section 1.6, it is a reasonable initial assumption that these passive aerosol collectors will not capture airborne particles with a diameter less than 1 μm. A typical ^{7}Be air concentration in ground level air is 3000 μBq m^{-3} (See Table 1.7), of which only 20% is attached to particles of diameter over 1μm [47] (See Table 1.6). The screens were therefore exposed to an effective "collectable" air concentration of 600 μBq m^{-3}. From the wind speed and direction data it is possible to estimate the volume of air, and so the ^{7}Be activity, which passed through the screens on the occasions of the short-term exposures. From the activity present afterwards the efficiency of ^{7}Be collection by the muslin cloth from the air forced through it by the wind can be estimated.

Using the mean ^{7}Be activity collected on the screens exposed during the S1 and S3 short-term exposures, periods during which there was no rainfall, the screen collection efficiencies for the ^{7}Be-bearing aerosol are calculated as 7.7$\pm$1.6 and 8.8$\pm$1.7%. Considering that all the ^{7}Be was collected by dry impaction during the S4 exposure gives an estimate of the collection efficiency from the air of 9.8$\pm$0.6%. The collection efficiency for particles of 2μm diameter expected for the muslin screens is of the order of 10% (See Section 1.6).

There was, however, a period of rainfall during the S4 exposure. A rainfall of 0.8 mm was measured at Eskmeals, in a mean wind speed of 10.3 ms^{-1}. Resolving this horizontal velocity with a typical raindrop fall speed of 7 ms^{-1} [77], it is possible to estimate the volume of rain striking the screens, and thus approximate

the ^{7}Be activity which may have been collected in the rain. If all the ^{7}Be present in this rain is assumed to be collected by the screens, and a typical activity in rainfall of 1.7 Bql^{-1} (Table 1.8) is assumed, the predicted ^{7}Be collection on the S4 screens is 0.56 Bq. The mean ^{7}Be activity actually present on these screens after exposure was 1.9 Bq.

The conclusion which can be drawn from these short-term data is that it is possible to explain the ^{7}Be activity collected on the exposed muslin screens by considering the impaction of the ^{7}Be-bearing aerosol onto the screen fibres. This must be the explanation of the collections made during periods when there was no rainfall. It is possible however that there may be a contribution to the collected ^{7}Be in rainfall striking the exposed cloth.

The longer term exposures at Drigg C and D all had periods of rainfall. Table 5.10 calculates the collection efficiencies of the screens from the mean ^{7}Be levels present after each exposure and the volume of air estimated to have passed through them on each occasion. An effective air concentration of 600 μBq m^{-3} is again assumed.

The calculated collection efficiencies for the long-term exposures are markedly lower than the estimations from the short-term data. The possibility that the screen collection efficiency could decrease with age has been proposed by McHugh et al. [50], so longer term exposures may be expected to result in a reduced collection. Figure 5.13 illustrates a plot of the ^{7}Be collection efficiency from each long-term exposure along transects C and D against the total rainfall collected at Eskmeals in each exposure period. The line is a least-square linear fit to the data points and has a correlation coefficient of -0.677, a correlation significant to the 95% confidence limit [74]. There is certainly little evidence of an increased collection of ^{7}Be during periods of high rainfall, implying that the screens are not collecting ^{7}Be from rain. These data imply, moreover, that the rain causes the removal of ^{7}Be from the screens, which would explain the reduced ^{7}Be collection efficiency of the long-term screens relative to the ones exposed for shorter periods.

Exposure	Mean ^{7}Be Collected (Bq)	Air Flux ($m^3/10^6$)	Effective air Concentration ($\mu Bq\,m^{-3}$)	Collection Efficiency %
S1	0.78±0.16	0.017	45.9±9.4	7.7±1.6
S3	0.84±0.16	0.016	52.5±10	8.8±1.7
S4	2.06±0.12	0.035	58.9±3.4	9.8±0.6
C1	23.4±2.0	1.95	12.0±1.0	2.00±0.17
C2	5.4±0.6	1.93	2.8±0.3	0.47±0.05
C3	22.2±2.1	2.32	9.6±0.9	1.59±0.14
C4	40.0±3.0	6.26	6.4±0.5	1.06±0.08
C5	21.1±1.3	1.54	13.7±0.8	2.28±0.14
C6	28.8±4.6	5.96	4.8±0.8	0.81±0.13
C7	12.2±1.6	6.17	2.0±0.3	0.33±0.04
D1	44.3±3.8	3.76	11.8±1.0	1.96±0.17
D2	16.7±2.4	2.28	7.3±1.1	1.22±0.18
D3	11.0±2.9	6.17	1.8±0.5	0.30±0.08
D4	10.7±2.8	5.60	1.9±0.5	0.32±0.08

Table 5.10: Estimated ^{7}Be collection efficiency for the muslin screens exposed along the transects C and D at Drigg. The collectable air concentration is assumed to be $600\,\mu Bq\,m^{-3}$

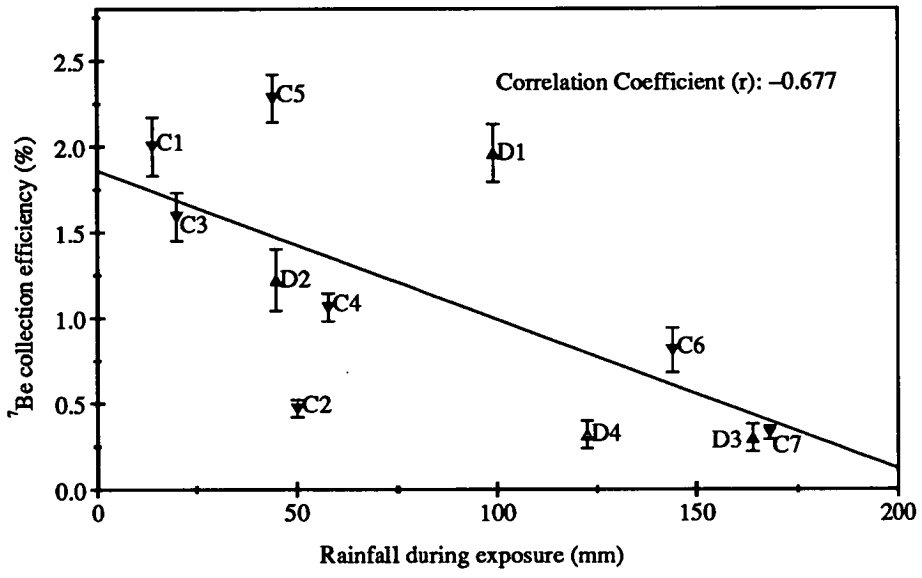

Figure 5.13: Calculated ^{7}Be collection efficiencies for exposures along Drigg C and D against the total rainfall collected at Eskmeals during each period

5.2.3 Using ^{7}Be to plot the wind flow along the transects

Having considered how the muslin screens collect the ^{7}Be from the air, it is also necessary to discuss why the screens in each exposure set did not collect the same ^{7}Be activity during their exposure. From the plots of the ^{7}Be collected during the Drigg C exposures (Figures 3.12 and 3.13), it can be seen that there is a systematic pattern to the ^{7}Be collections at the different sites from each of the exposure sets. The ^{7}Be collection is reduced at the more inland sites compared to the ones nearer the sea, and there is a repeated dip in collection at sites 5, 6, 7 and 8. It is known that the instantaneous concentration of ^{7}Be in ground level air and rain is very variable, and that it can vary greatly from place to place. It is not possible, however, to explain how the ^{7}Be air concentration could vary over the short distance being considered here in such a consistent fashion.

This phenomenon is explained by considering how the wind flow might change along this exposure transect. In an onshore wind, the wind speed can be expected to reduce as it blows over the coastline, as the surface drag increases. Thus screens nearer the sea can be expected to sample a larger volume of air than the screens at the rear, which are exposed to winds of a slower speed. The most sea-ward screens can be expected to collect more ^{7}Be from the air.

The author has noted how in periods of onshore winds, the region behind the frontal dune is very sheltered compared to the top of the dune at site 4 (Figure 2.4). Further inland along the transect the wind speed increases again. The screens at sites 5, 6, 7 and 8 are therefore positioned in the shadow of the front dune during onshore wind flow and will be exposed to lower wind speeds than the screens exposed both closer to and further from the sea under such conditions. This explains their consistently reduced ^{7}Be collection. The same can expected to be true for screens at sites 1, 2 and 3 in periods of offshore wind flow. These sites will be sheltered in the shadow of the dune as the wind blows out to sea.

The screens exposed along the Drigg D transect also show a reduced collection of ^{7}Be by the inland screens relative to the ones nearer the sea (Figure 3.19). These data sets, however, do not show a reduced collection by any of the screens exposed in the middle of the transect. This transect has a much more shallow

gradient up the frontal dune (Figure 2.5) and there is no significant shadow cast by this dune. It has not been observed that the screens exposed in this area behind the frontal dune are particularly sheltered during onshore winds.

5.2.4 Extracting the effects of the wind flow from the radionuclide and sea-salt collection data

The variation in the wind flow along the Drigg transects will also have had an effect on the collection of the spray droplets thrown into the air in the nearby surf zone. Similar patterns to that seen in the collected ^{7}Be data can be seen in the radionuclide and sea-salt collections at the different sites, including the dip at the sites behind the large frontal dune on the Drigg C transect (Figures 3.6 to 3.20). The apparent reduction in radionuclide air concentration over the distance along the transects plotted in these diagrams must also contain the effects of the changing wind flow discussed above. Some of the apparent reduction in the radionuclide and sea-salt collection with distance inland must be due to the behaviour of the wind as it blows along the transect. This artefact of the measuring technique must be extracted if the true reduction in radionuclide air concentration with distance inland is to be established.

The assumption is made that the differing levels of ^{7}Be collected by the screens during each exposure are due entirely to the changing wind flow pattern along the transects. It is therefore possible to extract the effects of the changing wind flow on the collections of ^{241}Am, ^{137}Cs, ^{106}Ru and sea-salt by normalising the volume of air sampled by each screen using the collected ^{7}Be activity.

A proviso which should be kept in mind, however, is that while the exposed muslin screens will collect sea spray only during periods of onshore wind flow, they can collect ^{7}Be at all times, in winds from all directions. Considering the wind data from the exposures along Drigg C, a large fraction of the wind flux through the screens of the C1, C5, C6 and C7 exposures was from onshore winds (See Column 4, Table 3.4). For these exposures, the collection of the majority of the ^{7}Be will have occurred simultaneously with the sea spray collection. In exposure C3, and to a lesser extent C2 and C4, a significant fraction of the

^{7}Be will have been collected by the screens during periods when there will have been no sea spray collection. In these cases the changes in wind flow along the transect, plotted using the ^{7}Be collection pattern at the different sites, may not be relevant to the periods of sea spray collection.

The quantity of sea-salt collected on the screens exposed for short periods at Drigg D are illustrated in Figures 3.23 and 3.24. Only the data from the S1, S3 and S4 exposures will be considered here, as only the screens from these exposures contained measurable levels of ^{7}Be. The results from the sea-salt measurements on these screens are redrawn in Figure 5.14. The screens were exposed at the same sites on each occasion, but the distance between the edge of the sea and the screens was different for each exposure. All three exposures show a similarly shaped reduction in salt collection over the distance covered by the screens. It is obvious that the reduced sea-salt collection along the screen transect illustrated in these plots is not purely a result of the diminishing airborne sea-salt concentration with distance from the sea. As these screen sets were exposed at different distances from the sea they would be expected to show different falloff gradients along the transect. In the case of the S1 and S3 exposures the front screen was positioned 300 and 600 m, respectively, from the water's edge. The sea-salt air concentration can not have been decreasing at this rate at such large distances from the surf, as the air loading would have been unrealistically high close to the sea. It is a reasonable assumption that the falloff plotted with distance in these data includes the affects of the changing wind flow pattern along the section of the sand dunes covered by the screens. This also explains why the falloff pattern is so similar in the three data sets.

The effect of the changing wind flow pattern on the screens can be removed by using the ^{7}Be activity collected at each site. The calculated sea-salt : ^{7}Be ratio on each screen is illustrated in Figure 5.15, thus correcting the sea-salt collections for the different volume of air sampled at each exposure site. The reduced sea-salt collections over the distance covered by the screens are very much flattened out in the data from the S1 and S3 exposures, the occasions when the spray had already travelled relatively large distances before reaching the exposed screens. There is still, however, a significant change between front and back screens in

the S4 data, when the mean sea to front screen distance was only 17 m during the exposure.

The lines fitted to the data points in these diagrams are outputs from the Sea-to-Land Tansfer Model described in Chapter 4. The volume of spray collected downwind of a stationary source was calculated relative to a reference point positioned at the site of the most sea-ward muslin screen. The collection at this reference site was then scaled to fit the data points. Neutral atmospheric conditions were assumed for these fits (i.e. p=0.8). The falloff with distance inland in the S4 data is very well fitted by the model.

The success in using the ^{7}Be levels collected on the exposed screens to explain the peculiar results in the sea-salt collection data from the S1 and S3 exposures lends further credence to the hypothesis that the ^{7}Be collection on the exposed screens can be used to plot the changes in the wind flow pattern over the sand dunes.

Figures 5.16 and 5.17 show the ^{241}Am collections on the Drigg C screens corrected for the wind behaviour by dividing the collected ^{241}Am activity on each screen by the ^{7}Be activity. Having thus extracted the effects of the wind flow irregularities on the sea spray collections, it can be seen that there is a remaining reduction in the ^{241}Am air concentration with distance inland along the transect. The fits to the data in these plots were again produced by the Sea-to-Land Transfer Model. For these fits a value of p of 0.8, typical of neutral atmospheric stability conditions, has been used. The surf zone has been considered to move between the distances of 1000 and 10 m from the most sea-ward screen. This falloff pattern was then fitted to each data set by shifting it vertically relative to the points. Only in the C4 exposure could a reasonable fit not be obtained with these values of p and W. In this case a larger value of p of 0.95 (more typical of unstable atmospheric conditions) was used to give an improved fit.

It is interesting to note how the data points from sites 1, 2 and 3 are far above the fit lines to the data from the C3 and C4 exposures (Figure 5.16). As discussed above, these were exposures during which there were extensive periods of offshore wind flow. Thus the screens at Sites 1, 2 and 3 will have been more sheltered than the other screens, and are expected to have a reduced collection

of ^{7}Be. This explains the enhanced ^{241}Am : ^{7}Be ratio on these screens and why these data points are lifted off the fit line through the other data points.

The results of performing the same procedure on the ^{137}Cs activity collected on the muslin screens exposed along Drigg C are illustrated in Figures 5.18 and 5.19. Again the fits to the data are from the model, in this occasion all assuming a value of the parameter p of 0.8, with the surf moving between 10 and 1000 m from from the front screen. Again, the data points from screens 1, 2 and 3 of the C3 and C4 exposures can been seen to be well above the fit lines.

Outputs from the Sea-to-Land Transfer Model have been shown to simulate the reduction in sea-salt and radionuclide air concentrations with distance from the sea measured using a line of simultaneously exposed muslin screen collectors. In fitting the model to these measurements the input parameters have been given values which are typical of those quoted in the literature; the input parameter values are given in Table 4.1. None of the parameters have had to be given values far from what is expected in order to produce good fits to the muslin screen data.

The discussion of the model sensitivity to the values of the input parameters in Section 4.3 showed how the falloff pattern was sensitive to parameters p and W. These parameters were not measured during the course of the muslin screen exposures. Better fits to the Drigg C air volume corrected data in Figures 5.16 to 5.19 could have been obtained by varying the values of parameters p and W from the default values, but as no actual measurements were made there is no empirical basis for doing so. Even without the necessity of varying the values of the input parameters, however, the reduction in radionuclide air concentration with distance inland, as monitored by the muslin screens, has been well simulated using the model developed in the course of this study.

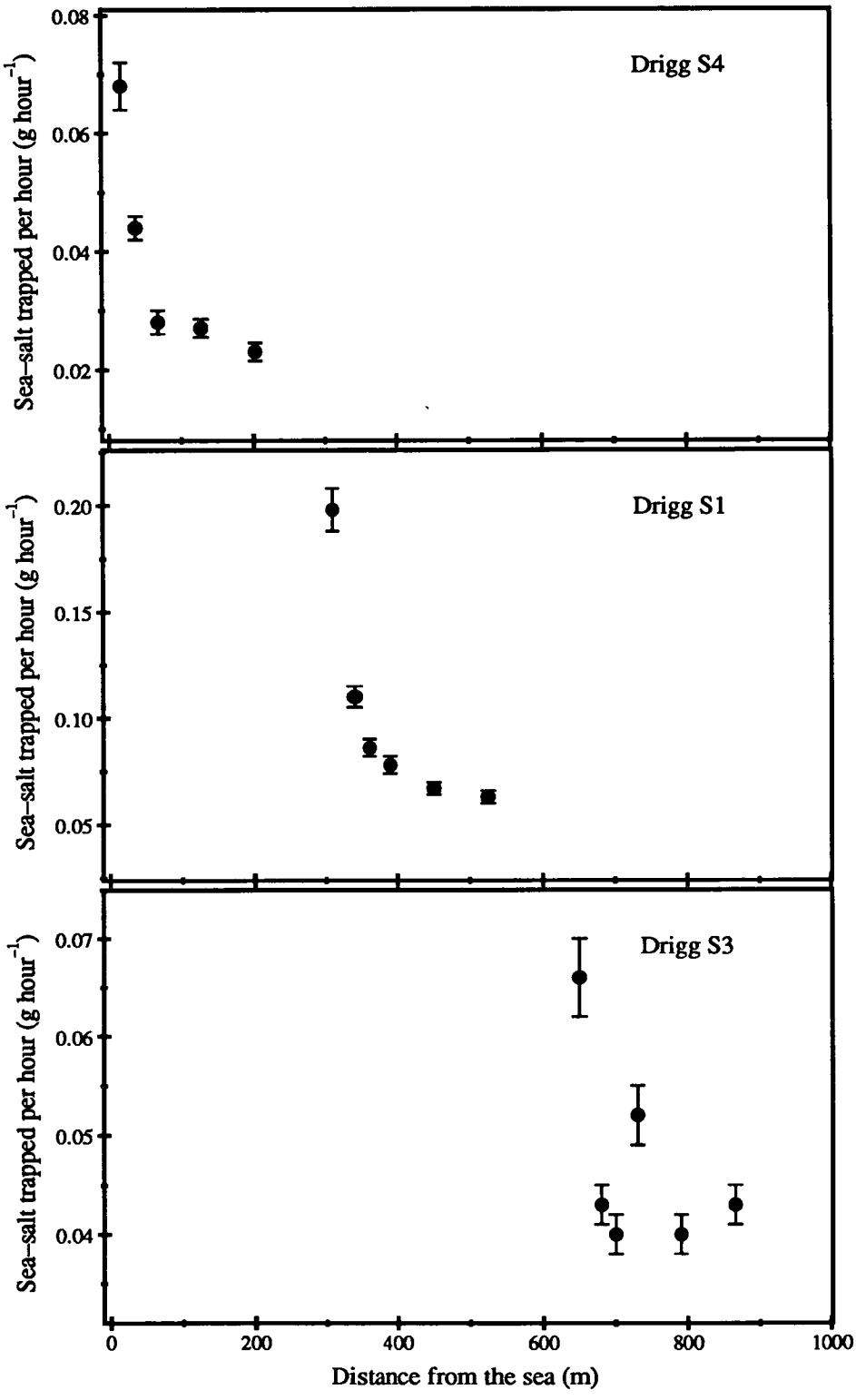

Figure 5.14: Sea-salt collections during the short-term exposures when measurable levels of ^{7}Be were collected. The sea–screen distance was different on each occasion

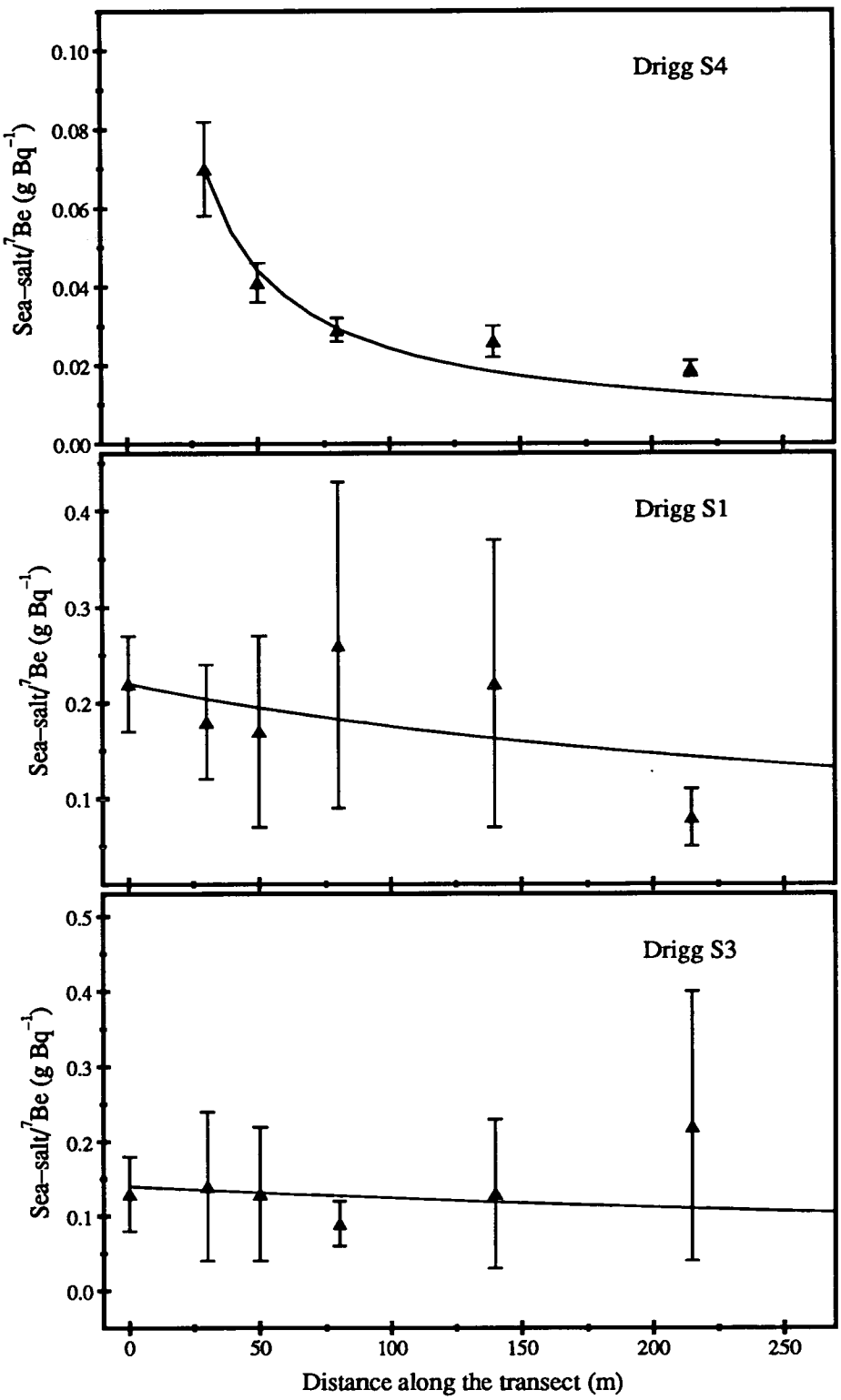

Figure 5.15: Sea-salt : ^{7}Be ratios on the screens exposed for short-term periods at Drigg D. Fits are produced by the Sea-to-Land Transfer Model

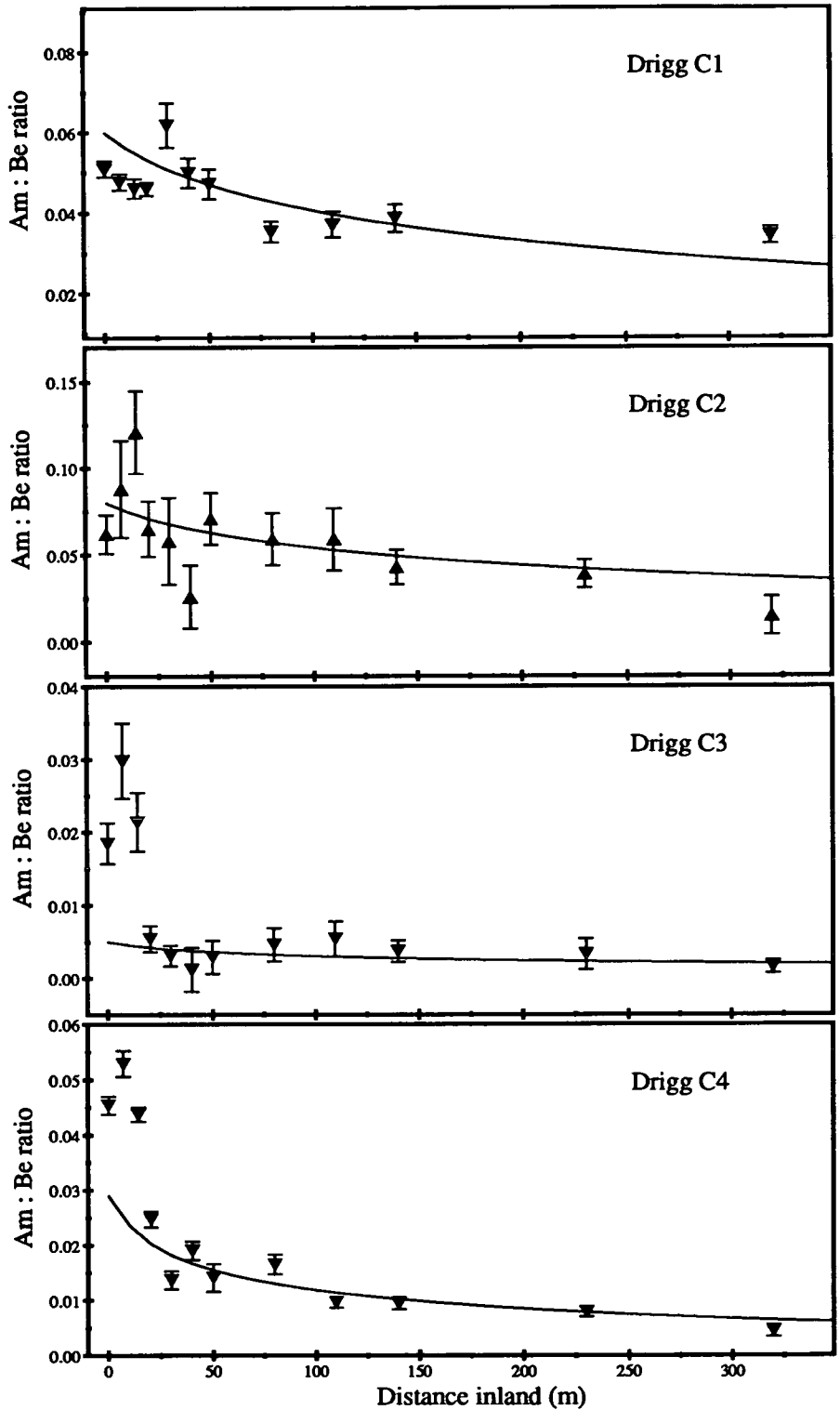

Figure 5.16: ^{241}Am : ^{7}Be ratios on the screens exposed along Drigg C. Fits are produced by the Sea-to-Land Transfer Model as discussed in the text

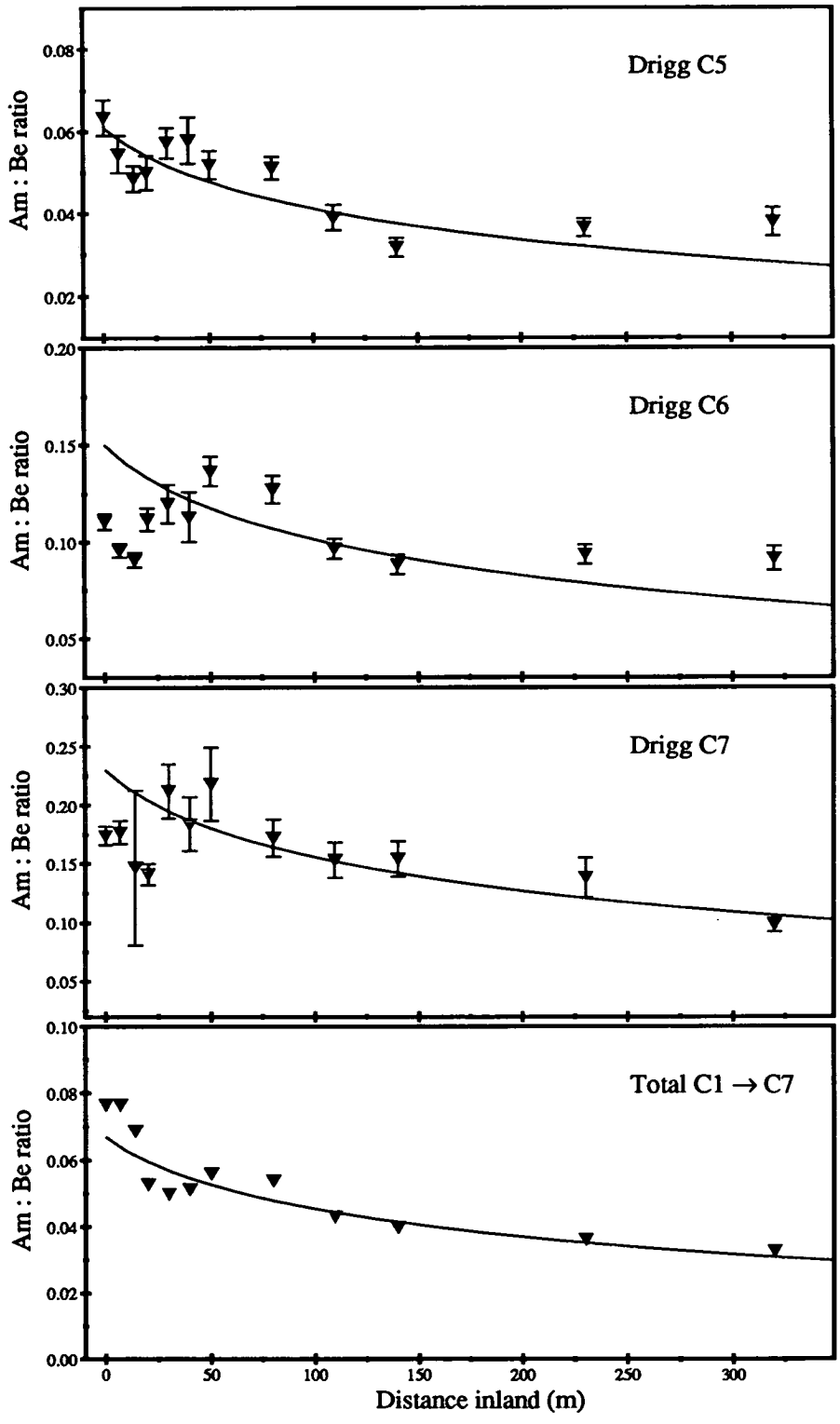

Figure 5.17: ^{241}Am : ^{7}Be ratios on the screens exposed along Drigg C. Fits are produced by the Sea-to-Land Transfer Model as discussed in the text

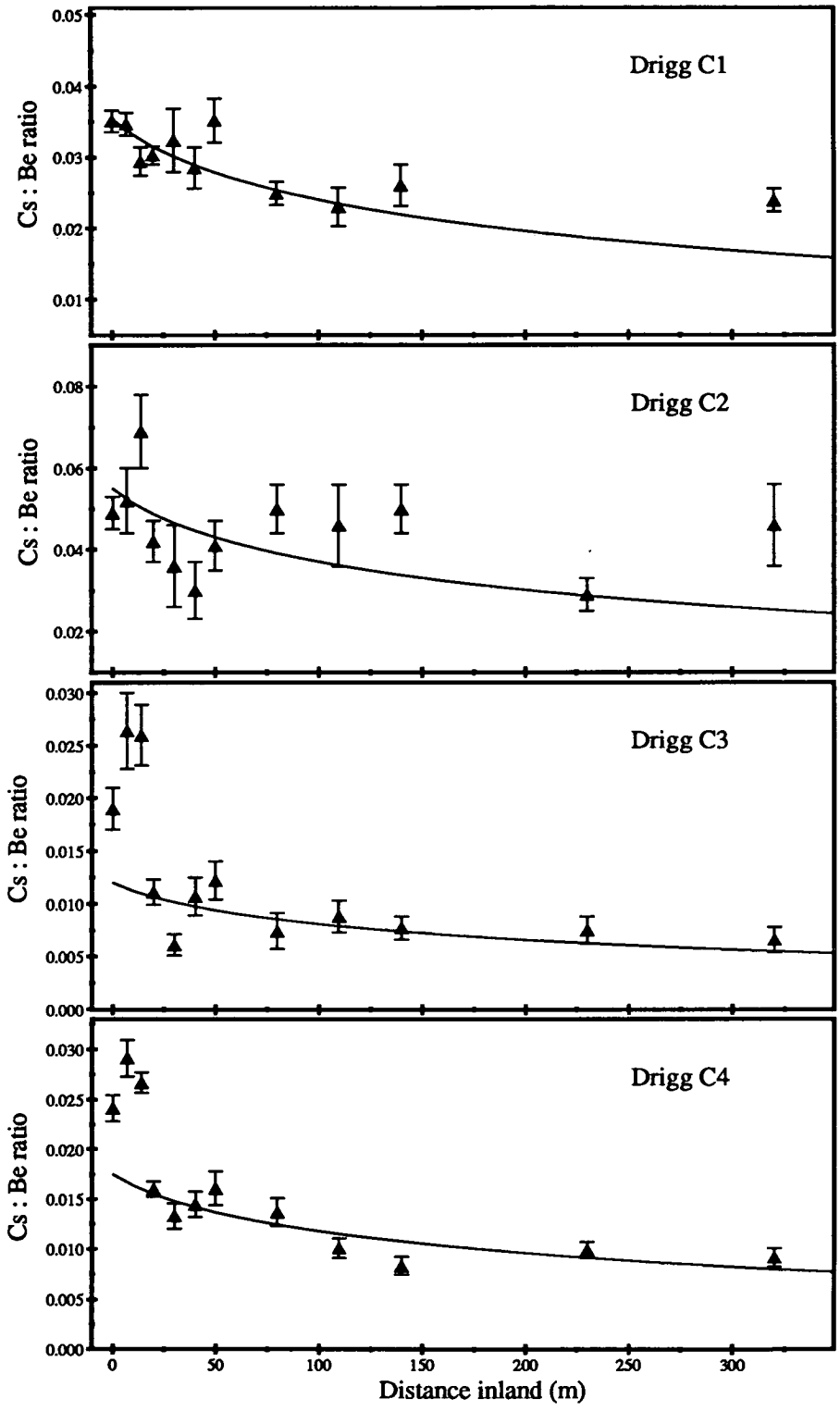

Figure 5.18: ^{137}Cs : ^{7}Be ratios on the screens exposed along Drigg C. Fits are produced by the Sea-to-Land Transfer Model as discussed in the text

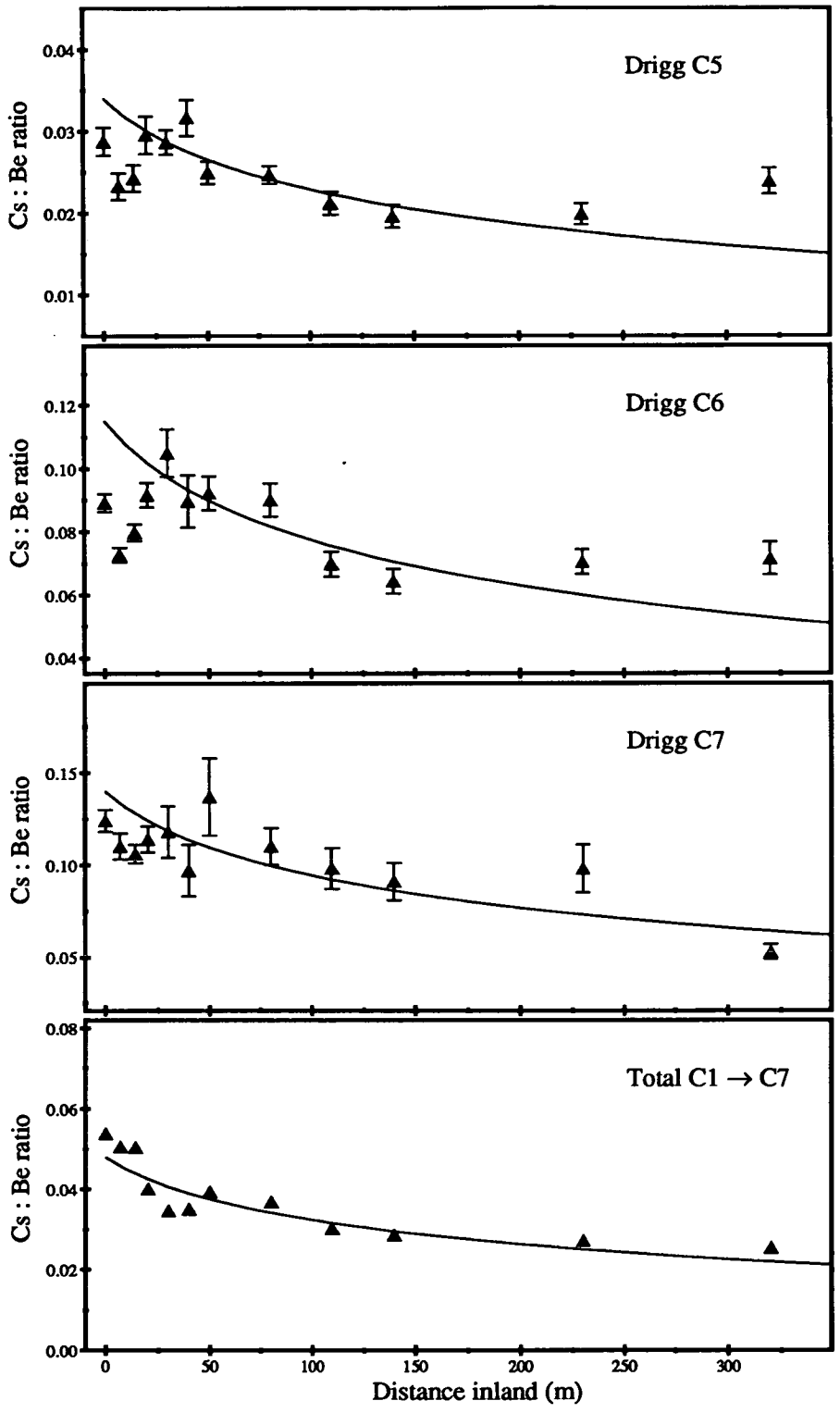

Figure 5.19: ^{137}Cs : ^{7}Be ratios on the screens exposed along Drigg C. Fits are produced by the Sea-to-Land Transfer Model as discussed in the text

5.2.5 Radionuclide air concentrations

The measurements made with the muslin screens along the Drigg transects can only be properly compared with other measurements of the intensity of the sea-to-land transfer of radionuclides, made with muslin screens or air samplers, when the collection characteristics of the screens are better understood. This work is currently being carried out at the E&MS section at Harwell, and should shed more light on the data being presented here [53].

Eakins et al. calculated the concentration of radionuclides present in the air passing through their exposed muslin screens by dividing the activity collected on the screens by the volume of air estimated to have passed through [18]. They used a collection efficiency for the screens of 20%. The results of their estimations of the ^{241}Am air concentrations are given in Table 1.3. The same procedure has been performed on the data obtained from the muslin screen exposures along the transects at Drigg C and D, and the estimated ^{241}Am air concentrations are quoted in Table 5.11. The mean level of ^{241}Am present on each set of exposed screens was used in the calculation, and an efficiency of 20% has again been assumed. The air flux from the sea-ward direction has been used in the calculation (See Table 3.4). On no occasion do these results approach the levels found by Eakins et al. on the extreme occasion at St. Bees (Table 1.3). The results however are of a similar order to their results from Eskmeals, but are generally lower. This reduction could be due to any or all of a number of different reasons.

One possibility is a reduction in muslin screen collection efficiency with time. Also, the conclusion that rainfall appeared to wash collected ^{7}Be off the screens could be extended to the Sellafield radionuclides. The reduced collection would result in an under-estimate of the air concentrations. The differences between these and the Eakins et al. results could also be due to the different wind conditions at the time of the exposures or to the expected differences in the rate of radionuclide sea-to-land transfer at different sites.

The mean air concentration present during the six months covered by the screen exposures at Drigg C was $2.0 \pm 0.3\,\mu\mathrm{Bq\,m^{-3}}$. This compares favourably with the annual mean of $2.4\,\mu\mathrm{Bq\,m^{-3}}$ measured by Fry with air samplers at Seascale in 1981 [27] and with other measurements performed with air samplers

at Eskmeals, quoted in Table 1.1.

Muslin screens are expected to collect droplets with diameters above 20 μm more efficiently than aerosol samplers [62]. Therefore a muslin screen exposed simultaneously with an aerosol sampler close to the surf would tend to measure a greater radionuclide air concentration. On the other hand, it also seems likely that 20% is too large a value for the muslin screen collection efficiency over an extended period, due to the possible removal caused by rainfall. Thus the mean air concentration estimated above from the muslin screen exposures along Drigg C will be an under-estimate of the true value.

A feature of interest from this work is the enhanced ^{241}Am : ^{137}Cs ratio on the exposed screens compared to that found by other workers. Pattenden et al. found a mean ^{241}Am : ^{137}Cs ratio of 0.03 in their air samplers at Eskmeals [62]. Eakins et al. found a higher mean ratio of 0.16 on exposed muslin screens [18]. On screens exposed at Drigg C in this study, the mean ^{241}Am : ^{137}Cs ratio was found to be 1.4$\pm$0.3, illustrating a much reduced collection of ^{137}Cs relative to that of other workers. This change may be due in part to the changes in the BNFL discharging protocol in the time between these measurements and those of the other workers. The mean annual ^{241}Am : ^{137}Cs ratio in the discharges from Sellafield increased from 0.003 to 0.06 between 1982 and 1987 [4]. Thus an increased isotopic ratio in the material being transferred inland might be expected over this period. It is also possible that geomorphological differences in the sediment offshore at Drigg and Eskmeals could lead to different radionuclide ratios in any sedimentary material being transferred inland.

There is some evidence from the muslin screen exposures at Drigg that periods of increased wind speed result in greater transfers of radioactive material inland. Figure 5.20 plots the air concentrations of ^{241}Am, ^{137}Cs and ^{106}Ru during each exposure at Drigg C against the mean wind speed during the exposure period. The lines are best fit straight lines to the data and are drawn to indicate the increased concentrations at higher wind speeds, and not to suggest a purely linear relationship. There is evidence here that the screens exposed during the stormier periods were exposed to air containing higher levels of radioactivity in the sea spray.

Exposure	Mean ^{241}Am Collected (Bq)	Air Flux from Sea ($m^3/10^6$)	Effective air Concentration ($\mu Bq\,m^{-3}$)
S4	0.09±0.12	0.035	13±3
C1	1.05±0.10	1.91	2.7±0.3
C2	0.33±0.06	1.43	1.2±0.2
C3	0.15±0.04	0.62	1.2±0.3
C4	0.87±0.21	3.77	1.2±0.3
C5	1.01±0.08	1.54	3.3±0.3
C6	2.97±0.44	5.50	2.7±0.4
C7	1.93±0.25	5.62	1.7±0.2
C1→C7	8.29±1.14	20.4	2.0±0.3
D1	5.2±1.2	3.52	7.4±1.7
D2	2.4±0.9	2.06	5.8±2.2
D3	2.0±0.9	5.62	1.8±0.8
D4	1.5±0.7	3.84	2.0±0.9

Table 5.11: Estimated ^{241}Am air concentrations from the muslin screens exposed along the Transects C and D at Drigg. A collection efficiency of 20% is assumed, after Eakins et al. [18]

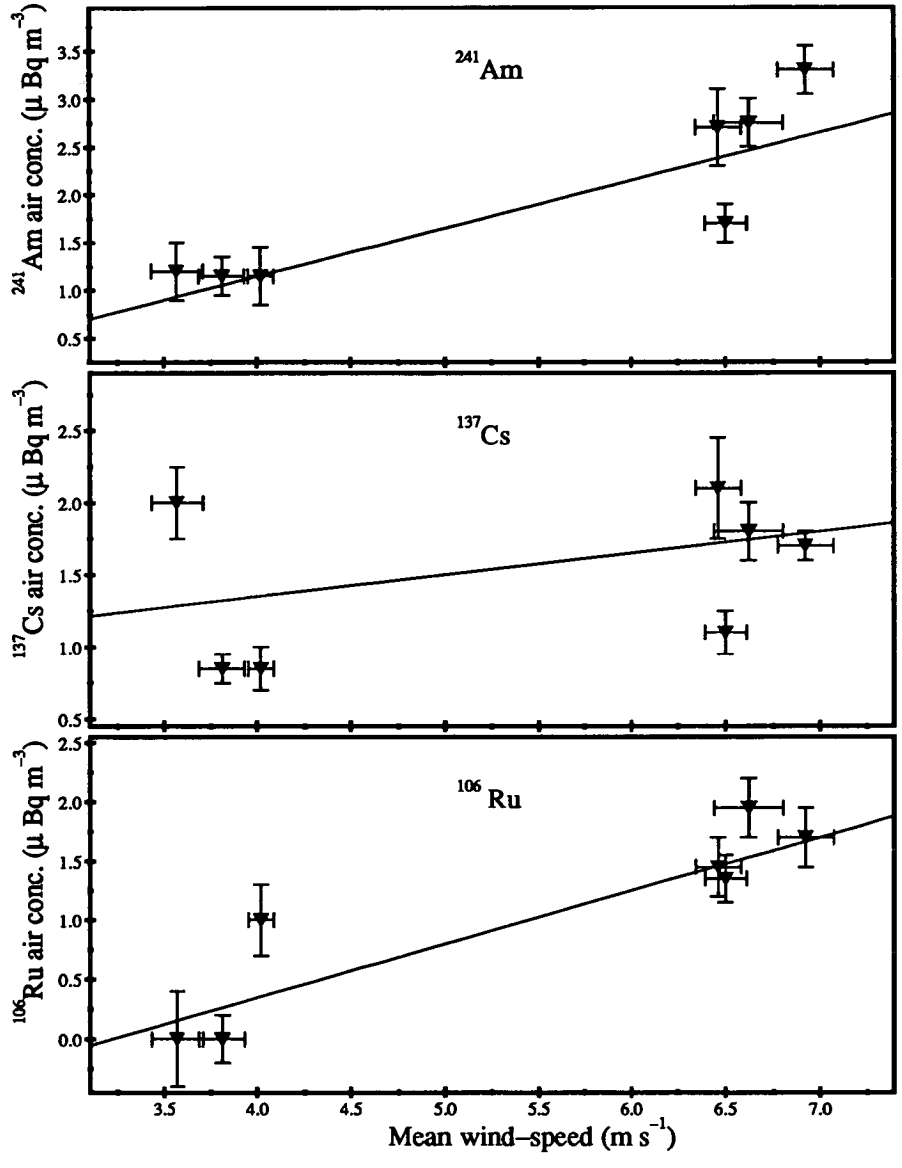

Figure 5.20: Air concentrations for the different radionuclides for each exposure along Drigg C plotted against the mean wind speed during each exposure

Chapter 6

Conclusions

In this final chapter the conclusions of this study are presented. Points where these conclusions concur and conflict with current thinking on this significant transfer mechanism of radionuclides into the human environment are highlighted and discussed.

These measurements, performed by collecting samples of coastal vegetation and exposing muslin cloth sea spray collectors near to the Cumbrian Irish Sea coast, constitute a systematic study of the inland transfer of sea spray-borne radioactivity. This is the most detailed analysis of the reduction in radionuclide air concentration with distance inland which has been performed close to the Cumbrian coastline. The measurements which have been carried out will therefore be useful in making better estimates of the radiation exposure of the local population in this region arising from the discharge to sea of the low-level wastes from Sellafield.

It is an ironic fact that the Sellafield radionuclides present in the coastal vegetation samples collected a few miles south of the plant were swamped by radionuclides released in a nuclear accident over 2500 miles away. Some of the marram grass samples collected in April 1987 had ^{137}Cs concentrations of 2000 $Bq\,kg^{-1}$, of which less than 50 $Bq\,kg^{-1}$ was thought to be of Sellafield origin (See Section 5.1.1). The ^{137}Cs to ^{134}Cs isotopic ratio in the initial deposition in this region from the Chernobyl plume in early May 1986 is estimated as 1.72 ± 0.08 from the analysis of these marram grass samples. This is in agreement with

measurements made on rainfall in Cumbria at the time of the deposition [9]. The ^{106}Ru to ^{134}Cs ratio in the initial deposition from the Chernobyl cloud is estimated at 0.43±0.16. No measurements of the ratio of these isotopes in Cumbria have been reported with which this estimate can be compared. Using the isotopic ratio between the Cs isotopes quoted above has allowed the ^{137}Cs of Chernobyl origin in the collected marram grass samples to be calculated, thus estimating the ^{137}Cs of Sellafield origin in the vegetation. Significant correlations were found between the changing ^{241}Am concentrations in the marram grass collected at different distances inland and the ^{137}Cs calculated to be of Sellafield origin. The concentrations of these radionuclides decrease at the same rate with distance from the sea, implying that they are being transferred inland by the same mechanism.

The mean retention time of marram grass for deposited ^{134}Cs was estimated, from a consideration of the changing concentrations in grass samples collected at the same sites at different times, to be 90±15 days during the months of early spring (Section 5.1.2). This loss rate is not expected to differ greatly for different depositing radionuclides and is expected to be even less rapid at other times of the year [10]. In the three months between November 1987 and February 1988 the ^{241}Am and Sellafield-originating ^{137}Cs concentration remained unchanged in vegetation collected along the Drigg C transect. As the loss mechanism is thought to be very inefficient in this grass species over the winter months, there is an implication in this data that the marram grass is an inefficient collector of the spray-borne radioactivity.

The simultaneous exposure of muslin screen collectors along transects inland proved to be a cheap, simple but effective method of measuring the reduction in radionuclide air concentration with distance from the sea. The technique of exposing the muslin screens also avoided many of the problems encountered in the attempts to plot the reduction in radionuclide intensity using the marram grass transects.

The apparent reduction in radionuclide air concentration along a line of exposed muslin collectors has been found to contain an artefact due to irregularities in the wind flow along the exposure transect. Although the screens were exposed

simultaneously and in a close formation, they collected airborne spray droplets from different air volumes. This results in different collections at the different sites, and would do so even if each screen were exposed to an identical air concentration. This problem with this collection technique has been solved with the use of the collected activity of ^{7}Be during the exposure period. The natural atmospheric radionuclide ^{7}Be has not been used in any previous studies to normalise the collection of exposed passive collectors in this manner. The method of using collected ^{7}Be to normalise for the sampling of different volumes of air can only be used for reasonably closely positioned collectors, as the surface air concentration of ^{7}Be can vary greatly from site to site (See Section 1.7).

The radionuclides of Sellafield origin collected on exposed muslin screens were found to be closely correlated with the collected sea-salt. This direct link, clearly implicating the sea spray transfer as the mechanism of the inland transport of the Sellafield radionuclides, has not been illustrated previously in such an explicit fashion.

As was the case in the marram grass data, there were also found to be significant correlations between the collected activities of different Sellafield radionuclides on the exposed muslin screens. Other studies have failed to find that fission products are being transferred inland by the same mechanism as the actinides. Cambray and Eakins found different falloff rates for ^{137}Cs, $^{239+240}Pu$ and ^{241}Am in soil cores collected along transects inland from the sea [8]. Pattenden et al. found correlations between ^{137}Cs and ^{106}Ru in deposited material in Cumbria, but did not find correlations of these isotopes with ^{241}Am [63]. The conclusions from this study, however, are that all the different radionuclides are being transferred inland by the same mechanism and that their intensity decreases at the same rate with distance inland. That the fission product ^{137}Cs can be efficiently transferred inland in sea spray is also strongly suggested from the muslin screen exposure at St. Bees by Eakins et al. [18], as discussed in Section 1.3.2.

Rough estimates of the sea spray enrichment factors relative to seawater have been made, using activities of ^{137}Cs and ^{241}Am typical of in-shore seawater in this region of Cumbria (See Section 5.2.1). Reasonable agreement has been found with the enrichment factors proposed in other studies. An interesting feature of

these results, however, is that the radionuclide to sea-salt ratio has been found to be constant with distance inland. There is no evidence from the data collected here for a varying enrichment factor with size of spray droplets, as has been predicted from other studies [19][63].

Radionuclide air concentrations close to the Irish Sea have been estimated from the muslin screen exposures. The mean air concentration of ^{241}Am determined from the muslin screen exposures over a six month period along the Drigg C transect agrees well with air concentrations averaged over long time periods in this region reported elsewhere (Section 5.2.5). The highest ^{241}Am air concentration estimated from the muslin screen data was $13\pm3\,\mu\mathrm{Bq\,m^{-3}}$ from the short-term exposure S4. It is reasonable to assume that at least a similar plutonium-alpha activity was also present in the air on this occasion. Together the Pu and ^{241}Am air concentrations, therefore, are equivalent to at least 3% of the ICRP recommended limit (See Section 1.3.5). There is also some evidence from the long-term muslin screen exposures along Drigg C that stormier weather conditions result in increased radionuclide air concentrations close to the Cumbrian coastline (Section 5.2.5).

The Sea-to-Land Transfer Model developed in the course of this study has been shown to be successful in simulating the reduction in radionuclide air concentration with distance inland from the Cumbrian coastline. It also closely fits other published data on the reduction in radionuclide concentration inland in coastal vegetation and soil.

This model accounts for the reduction in near surface air concentration by two mechanisms, the deposition of material to the ground and the mixing of the suspended material to increasing heights with distance travelled from the source. One of the conclusions arising from the successful application of the Sea-to-Land Transfer Model to the experimental data, is that the rapid reduction in airborne droplet concentration close to the source of the spray is due more to atmospheric turbulence, mixing the material vertically, than to the spray being deposited to the ground from the dispersing plume. Thus the reduction in air concentration with distance does not imply that the sea spray is limited in its extent to small distances inland. The spray droplets travel to greater distances

from their source than may be at first assumed when considering the plots of the reducing air concentrations with distance. In neutral atmospheric conditions the model predicts that a muslin screen exposed 1 km inland will collect only 2% of the spray volume collected by a screen positioned 10 m from the surf. However, 60% of the spray volume released by the source is calculated to be still airborne 1 km inland. Thus, the data discussed in Section 1.3.4 showing how radioactive material discharged to sea was found up to 60 km inland in Cumbria [20], is not surprising when considering this information provided by the Sea-to-Land Transfer Model.

Estimates of the rate at which radioactivity is released from the surf zone have also been made with the Sea-to-Land Transfer Model. These calculations have used measurements of radionuclide air concentrations close to the coast. The production rate of radioactivity in surf produced spray has not been previously estimated.

The highest airborne concentration in this study resulted in the collection of 0.081 Bq of ^{241}Am per hour on the front 0.5 m^2 screen of the S4 exposure, exposed a mean distance of 17 m from the edge of the surf in a wind of 11 $m\,s^{-1}$. It is calculated from the model that 10% of the material produced in the 1 m length of surf adjacent to the screen will have passed through the volume occupied by it under these conditions. Assuming a collection efficiency of 20% implies that ^{241}Am was being produced at a rate of 4.1 Bq per hour per metre length of surf. These conditions would result in the transfer of 3.9×10^6 Bq (100 μCi) of ^{241}Am along 40 km of the Cumbrian coastline from St. Bees to Barrow over a 24 hour period. A similar activity level of $^{239+240}$Pu could also be expected to be transferred inland under such conditions. It should be noted that this exposure was not during a particularly stormy period, and that winds of up to 3 times this speed occur in the Irish Sea.

The very high air concentration measured by Eakins et al. with a muslin screen at St. Bees is of significance here (See Section 1.3.2). This 5 m wide screen collected 35 Bq of $^{239+240}$Pu and 25 Bq of ^{241}Am when positioned 33 m from the sea for 105 minutes in 6.9 ms^{-1} winds. The Sea-to-Land Transfer Model calculates that this screen will have sampled 13% of the produced material; assuming a

20% collection efficiency, this implies a production rate of 2.6 Bq of $^{239+240}$Pu and 1.8 Bq of ^{241}Am per metre of source per minute. Under such intense conditions a 1 km length of shoreline will have been responsible for the transfer of 1.54×10^5 Bq (4.2 μCi) of $^{239+240}$Pu and 1.10×10^5 Bq (3.0 μCi) of ^{241}Am per hour to the adjacent shoreline. This constitutes a very significant rate of transfer of these long-lived and extremely toxic radionuclides from the sea to the land.

It is useful here to outline the direction further research into the sea-to-land transfer of radioactivity and other pollutants should take to continue the work carried out in this study and to further investigate the conclusions arising from the measurements performed here.

It would be of use to perform a series of measurements of muslin screen exposures along transects which extend to greater distances inland from the coastline. Such measurements would provide excellent further tests on the applicability of the Sea-to-Land Transfer Model.

More information on the collection characteristics of these muslin cloth screens will be of great use and increase the applicability of the type of measurements performed here. This knowledge would allow a better comparison between the air concentrations estimated from muslin screen exposures and those made by other workers with bulk aerosol samplers. This method of collecting aerosol of diameter over 1 μm is extremely simple and effective. Other studies of airborne particle transport would certainly benefit from the use of techniques tried here. It is suggested that the method of using collected ^{7}Be to normalise sample volumes, developed here, could be of great use in such studies.

An aspect of the sea-to-land transfer of radioactivity which has not been closely investigated here and which is of great significance, concerns the periods when very high radioactivity levels are transferred inland. One such occasion was caught during one of the short-term muslin screen exposures of Eakins et al. (See Section 1.3.2). As discussed in Section 1.3.5 the air concentration measured on this occasion was greater than the current ICRP recommended limit for exposure of the general public. The meteorological conditions and the geomorphology of the sea-bed which give rise to such large air concentrations merit further study.

The regularity with which these occasions arise and the typical rate at which radioactivity is coming inland during such periods merits a detailed investigation. The obvious site to perform such measurements is on the beach at Seascale. This would then give direct evidence of the radiation exposure of the public in this town; this population is possibly the group most at risk from the radionuclides coming inland in the sea spray.

Sewage waste outlets to the sea are possibly the source of bacteria and viruses which can become incorporated into airborne and respirable spray droplets [1][2]. The transport of pathogenic pollutants other than radioactive ones therefore deserves further investigation.

It is very possible that the increased incidences of childhood cancers in the vicinity of Britain's nuclear reprocessing facilities are related to the enhanced radioactivity levels in these localities, caused by the environmental discharges to air and sea from these plants. If this is the case, one of the most significant pathways of this released radioactivity to the local populations, certainly of the long-lived actinides Pu and ^{241}Am, is by the transfer of marine discharged material inland in sea spray.

A body burden of 0.04 μCi of ^{239}Pu will cause a radiation exposure equal to an annual dose level of 5 mSv [57]. As the current ICRP limits for the general public are now 1 mSv [38], the maximum permissible body burden for members of the public can now be considered to be approximately 20% of this. When considered in these terms it can be seen that the transfer of radioactivity inland in sea spray is responsible for transporting very significant levels of long-lived radionuclides inland from the sea. A calculation performed here has shown how, in extreme conditions, the order of 4.2 μCi of $^{239+240}$Pu can be expected to be produced along 1 km of coastline in one hour. This transfer rate brings ashore a quantity of Pu activity per km of shoreline which is equivalent to the maximum permissible body burdens of over 500 members of the general public for every hour these conditions persist. In addition, the associated ^{241}Am transfer carries an activity level equivalent to the permissible body burdens of another 500 people per hour. It should also be noted that other radionuclides are transported inland

in significant quantities and that the spray-borne contaminants are expected to be efficiently carried to distances much greater than several kilometres inland from the sea.

It may be that the extreme conditions considered here are very rare and that all the radioactivity transported inland is very unlikely to find its way into the bodies of people. However, the above discussion does give an indication of the quantities of the long-lived radionuclides discharged to sea which are being returned to land by what is often a disregarded pathway. It also highlights the possible significance of this pathway in causing an increased radiation exposure of those resident in the coastal strip of Cumbria. It is to be concluded that this transfer mechanism merits further consideration and investigation as the causes of the leukaemia clusters in this region are sought.

References

[1] Baylor, E.R., Baylor, M.B., Blanchard, D.C., Syzdek, L.D. & Appel, C. (1977). Virus transfer from surf to wind. *Science* **198**, 575–580

[2] Blanchard, D.C. & Syzdek, L.D. (1970). Mechanism for the water-to-air transfer and concentration of bacteria. *Science* **170**, 626–628

[3] Blanchard, D.C. (1983). The production, distribution and bacterial enrichment of the sea-salt aerosol. In: *Air-Sea exchange of gases and particles* pp 407–454 (Ed. by Liss, P.S. & Slinn, W.G.N.). D. Reidel Publishing Comp., Dordrecht, Holland

[4] British Nuclear Fuels plc (1988). Radioactive discharges and monitoring of the environment 1987. Health & Safety Directorate, BNF plc, Cheshire

[5] Boyce, S.G. (1954). The salt spray community. *Ecological Monographs* **24**, 29–67

[6] Brown, E. & Firestone, R.B. (1986). Table of Radioactive Isotopes (Ed. by Shirley, V.S.). John Wiley & Sons

[7] Cambray, R.S. & Eakins, J.D. (1980). Studies of Environmental Radioactivity in Cumbria Part 1: Concentration of Pu and ^{137}Cs in environmental samples from West Cumbria and a possible maritime effect. London, HMSO **AERE-R 9807**

[8] Cambray, R.S. & Eakins, J.D. (1982). Pu, ^{241}Am and ^{137}Cs in West Cumbria and a maritime effect. *Nature* **300**, 46–48

[9] Cambray, R.S., Cawse, P.A., Garland, J.A., Gibson, J.A.B., Johnson, P., Lewis, G.N.J., Newton, D., Salmon, L. & Wade, B.O. (1987). Observations on radioactivity from the Chernobyl accident. *Nuclear Energy* **26(2)**, 77–101

[10] Chamberlain, A.C. (1970). Interception and retention of radioactive aerosols by vegetation. *Atmospheric Environment* **4**, 57–78

[11] Chamberlain, A.C. (1975). The movement of particles in plant communities. In: *Vegetation and the Atmosphere Vol. 1* pp 155–203 (Ed. by Monteith, J.L.). Academic Press, London

[12] Clarke, R.H. (1979). The 1st Report of a Working Group on Atmospheric Dispersion: A model for a short and medium range dispersion of radionuclides released to the atmosphere. London, HMSO **NRPB-R91**

[13] Cohen, B.L. (1983). Before it's too late; a scientist's case for nuclear energy. Plenum Press, New York and London

[14] Committee on Medical Aspects of Radiation in the Environment (COMARE), Chairman: Prof. M. Bobrow (1988). Second Report: Investigation of the possible increased incidence of leukaemia in young people near the Dounreay Nuclear Establishment, Caithness, Scotland. London, HMSO

[15] Crecelius, E.A. (1981). Prediction of marine atmospheric deposition rates using total ^{7}Be deposition velocities. *Atmospheric Environment* **15**, 579–582

[16] De Leeuw, G. (1986). Vertical profiles of giant particles close above the sea surface. *Tellus* **38B**, 51–61

[17] Dibb, J.E. (1989). Atmospheric deposition of ^{7}Be in the Chesapeake Bay region. *Journal of Geophysical Research* **94(D2)**, 2261–2265

[18] Eakins, J.D., Lally, A.E., Burton, P.J., Kilworth, D.R. & Pratley, F.A. (1982). Studies of Environmental Radioactivity in Cumbria Part 5: The magnitude and mechanism of enrichment of sea spray with actinides in West Cumbria. London, HMSO **AERE-R 10127**

[19] Eakins, J.D., & Lally, A.E. (1984). The transfer to land of actinide-bearing sediments from the Irish Sea by spray. *The Science of the Total Environment* **35**, 23–32

[20] Eakins, J.D., Lally, A.E., Cambray, R.S., Kilworth, D.R., Morrison, R.T. & Pratley, F.A. (1984). Plutonium in sheep faeces as an indicator of deposition on vegetation. *Journal of Environmental Radioactivity* **1**, 87–105

[21] Eisenbud, M. (1987). Environmental Radioactivity (3^{rd} Edition). Academic Press, Inc. San Diego, California

[22] England, J.B.A. (1976). Review Article: Detection of ionising radiations. *Journal of Physics E* **9**, 233–251

[23] Exton, H.J., Latham, J., Park, P.M., Perry, S.J., Smith, M.H. & Allan, R.R. (1985). The production and dispersal of marine aerosol. *The Quarterly Journal of the Royal Meteorological Society* **111**, 817–837

[24] Fairall, C.W., Davidson, K.L. & Schacher, G.E. (1983). An analysis of the surface production of sea-salt aerosols. *Tellus* **35B**, 31–39

[25] Feely, H.W., Larsen, R.J. & Sanderson, C.G. (1989). Factors that cause seasonal variations in ^{7}Be concentrations in surface air. *Journal of Environmental Radioactivity* **9**, 223–249

[26] Fraizier, A., Masson, M. & Guary, J.C. (1977). Recherches preliminaires sur le role des aerosols dans le transfert de certains radioelements du milieu marin au milieu terrestre. *Journal de Recherches Atmospheriques* **11**, 49–60

[27] Fry, F.A., Dodd, N.J., Green, N., Major, R.O. & Wilkins, B.T. (1982). Environmental radioactivity surveillance programme: Results for the U.K. for 1981. London, HMSO **NRPB-R134**

[28] Fujiwara, K. & Umejima, S. (1962). On the distribution of wind-borne salt on the coastal terrace. *Research Bulletins of the College of Experimental Forests, Hokkaido University* **21(2)**, 453–464

[29] Gardner, M.J., Snee, M.P., Hall, A.J., Powell, C.A., Downes, S. & Terrell, J.D. (1990). Results of case-control study of leukaemia and lymphoma among young people near Sellafield nuclear plant in West Cumbria. *British Medical Journal* **330**, 423–429

[30] Gathman, S.G. (1983) Optical properties of the marine aerosol as predicted by a BASIC version of the Navy Aerosol Model. Naval Research Laboratory, Washington, D.C. **NRL Memorandum Report 5157**

[31] Gathman, S.G. (1989) A preliminary description of NOVAM, the Navy Oceanic Vertical Aerosol Model. Naval Research Laboratory, Washington, D.C. **NRL Report 9200**

[32] Gustafson, P.F., Kerrigan, M.A. & Brar, S.S. (1961). Comparison of ^{7}Be and ^{137}Cs radioactivity in ground-level air. *Nature* **191**, 454–456

[33] Hama, K. & Takagi, N. (1970). Measurements of sea-salt particles on the coast under moderate winds. *Papers in Meteorology and Geophysics* **21(4)**, 449–458

[34] Hetherington, J.A. & Jeffries, D.F. (1974). The distribution of some fission product radionuclides in sea and estuarine sediments. *Netherlands Journal of Sea Research* **8(4)**, 319–338

[35] Hetherington, J.A. (1976). The behaviour of Plutonium nuclides in the Irish Sea. In: *Environmental Toxicity of Aquatic Radionuclides: Models and Mechanisms* pp 81–106 (Ed. by Miller, M.W. & Stannard, J.N.). Ann Arbor Scientific Publications Inc., Ann Arbor, Michigan

[36] Horrocks, W.H. (1907). Experiments made to determine the conditions under which "specific" bacteria derived from sewage may be present in the air of ventilating pipes, drains, inspection chambers and sewers. *Proceedings of the Royal Society of London, Series B* **79**, 255–266

[37] Hotzl, H. & Winkler, R. (1987). Activity concentrations of ^{226}Ra, ^{228}Ra, ^{210}Pb, ^{40}K and ^{7}Be and their temporal variations in surface air. *Journal of Environmental Radioactivity* **5**, 445–458

[38] Howorth, J.M. & Eggleton, A.E.J. (1988). Studies of Environmental Radioactivity in Cumbria Part 12: Modelling of the sea-to-land transfer of radionuclides and an assessment of the radiological consequences. London, HMSO **AERE R 11733**

[39] Hunt, G.J. (1985). Timescales for the dilution and dispersion of transuranics in the Irish Sea near Sellafield. *The Science of the Total Environment* **46**, 261–278

[40] Independent Advisory Group, Chairman: Sir D. Black (1984). Investigation of the possible increased incidence of cancer in West Cumbria ("The Black Report"). London, HMSO

[41] Jeffries, D.F., Preston, A. & Steele, A.K. (1973). Distribution of ^{137}Cs in British coastal waters. *Marine Pollution Bulletin* **4**, 118–122

[42] Jeffries, D.F., Steele, A.K. & Preston, A. (1982). Further studies on the distribution of ^{137}Cs in British coastal waters – 1. Irish Sea. *Deep-Sea Research* **29(6A)**, 713–738

[43] Jones, J.A. (1981). The 2nd Report of a Working Group on Atmospheric Dispersion: A procedure to include deposition in the model for short and medium range atmospheric dispersion of radionuclides. London, HMSO **NRPB-R122**

[44] Junge, C.E. (1963). Air Chemistry and Radioactivity. Academic Press New York, N.Y.

[45] Knoll, G.F. (1979). Radiation Detection and Measurement. John Wiley & Sons

[46] Lassey, K.R. (1982). The interception and retention of aerosols by vegetation, 1: The formulation of a filtration model. *Atmospheric Environment* **15(1)**, 13–24

[47] Ludwick, J.D., Fox, T.D., Thomas, C.W. & Wendell, L.L. (1975). Inter-relations of chemical and physical information at Quillayute, Washington for 1974. *Report prepared for the U.S. Dept. of Energy, Research & Development Administration*

[48] Malloch, A.J.C. (1972). Salt-spray deposition on the maritime cliffs of the Lizard Peninsula. *Journal of Ecology* **60**, 103–112

[49] Martin, J.M., Thomas, A.J. & Jeandal, C. (1981). Transfert atmospherique des radionucleides artificiels de la mer vers le continent. *Oceanologica Acta* **4(3)**, 262–266

[50] McHugh, J.O., Smith, B.D., Hunt, G.J. & Thomas, R.E.G. (1986). The MAFF dry cloth collector programme for monitoring airborne radioactivity. *Journal of the Society of Radiological Protection* **6(2)**, 63–67

[51] McHugh, J.O. & Hetherington, J.A. (1987). Airborne radioactivity on the Scottish Solway coast. *Journal of Environmental Radioactivity* **5**, 333–342

[52] McKay, W.A., Pattenden, N.J. & Branson, J.R. (1987). Studies of Environmental Radioactivity in Cumbria Part 10: Some radionuclides in near-shore seawater 1980–84. London, HMSO **AERE R 11912**

[53] McKay, W.A. Personal Communication

[54] Minnema, D.M., Hudson, C.G. & Jones, J.D. (1981). A comparison of Ge(Li) detectors with different efficiencies for low-level general purpose counting. *Health Physics* **40**, 55–61

[55] Monteith, J.L. & Unsworth, M.H. (1990). Principles of Environmental Physics (2^{nd} Edition). Edward Arnold, London

[56] Muggleton, A.H.F. (1972). Semi-conductor X-ray spectrometers. *Nuclear Instruments & Methods* **101**, 113–125

[57] Nenot, J.C. & Stather, J.W. (1979). The toxicity of plutonium, americium and curium. Pergamon Press, Oxford for the Centre of the European Communities

[58] Olsen, C.R., Larsen, I.L., Lowry, P.D., Cutshall, N.H., Todd, J.F., Wong, G.T.F. & Casey, W.H. (1985). Atmospheric fluxes and marsh-soil inventories of ^{7}Be and ^{210}Pb. *Journal of Geophysical Research* **90(D6)**, 10487–10495

[59] Parker, R.P. (1962). ^{7}Be and fission products in surface air. *Nature* **193**, 967–968

[60] Parkin, D.W., Phillips, D.R., Sullivan, R.A.L. & Johnson, L. (1970). Airborne dust collections over the North Atlantic. *Journal of Geophysical Research* **75(9)**, 1782–1793

[61] Pasquill, F. & Smith, F.B. (1983). Atmospheric Diffusion (3^{rd} Edition). Ellis Horwood Ltd., Chichester, U.K.

[62] Pattenden, N.J., Cambray, R.S., Playford, K., Eakins, J.D. & Fisher, E.M.R. (1981). Atmospheric measurements on radionuclides previously discharged to sea. In: *The Impacts of Radionuclide Releases into the Marine Environment. Vienna, October 1980.* pp 201–221. IAEA, Vienna **IAEA STI/PUB/565**

[63] Pattenden, N.J., Cambray, R.S. & Playford, K. (1987). Studies of Environmental Radioactivity in Cumbria Part 15: The variation of radionuclide atmospheric deposition with distance from the sea. London, HMSO **AERE R 12478**

[64] Peirson, D.H. (1963). ^{7}Be in air and rain. *Journal of Geophysical Research* **68(13)**, 3831–3832

[65] Pentreath, R.J., Lovett, M.B., Jeffries, D.F., Woodhead, D.S., Talbot, J.W. & Mitchell, N.T. (1983). Impact on public radiation exposure of transuranium nuclides discharged in liquid wastes from fuel element reprocessing at Sellafield, U.K. In: *Radioactive Waste Management, 5. Seattle, May 1983.* pp 315–329. IAEA, Vienna **IAEA-CN 43/32**

[66] Pentreath, R.J., Harvey, B.R. & Lovett, M.B. (1986). Chemical speciation of transuranium nuclides discharged into the marine environment. In: *Speciation of Fission and Activation Products in the Environment* pp 312–325 (Ed. by Bulman, R.A. & Cooper, J.R.). Elsevier Appl. Sci. Pubs., London and New York

[67] Petrenchuk, O.P. (1977). Influence of coastal-zone physico-geographic conditions on the influx of marine aerosols into the atmosphere. *Meteorologiya i Gidrologiya* **6**, 5–10

[68] Sanak, J., Lambert, G. & Ardouin, B. (1985). Measurements of the stratosphere-to-troposphere exchange in Antarctica by using short-lived cosmo-nuclides. *Tellus* **37B**, 109–115

[69] Shapiro, M.H. & Forbes-Resha, J.L. (1976). Mean residence time of ^{7}Be-bearing aerosols in the troposphere. *Journal of Geophysical Research* **81(15)**, 2647–2649

[70] Slinn, S.A. & Slinn, W.G.N. (1980). Predictions for particle deposition on natural waters. *Atmospheric Environment* **14**, 1013–1016

[71] Smith, F.B. & Clark, M.J. (1986). Radionuclide deposition from the Chernobyl cloud. *Nature* **322**, 690–691

[72] Smith, M.H., Consterdine, I.E. & Park, P.M. (1989). Atmospheric loadings of marine aerosol during a Hebridean cyclone. *The Quarterly Journal of the Royal Meteorological Society* **115**, 383–395

[73] Smith, M.H., Consterdine, I.E. & Park, P.M. (1990). North Atlantic aerosol background concentrations measured at a Hebridean coastal site. Submitted to *Atmospheric Environment*

[74] Taylor, J.R. (1982). An introduction to error analysis: the study of uncertainties in physical measurements. University Science Books, California

[75] Turekian, K.K., Benninger, L.K. & Dion, E.P. (1983). ^{7}Be and ^{210}Pb total deposition fluxes at New Haven, Connecticut and at Bermuda. *Journal of Geophysical Research* **88(C9)**, 5411–5415

[76] Wagenbach, D., Gorlach, U., Moser, K. & Munnich, K.O. (1988). Coastal Antarctic aerosol: the seasonal pattern of its chemical composition and radionuclide content. *Tellus* **40B**, 426–436

[77] Wallace, J.M. & Hobbs, P.V. (1977). Atmospheric Science: An introductory survey. Academic Press, London

[78] Wells, N. (1986). The Atmosphere and Ocean: A Physical Introduction. Taylor & Francis, London and Philadelphia

[79] Williams, D.J. & Moser, B.C. (1976). Airborne sea salt sedimentation measurements and a method of reproducing ambient sedimentation rates for study of its effect on vegetation. *Atmospheric Environment* **10**, 531–534

[80] Wu, J. (1979). Spray in the atmospheric surface layer: Review and analysis of laboratory and oceanic results. *Journal of Geophysical Research* **84(C4)**, 1693–1704

[81] Young, J.A. & Silker, W.B. (1974). The determination of air-sea exchange and oceanic mixing rates using ^{7}Be during the BOMEX experiment. *Journal of Geophysical Research* **79(30)**, 4481–4489

[82] Young, J.A. & Silker, W.B. (1980). Aerosol deposition velocities on the Pacific and Atlantic oceans calculated from ^{7}Be measurements. *Earth and Planetary Science Letters* **50**, 92–104